Exploring CRISPR-Based Detection of *Lecanosticta acicola* in Loblolly Pine: From DNA Extraction to Field-Forward Diagnostics for Brown Spot Needle Blight

by

Alexia Alford

A thesis submitted to the Graduate Faculty of
Auburn University
in partial fulfillment of the
requirements for the Degree of
Master of Science

Auburn, Alabama
May 2, 2026

Keywords: Brown spot needle blight, CRISPR-Cas9, Loblolly pine, Diagnostics

Approved by

Hao Chen, Chair, Assistant Professor of Forest Genomics
Janna Willoughby, Associate Professor, College of Forestry, Wildlife, and Environment
Iris Vega Erramuspe, Assistant Research Professor - Biosensors

Abstract

Brown spot needle blight (BSNB), caused by Lecanosticta acicola, reduces growth and may contribute to mortality in loblolly pine (Pinus taeda), but diagnosis is complicated by symptom overlap with other needle diseases and by inhibitor-rich conifer tissues. This thesis presents an exploratory evaluation of CRISPR-based diagnostics for L. acicola, with a particular focus on the pre-analytical steps that determine whether sufficient pathogen DNA can be reliably recovered from BSNB-infected needles. Chapter 1 reviews classical, molecular, and point-of-care diagnostic approaches for woody plant pathogens and highlights CRISPR-Cas platforms as a promising bridge between laboratory-level specificity and field deployment. Chapter 2 compares five DNA extraction workflows and six ITS2 amplification conditions, including PNA-based host DNA suppression, and shows that fungal-enriching chemistries combined with selective amplification yield stronger and more consistent detection of L. acicola than plant- or microbiome-focused kits. Chapter 3 builds on these optimized conditions to develop and validate proof-of-concept CRISPR-Cas assays targeting the ITS and TEF1 loci of L. acicola, using in vitro Cas9 ribonucleoprotein cleavage to screen guide RNAs and confirm target suitability for diagnostic application. Together, these results demonstrate that combining extraction strategies that favor fungal DNA with CRISPR-based detection improves diagnostic performance from pine needles and provides a practical foundation for future field-deployable BSNB diagnostic tools.

Keywords: Brown spot needle blight, CRISPR-Cas9, Loblolly pine, Diagnostic

Artificial Intelligence (AI) Use Disclosure Statement

In the preparation of this thesis / dissertation, the following Artificial Intelligence (AI) tools were used: Perplexity and Grammarly. These tools were used primarily to troubleshoot and refine R code, to clarify and interpret thesis formatting guidelines, and to assist with grammar and wording of existing text. The author acknowledges full responsibility for the intellectual content of this work and has ensured that all AI-assisted sections have been reviewed and revised for accuracy and appropriate academic style. All AI-generated content was reviewed and validated for relevance, appropriateness, and accuracy before incorporation into the final document to maintain scholarly integrity of this research.

Digital Accessibility Use Disclosure Statement

In the preparation of this thesis / dissertation, the following digital accessibility tools were used to ensure this document complies with federal requirements: [list specific software/tools]. The author acknowledges full responsibility for the intellectual content of this work and has made a good faith effort to comply with digital accessibility requirements in publishing, wherein the nature of the content does not significantly change in order to do so. Furthermore, all content has been reviewed and revised to meet these requirements prior to final publication.

Acknowledgments

I would like to thank my advisor, Dr. Hao Chen, for his guidance, mentorship, and help throughout this entire process. I am honored to have been selected for this program and to have worked under his supervision. I am also grateful to my committee members, Dr. Janna Willoughby and Dr. Beatriz Vega, for their thoughtful feedback and support, which strengthened both this thesis and my growth in this program.

I am incredibly thankful for the help of Dr. Eckhardt and her lab members for their assistance with field sampling. I would also like to extend my thanks to graduate students Temitope Folorunso and Gabriel Silva for their advice, encouragement, and practical assistance along the way.

This project would not have been possible without the support of my family, friends, and Auburn family, whose steady love and encouragement I am exceedingly thankful for.

Table of Contents

List of Tables

List of Figures

List of Abbreviations

BSNB Brown spot needle blight

CRISPR Clustered regularly interspaced short palindromic repeats

Cas CRISPR-associated

Cas9 CRISPR-associated protein 9

Cas12a CRISPR-associated protein 12a

DNA Deoxyribonucleic acid

gDNA Genomic DNA

ITS Internal transcribed spacer

LAMP Loop-mediated isothermal amplification

L. acicola Lecanosticta acicola

PCR Polymerase chain reaction

qPCR Quantitative polymerase chain reaction

ddPCR Droplet digital polymerase chain reaction

RPA Recombinase polymerase amplification

RNP Ribonucleoprotein

1 Chapter 1: Introduction and Review of Literature

1.1 Why Diagnostics Decide Outcomes in Woody Plant Disease

Accurate and timely diagnosis is the foundation of plant disease management because it enables intervention before pathogens spread, outbreaks escalate, or infected plant materials move through trade and planting systems (Sarmah et al., 2025). In practice, the “value” of a diagnostic result is not only whether it is correct, but whether it arrives early enough to change decisions—such as quarantine actions, sanitation harvests, fungicide timing, nursery stock movement, or replanting choices. This need is amplified in woody hosts (i.e., forest trees, orchard trees, and ornamentals) because infections can remain cryptic for long periods, trees are long-lived, and epidemics can expand across landscapes while remaining undetected during early phases (Luchi et al., 2020). Woody systems also have distinct epidemiology: long-distance dispersal may be driven by storm events, insect vectors, or human-mediated movement of asymptomatic seedlings, while local spread is shaped by stand structure and canopy microclimate, creating strong incentives for early detection and containment.

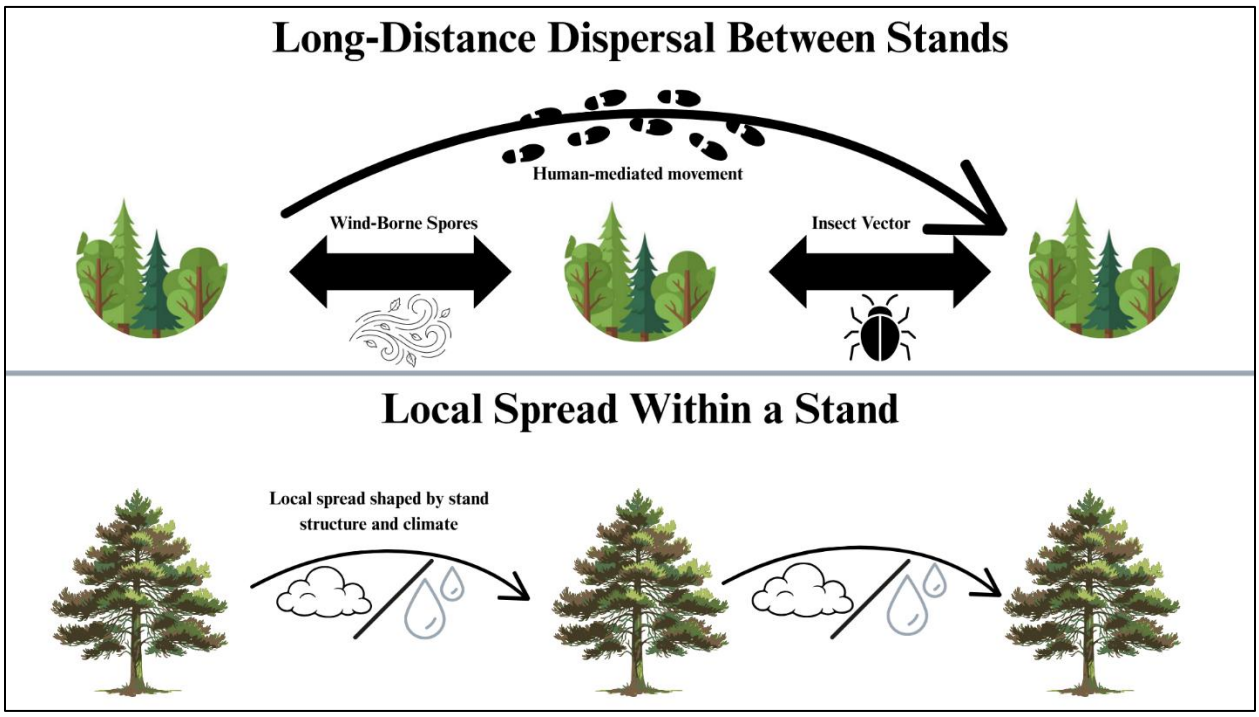

Figure 1.1 Long-distance dispersal of woody plant pathogens between stands via wind-borne spores, insect vectors, and human-mediated movement of asymptomatic seedlings, contrasted with local spread within a stand shaped by stand structure and microclimate.

In addition, woody tissues (needles, bark, phloem, xylem, roots) contain polysaccharides, polyphenols, resins, and other secondary metabolites that inhibit nucleic-acid amplification, and the physical toughness of tissues complicates extraction consistency—so “pre-analytical” steps (sampling strategy, tissue choice, disruption method, and inhibitor mitigation) are often as important as the detection chemistry itself (Baldi and La Porta, 2020). For example, pathogen distribution may be patchy within a crown or along a stem, and the best diagnostic tissue for one pathogen (e.g., cambium

for some canker fungi) may be suboptimal for another (e.g., needles for needle blights). For these reasons, diagnostic workflows in woody plant pathology are increasingly designed as tiered systems: field reconnaissance and symptom triage, rapid molecular screening near the sampling site when possible, and laboratory confirmation for regulatory or high-stakes decisions (Luchi et al., 2020; Baldi and La Porta, 2020). A well-designed tiered workflow also includes explicit quality safeguards—field blanks, extraction controls, positive controls, and confirmatory assays—so decisions are resilient to contamination, inhibitors, and low-titer infections.

1.2 Classic Diagnostic Procedures

Classical diagnosis begins with symptoms and sign recognition and remains indispensable for rapid scouting, delimitation surveys, and deciding which individuals and tissues to sample. Symptoms such as chlorosis, needle browning, defoliation, resin exudation, cankers, or crown thinning provide crucial context about the likely disease process, and visible signs such as sporulation, fruiting bodies, or insect galleries can narrow hypotheses rapidly (Sarmah et al., 2025). In forestry operations, this first layer is essential because it allows large areas to be assessed quickly and directs limited laboratory resources toward the most informative samples. However, symptom-based diagnosis generally detects disease only after symptoms appear and is often non-specific, since drought, nutrient limitation, insects, and multiple pathogens can produce similar cankers, dieback, or needle discoloration (Sarmah et al., 2025; Luchi et al., 2020). In many woody pathosystems, the latent period is long enough that symptoms lag behind

infection by weeks to months, and visible decline may reflect cumulative stress rather than a single causal agent.

Microscopy and isolation/culture provide stronger etiological evidence and enable downstream work (pathogenicity testing, isolate archiving, fungicide sensitivity, population genetics analyses), but they are time-consuming and may fail for slow-growing, unculturable, or low-abundance pathogens; they are also vulnerable to overgrowth by faster saprophytes and endophytes (Sarmah et al., 2025; Luchi et al., 2020). Even when culturing succeeds, morphology-based identifications can be ambiguous in species complexes, and culturing may bias recovery toward organisms that grow well on standard media rather than those most responsible for disease. Nonetheless, classical methods remain vital for generating reference isolates used to validate molecular assays and for answering questions that molecular tests alone cannot—such as whether a recovered organism is viable, aggressive, and consistent with observed symptoms under controlled inoculation. These limitations, especially the inability to reliably detect latent infections quickly—have driven the widespread adoption of molecular diagnostics in woody plant pathology, particularly for early detection and biosecurity surveillance (Luchi et al., 2020).

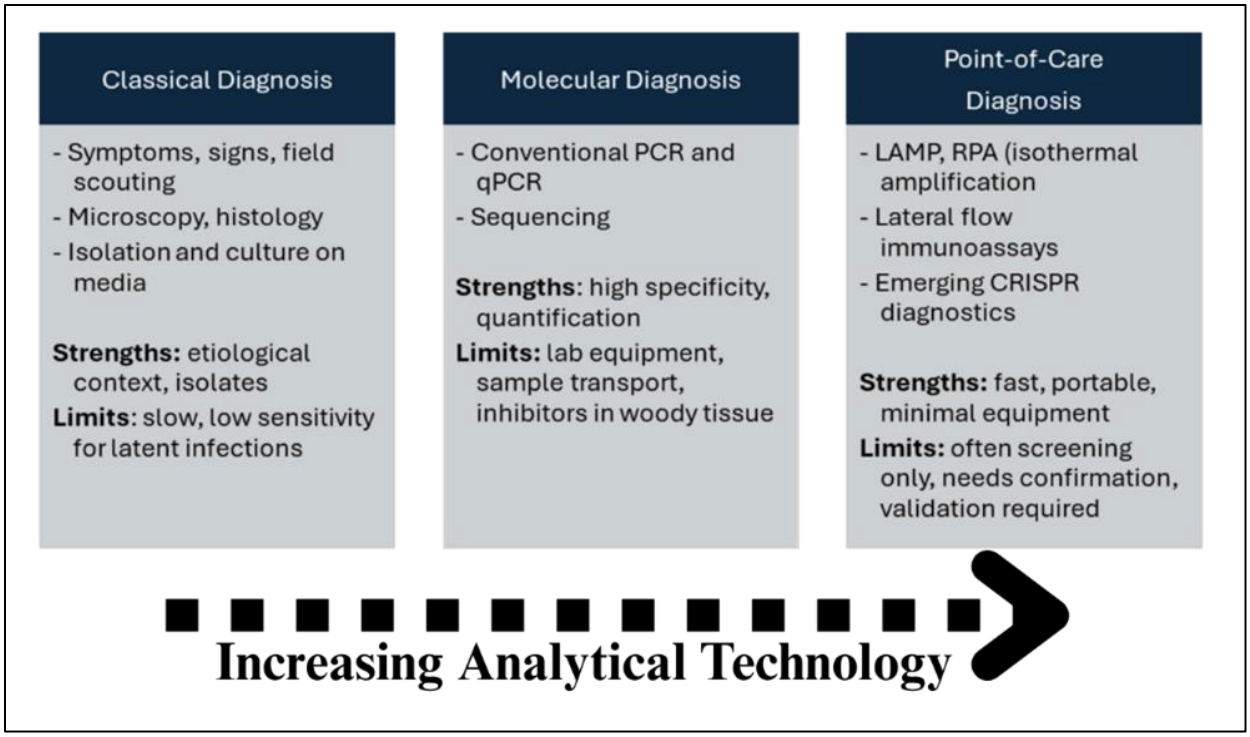

Figure 1.2 Classical, molecular, and point-of-care diagnostic methods used in woody plant pathology, summarizing their main applications, strengths, and limitations across field and laboratory contexts.

1.3 Fast Screening in the Field: Serology and Lateral Flow Tests

Immunological methods (e.g., ELISA) and lateral flow immunoassays provide fast screening that can be scaled to large surveys and used outside specialized molecular laboratories (Sarmah et al., 2025). Their core advantage is operational simplicity: they typically require minimal sample processing, can be interpreted visually, and are well suited to routine monitoring where hundreds or thousands of samples may be screened. In woody systems, lateral flow devices can support in-field decisions because they are simple and rapid; however, performance depends on antibody quality and antigen abundance, and cross-reactivity or reduced sensitivity compared with nucleic-acid

methods can be problematic when pathogen loads are low during early or latent infection (Luchi et al., 2020; Baldi and La Porta, 2020). This is especially relevant in woody tissues where pathogen biomass may be low, unevenly distributed, or localized in specific tissues not captured by the field sample.

Consequently, serology is often most effective as a triage layer especially useful for routine monitoring and rapid sorting of samples, while molecular confirmation is used for definitive identification, regulatory decisions, and fine-scale discrimination among closely related taxa (Luchi et al., 2020). In an integrated workflow, immunoassays can reduce the load on molecular labs by identifying likely positives quickly, while molecular assays provide the specificity needed to avoid costly false alarms. Immunoassays also fit well into training and extension contexts, where stakeholders need accessible tools and clear guidance on what a “screen positive” does and does not mean.

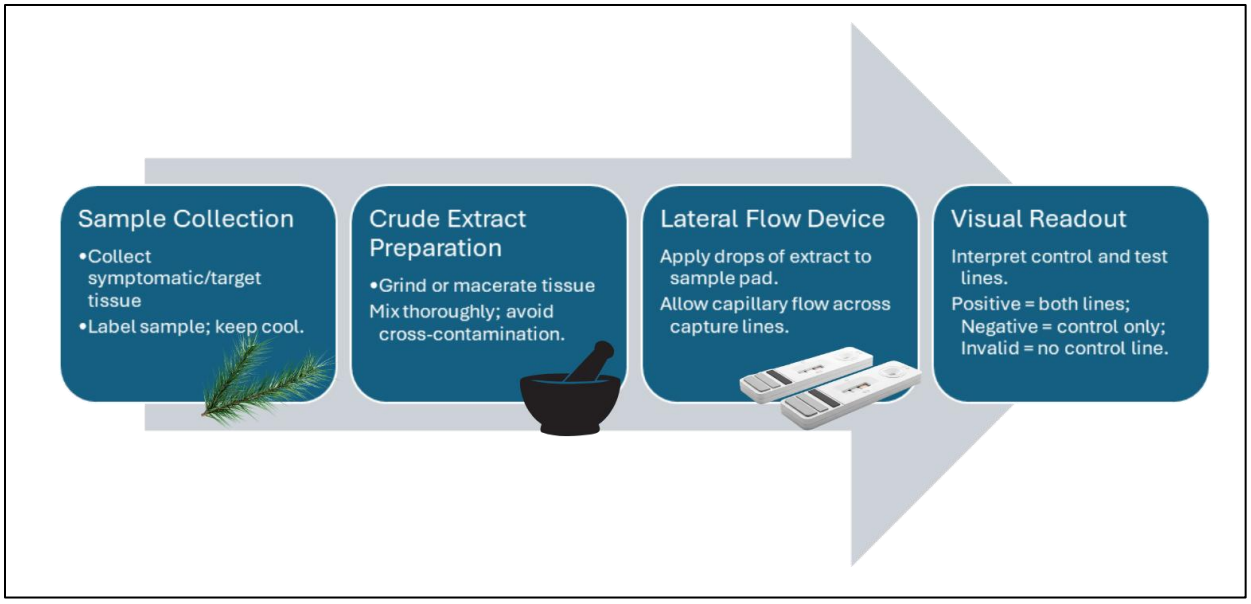

Figure 1.3. Workflow for lateral flow immunoassays in woody plant diagnostics, from sample collection and crude extract preparation through application to a lateral flow device and visual interpretation of control and test lines.

1.4 PCR and qPCR: The Laboratory Backbone for Sensitive Confirmation

PCR-based diagnostics form the backbone of modern plant pathogen detection because they are sensitive, specific, and supported by decades of assay development across fungi, oomycetes, bacteria, viruses, and nematodes (Wu et al., 2025; Sarmah et al., 2025). Conventional PCR remains robust and cost-effective for confirming presence/absence and for amplifying marker regions for sequencing-based identification, but it typically requires laboratory equipment and post-amplification handling, which slows turnaround and increases contamination risk. In woody plant diagnostics, conventional PCR also places higher demands on nucleic acid quality; inhibitors in bark, needles, and woody tissues can cause false negatives unless extraction and cleanup are optimized

(Baldi and La Porta, 2020). Despite these constraints, conventional PCR is widely used for routine confirmation and for building reference sequences from isolates and field samples.

Quantitative PCR (qPCR) improves sensitivity and adds quantification, enabling detection directly from symptomatic and asymptomatic tissues and supporting risk assessment and surveillance, particularly for invasive forest pathogens (Luchi et al., 2020). Quantification matters because it can help distinguish trace contamination from meaningful infection, track pathogen loads over time, compare sites or treatments, and support models of disease risk. qPCR assays are also well suited to high-throughput programs because they can be standardized, automated, and run with strict controls, which is important for diagnostic labs that must report defensible results. Digital droplet PCR (ddPCR) can further increase precision and inhibitor tolerance by partitioning reactions and enabling absolute quantification (Hindson et al., 2011; Sarmah et al., 2025), offering advantages when targets are rare, samples are highly inhibited, or absolute quantification is needed. However, ddPCR instrumentation and per-sample costs generally keep it in specialized laboratories and high-value use cases rather than routine field deployment (Wu et al., 2025). In forestry practice, the best use cases for ddPCR often involve difficult matrices, low-titer detection, or applications where precise quantification directly changes management decisions.

Table 1.1. Comparison of conventional PCR, quantitative PCR (qPCR), and droplet digital PCR (ddPCR) for detection of woody plant pathogens, highlighting differences in sensitivity, quantification, and instrumentation requirements.

Method	Sensitivity	Quantification	Equipment & Speed
Conventional PCR	- High but <qPCR and ddPCR	None	- Standard thermocycler, gel electrophoresis - Moderate turnaround
Quantitative PCR (qPCR)	- Very high - Good for low-titer infections	- Relative quantification via standard curve	- Real-time thermocycler - Faster than PCR
Digital Droplet PCR (ddPCR)	- Highest - Strong performance with inhibitors and rare targets	- Absolute copy number without standard curve	- Droplet generator+ reader - Slower and higher cost

Portable Speed Without a Thermocycler—Isothermal Amplification for Point-of-Care Testing

Because forestry diagnostics often require speed, portability, and minimal instrumentation, isothermal amplification methods have become central to point-of-care (POC) testing. LAMP amplifies nucleic acids at a constant temperature and can yield results rapidly with simple heating devices; it is often more field-deployable than PCR and can be coupled with fluorescence, turbidity, or colorimetric readouts (Notomi et al., 2000; Baldi and La Porta, 2020). LAMP is attractive in forestry because it can be implemented with compact equipment, can tolerate somewhat cruder extracts than PCR in many cases, and can be adapted to quick workflows suitable for nurseries, inspection stations, and field teams. It also supports targeted detection for known pathogens and can be designed for strong specificity when primer sets are carefully optimized and validated.

RPA operates at even lower temperatures and can be faster than LAMP, which is attractive for portable, battery-powered testing platforms and rapid workflows in remote field sites (Piepenburg et al., 2006; Baldi and La Porta, 2020). Its low-temperature operation is especially useful where precise thermal control is difficult, and its speed makes it compatible with same-visit decision-making. However, isothermal amplification can be vulnerable to non-specific amplification and false positives in some settings, particularly when crude extracts contain inhibitors or when primer design is suboptimal, so confirmatory strategies, contamination control, and careful validation remain essential (Baldi and La Porta, 2020; Luchi et al., 2020). In best practice, isothermal assays are deployed with clear interpretation rules, appropriate internal controls, and confirmatory follow-up (e.g., qPCR or sequencing) when outcomes are high-stakes or when a new location or host is involved.

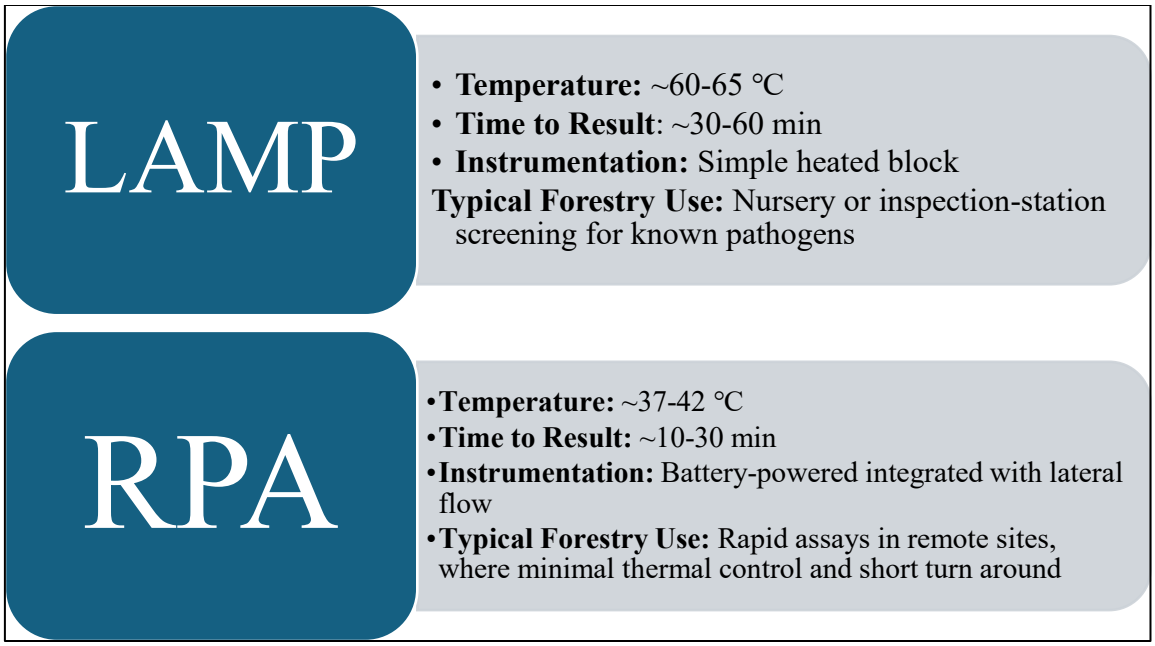

Figure 1.4. Summary of key operating features of loop-mediated isothermal amplification (LAMP) and recombinase polymerase amplification (RPA), including typical temperature ranges, time to result, instrumentation, and forestry use cases.

1.5 Traditional Methods That Keep Forestry Diagnostics Running

Beyond PCR and isothermal amplification, woody plant pathology relies on traditional and operational diagnostic tools that remain highly valuable, especially for landscape surveillance and for pathogens that are difficult to detect directly from woody tissues. One widely used approach is baiting and selective isolation—particularly for oomycetes such as *Phytophthora*—where soil, water, or root-zone samples are baited with susceptible plant tissues to enrich the pathogen prior to culturing and downstream identification (Luchi et al., 2020; Wu et al., 2025). This approach is powerful because it increases the chance of recovering viable propagules from complex environmental matrices, and it supports downstream characterization (e.g., mating type, aggressiveness,

and fungicide sensitivity). In forestry and nursery contexts, baiting can be integrated into routine monitoring programs for irrigation water, potting substrates, and field soils.

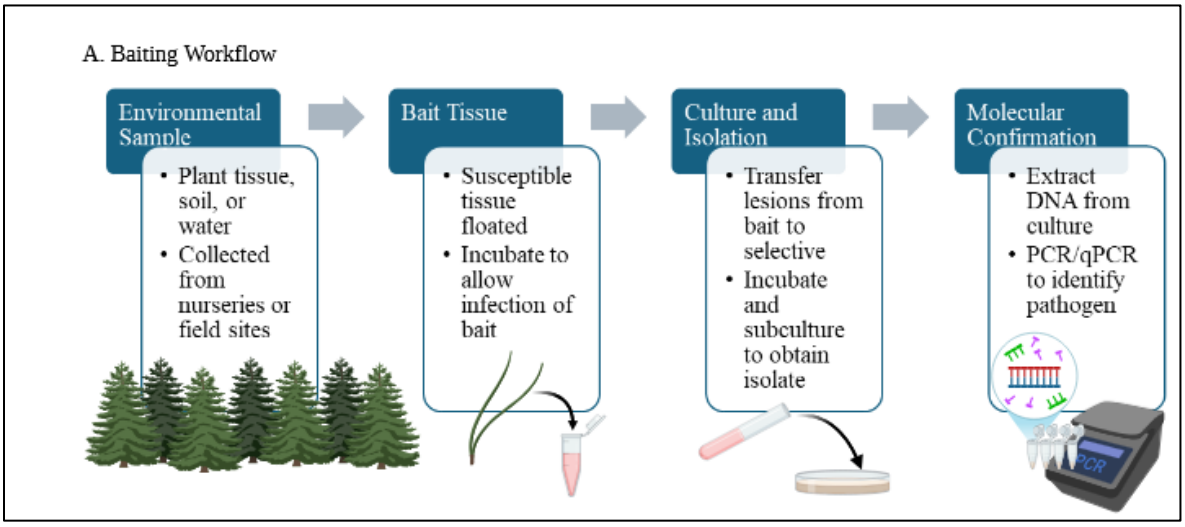

Figure 1.5. Baiting workflow for enriching water- and soil-borne pathogens, from environmental sample collection through bait infection and culture to molecular confirmation by PCR/qPCR. Schematic created with BioRender.com.

At the same time, baiting is slow relative to molecular tests and can be biased by bait choice, water temperature, seasonality, and competition among microbes. It requires time (days to weeks), laboratory handling, and taxonomic expertise; it can also miss organisms that do not bait efficiently or are outcompeted by faster-growing microbes (Luchi et al., 2020; Sarmah et al., 2025). For that reason, baiting is often paired with molecular assays applied either directly to environmental DNA or to cultures recovered from baiting, allowing faster identification and higher confidence once isolates are obtained (Luchi et al., 2020).

Reading the Wood's "Forensics"—Histopathology and Tissue Anatomy

A second group of traditional methods involves histopathology and wood/tissue examination, including thin-sectioning, staining, and microscopic assessment of colonization patterns, resin duct responses, vascular discoloration, tyloses/occlusions, and structural changes in xylem/phloem that are characteristic of particular disease syndromes (Sarmah et al., 2025). These approaches are especially informative for tree wilts and cankers because they connect symptoms to host tissue responses and can help distinguish infectious processes from abiotic injury or mechanical damage. In addition, histological observations can guide targeted molecular sampling by identifying the most relevant tissues (e.g., active lesion margins, discolored sapwood, or symptomatic needle zones) rather than relying on bulk tissue that may dilute pathogen signal.

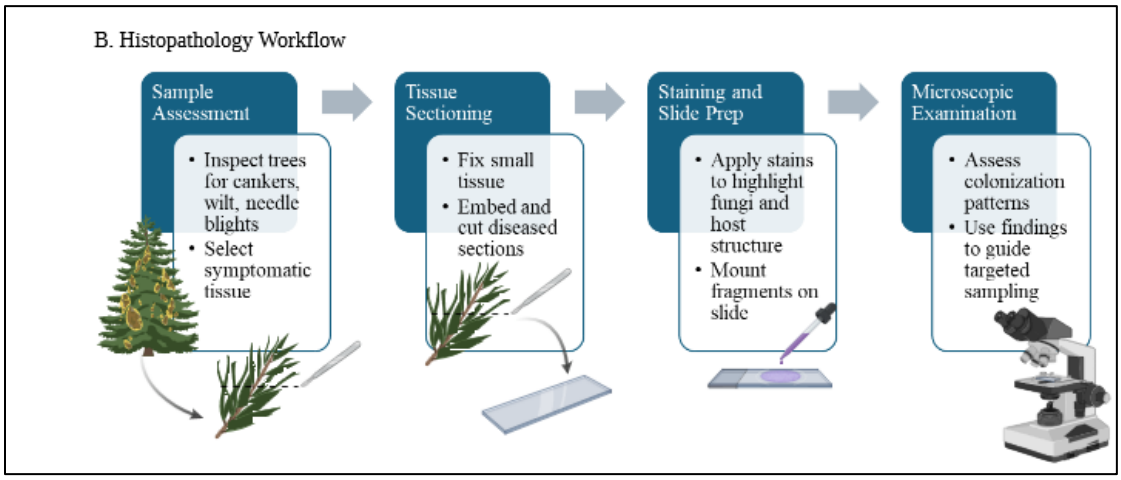

Figure 1.6. Histopathology workflow for woody tissues, showing progression from field symptom assessment and targeted tissue sampling through sectioning and staining to

microscopic examination used to interpret host responses and guide diagnostics. Schematic created with BioRender.com.

However, histopathology rarely provides species-level identification without additional molecular confirmation, and accuracy depends heavily on expertise and the presence of diagnostic signs at the time of sampling (Luchi et al., 2020; Sarmah et al., 2025). It can be less informative when infections are early, when tissues are highly degraded, or when the causal agent is present at low abundance. For this reason, histopathology is often used as a complementary “evidence layer” that strengthens interpretation and guides follow-up testing.

Catching Pathogens in Motion—Spore Trapping and Vector Monitoring

Woody pathosystems also commonly use spore trapping and vector monitoring as operational diagnostics. Spore traps (passive or active) can provide early warning by detecting airborne inoculum and informing risk windows for infection and management actions, while vector monitoring (e.g., bark beetles and other insects associated with fungal pathogens) can indicate pathogen pressure and dispersal pathways before severe symptoms appear (Sarmah et al., 2025; Wu et al., 2025). These tools are particularly valuable in forest landscapes where direct sampling of every tree is impossible, and where management may depend on forecasting periods of highest infection risk. Monitoring also supports outbreak investigations by identifying potential dispersal routes and by linking pathogen presence to vector dynamics.

The limitations are that trapping and vector monitoring usually measure exposure risk rather than confirmed infection, and they typically do not identify pathogens to species level unless paired with microscopy, immunoassays, or nucleic-acid tests (Luchi et al., 2020; Sarmah et al., 2025). Capture efficiency can vary with weather, canopy structure, and sampling design, so interpretation requires careful calibration. In modern programs, traps often function as “sample concentrators” whose contents are then tested by qPCR, metabarcoding, or other molecular assays to improve specificity and responsiveness.

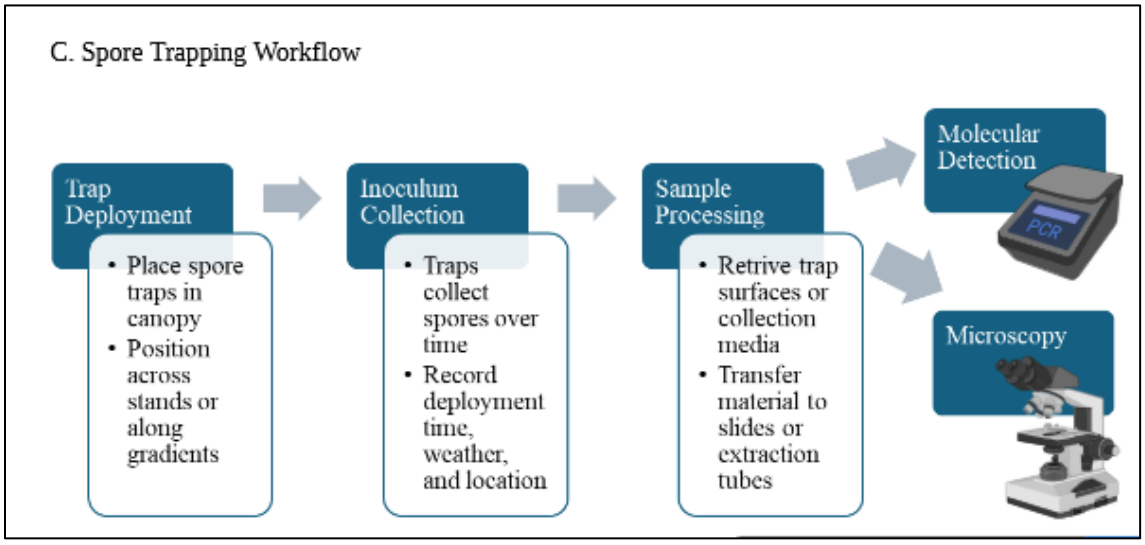

Figure 1.7. Spore trapping workflow for woody plant pathogens, from canopy trap deployment and airborne inoculum capture through recovery and processing of trap contents to microscopic and molecular detection. Schematic created with BioRender.com.

Seeing Disease from the Sky—Remote and Proximal Sensing

Remote sensing and proximal sensing (UAV/satellite imagery, vegetation indices, thermal imaging, and spectroscopy) are becoming essential for forestry because outbreaks can span large areas and individual-tree inspection is unrealistic (Sarmah et al., 2025). Their main strength is scale: remote sensing can detect canopy-level changes, quantify severity across stands, track progression through time, and support prioritization of ground surveys. This can be decisive in early outbreak phases where rapid delimitation is needed and resources are limited. Remote sensing also integrates well with forest inventory systems and can support post-treatment evaluation (e.g., after thinning, sanitation harvest, or prescribed burning).

However, remote sensing typically detects host stress rather than the causal organism, so it cannot replace confirmatory diagnostics; instead, it functions best as a triage layer that guides molecular testing toward the most informative samples (Baldi and La Porta, 2020; Sarmah et al., 2025). In practice, remote sensing is most valuable when linked to a sampling plan that includes confirmatory laboratory testing, allowing managers to translate “spectral stress signals” into pathogen-specific actions rather than generalized stress responses.

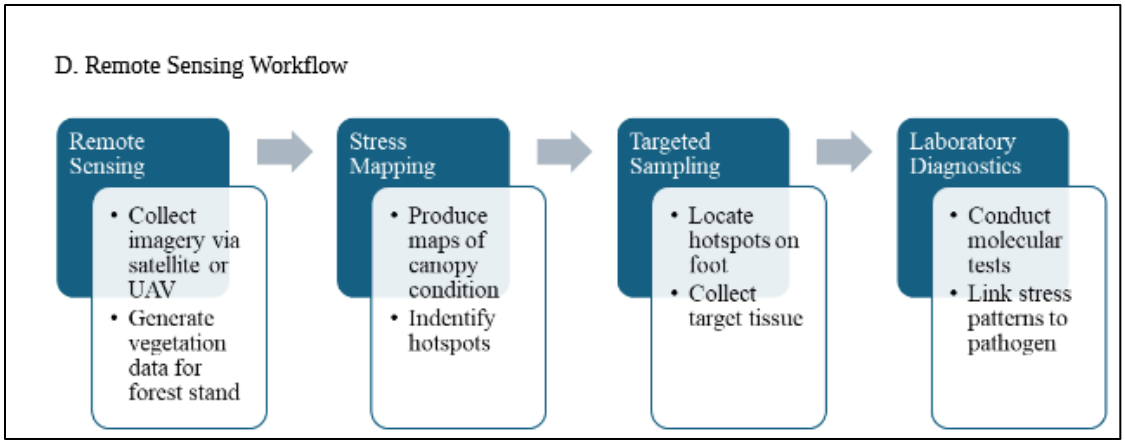

Figure 1.8. Remote and proximal sensing integrated with ground diagnostics, illustrating how satellite or UAV imagery is used to map canopy stress, guide targeted field sampling, and link stress patterns to specific pathogens via laboratory tests. Schematic created

How These Traditional Methods Compare with CRISPR Diagnostics

Traditional approaches excel at situational awareness and evidence-building: remote sensing helps answer “where is stress occurring,” spore/vector monitoring helps answer “is inoculum pressure rising,” baiting and culture help answer “can we recover the organism for deeper study,” and histopathology helps answer “how is the host responding anatomically” (Luchi et al., 2020; Sarmah et al., 2025). CRISPR-based diagnostics, by contrast, are designed to answer “what is it—exactly?” quickly and confidently at the point-of-need, with sequence-guided specificity that is hard to match by morphology or stress signals alone (Cao et al., 2024; Wu et al., 2025). This distinction matters in woody systems because management actions (quarantine, destruction of stock, movement restrictions) often require species-level confidence, and delays can mean irreversible spread.

In practice, the strongest forestry workflows integrate these tools rather than replacing one with another: sensing and trapping prioritize sites and timing, baiting/culture supports isolate recovery and reference collections, and CRISPR-Dx (or qPCR) provides rapid and specific confirmation from prioritized samples to enable timely management and containment (Luchi et al., 2020; Wu et al., 2025). A clear operational advantage of CRISPR-Dx is that it can be deployed closer to the sampling site than qPCR in many scenarios, potentially shrinking the time between suspicion and confirmation from days to hours—an especially important gain in nursery and port-of-entry settings.

Sequencing as the Ultimate Resolver—From Barcodes to Metabarcoding

Sequencing-based diagnostics complement targeted assays by enabling identification when the causal agent is unknown, mixed infections are suspected, or strain-level resolution is needed for epidemiology. Barcoding (e.g., fungal ITS) supports species identification, while metabarcoding and metagenomics can profile entire microbial communities without isolating organisms (Luchi et al., 2020). This is particularly valuable in woody hosts, where endophytes, opportunistic pathogens, and secondary invaders commonly co-occur, and where symptom expression may reflect combined stressors rather than a single organism. Sequencing can also identify unexpected or novel pathogens, which is critical for invasive species surveillance and for emerging disease syndromes linked to climate-driven range shifts.

Portable sequencing platforms can compress time-to-answer and support outbreak response, but accuracy, sample prep, and bioinformatics still constrain routine field use (Baldi and La Porta, 2020; Ansari et al., 2026). Even when sequencing is

technically feasible, translating complex community profiles into actionable management decisions can be challenging, especially when detected organisms include both pathogens and harmless commensals. Across all molecular approaches, woody plant diagnostics must be designed around difficult matrices: protocols that tolerate crude extracts, minimize equipment dependence, and include strong controls often outperform theoretically “best” assays that are too fragile operationally (Baldi and La Porta, 2020; Wu et al., 2025). For this reason, sequencing is often positioned as a “resolver” tool—used when targeted assays are insufficient, when mixed infections complicate interpretation, or when epidemiological tracking is required.

1.6 Why CRISPR Diagnostics Are a Breakthrough for Woody Plant Pathogen Detection

CRISPR-based diagnostics (CRISPR-Dx) are increasingly positioned as a next-generation solution because they combine high specificity with rapid, portable readouts. The central advantage is that guide-RNA-directed target recognition triggers a signal-generating nuclease activity, often through collateral cleavage of reporter molecules in Cas12 (DNA-targeting) and Cas13 (RNA-targeting) systems (Gootenberg et al., 2017; Chen et al., 2018). In foundational demonstrations, Cas13-based SHERLOCK enabled sensitive nucleic-acid detection with isothermal amplification and flexible readouts, while Cas12a-based approaches established strong trans-cleavage activity that enables highly sensitive detection following target recognition (Gootenberg et al., 2017; Chen et al., 2018). Forestry-focused reviews emphasize that integrating CRISPR detection with isothermal amplification (e.g., RPA or LAMP) enables ultrasensitive assays without thermocyclers and supports field-deployable kits with fluorescence or lateral-flow

outputs—directly aligned with the needs of nurseries, ports, and remote forest sites where rapid, confident decisions are required (Cao et al., 2024; Wu et al., 2025).

Practically, CRISPR-Dx is especially valuable in woody pathology for three reasons. First, it adds a second layer of sequence verification beyond amplification, which can reduce false positives that sometimes occur in isothermal methods when readouts rely on bulk amplification signals alone (Wu et al., 2025). Second, CRISPR guide design can discriminate among closely related organisms or even single-nucleotide differences, which is crucial when multiple pathogens produce similar symptoms (needle blight complexes, canker syndromes) or when regulated organisms require confident identification (Luchi et al., 2020; Wu et al., 2025). Third, CRISPR readouts can be adapted to field-friendly formats, including lateral flow strips, enabling faster operational decisions and tighter biosecurity response loops (Baldi and La Porta, 2020). While CRISPR-Dx still depends on reliable sample preparation and standardized validation (controls, inclusivity/exclusivity panels, reproducibility), its development trajectory strongly matches forestry's demand for low-infrastructure, high-confidence diagnostics (Luchi et al., 2020; Wu et al., 2025).

CRISPR also matters in forest pathology beyond detection as it is a powerful research tool for dissecting host–pathogen interactions and for engineering resistance in hosts or attenuating virulence in pathogens. Reviews emphasize that forest pathology has historically lagged behind annual-crop systems in deploying CRISPR approaches due to long generation times, transformation/regeneration bottlenecks, and regulatory constraints in trees, yet argue that expanding forest pathogen genomic resources and

improved delivery/regeneration methods can accelerate CRISPR-enabled discovery and resistance strategies (Dort et al., 2020; Cao et al., 2024). Importantly, these research advances feed back into diagnostics: better genomic resources and population data improve marker selection, increase the robustness of guide design, and enable assays that discriminate regulated lineages or track outbreak sources.

Brown Spot Needle Blight—Diagnostics That Separate Look-Alikes

Brown spot needle blight (BSNB), caused by *Lecanosticta acicola*, is an important needle disease of *Pinus* species and is increasingly recognized as a growing threat to pine forests and plantations (van der Nest et al., 2019). A central diagnostic challenge is that multiple needle blight agents can produce overlapping symptom patterns on needles and in crowns, and infection can precede obvious symptoms—making visual diagnosis unreliable for surveillance, quarantine inspections, and delimitation surveys (Luchi et al., 2020). Needle blights also vary by host susceptibility, canopy microclimate, and site conditions, which can blur symptom interpretation across stands and seasons. Therefore, molecular approaches are essential for distinguishing *L. acicola* from other key needle blight pathogens such as *Dothistroma pini* and *D. septosporum*, especially when rapid management decisions are required (Luchi et al., 2020).

Probe-based LAMP assays have been developed for rapid detection of *L. acicola*, *D. pini*, and *D. septosporum* directly from infected needles using species-informative targets, demonstrating a practical path toward field-forward screening (Aglietti et al., 2021). In a diagnostic workflow, LAMP can be deployed as an early screening layer in nurseries and surveys because it is fast and requires limited equipment, but best practice

still emphasizes careful handling to avoid contamination, inclusion of internal controls, and confirmatory testing (often qPCR or sequencing) when results carry regulatory consequences (Luchi et al., 2020; Baldi and La Porta, 2020). Standardized diagnostic guidance and validated assays are especially important for BSNB because false positives can disrupt trade and nursery operations, while false negatives can facilitate silent spread.

CRISPR-based approaches are a logical extension for BSNB diagnostics because they can provide highly specific post-amplification confirmation and can be designed to differentiate closely related taxa or lineages when needed. A practical RPA–CRISPR/Cas12 or LAMP–CRISPR workflow would combine an extraction approach tailored to inhibitor-rich needles, short isothermal amplification, and a CRISPR readout via fluorescence or lateral flow—yielding a rapid, field-deployable assay with strong sequence-level specificity (Chen et al., 2018; Gootenberg et al., 2017; Wu et al., 2025). In needle blight complexes—where “look-alike” symptoms are common—this added specificity is particularly valuable for quarantine decisions, nursery stock movement, and early containment, because it supports confident discrimination without requiring immediate access to a full diagnostic laboratory.

1.7 Building Framework for Diagnostic Pipelines

In woody plant pathology, diagnostic methods should be selected and integrated based on the decision being supported: classical methods provide etiological context and

isolates, PCR/qPCR provide sensitive laboratory confirmation, isothermal methods enable rapid field screening, sequencing resolves unknowns and mixed infections, and CRISPR-Dx offers a uniquely strong bridge between laboratory-grade specificity and point-of-need deployment (Luchi et al., 2020; Baldi and La Porta, 2020; Wu et al., 2025). Across these options, CRISPR-based diagnostics deserve special emphasis because they directly address forestry constraints—speed, portability, specificity, and operational simplicity—while remaining compatible with isothermal amplification formats already used in field biosecurity workflows (Cao et al., 2024; Wu et al., 2025). Importantly, CRISPR-Dx should be evaluated not only on analytical sensitivity, but also on operational performance: robustness to inhibitors, stability of reagents, clarity of readout, ease of training, and reproducibility across users and sites.

For brown spot needle blight, where symptom overlap and early crypticity complicate surveillance, combining validated LAMP/RPA screening with CRISPR confirmation offers a compelling pathway toward adoption-ready diagnostics that can support both plantation management and regulatory biosecurity needs (Aglietti et al., 2021; van der Nest et al., 2019; Luchi et al., 2020). More broadly, the future of woody plant pathogen detection will likely emphasize integrated systems in which remote sensing and environmental monitoring guide sampling, rapid molecular tools provide near-site screening and confirmation, and laboratory assays plus sequencing provide deep resolution when outbreaks, invasions, or research questions demand it.

2 Chapter 2. Evaluation of DNA Extraction Methods for Recovery of *Lecanosticta acicola* DNA from Loblolly Pine Needles Infected with BSNB

2.1 Abstract

Brown spot needle blight (BSNB), caused by *Lecanosticta acicola*, is an emerging foliar disease of pines that reduces growth, causes premature needle cast, and, in severe cases, contributes to tree mortality. BSNB diagnosis directly depends on reliable recovery of *L. acicola* DNA from mixed host-pathogen needle tissue. DNA extraction serves as a crucial pre-analytical step for molecular diagnostics, ecological studies, and downstream genomic work, like CRISPR-Cas complexes. This chapter evaluates five DNA extraction workflows: 1) YeaStar, 2) Quick-DNA Fungal/Bacterial, 3) Quick-DNA Plant/Seed, 4) ZymoBIOMICS, and 5) a modified CTAB protocol. Together, with six ITS2-oriented amplification conditions based on three primer systems (gITS7/ITS4, fITS7/ITS4, 5.8S-Fun/ITS4-Fun) with and without peptide nucleic acid (PNA) host-DNA suppression treatment. Infected loblolly pine needles, healthy needles, and *L. acicola* cultures were used to compare total DNA yield, purity, amplification performance, and the fungal to plant balance of recovered DNA. Across kits and assays, methods differed sharply in both total amplification and fungal enrichment: the YeaStar and Quick-DNA Fungal workflows produced the strongest fungal representation and the most stable performance across selective primer/PNA conditions, whereas ZymoBIOMICS, Quick-DNA Plant, and CTAB extractions were strongly plant-dominated despite sometimes high total DNA yield. The results demonstrate that successful recovery of *L. acicola* DNA from BSNB-infected

needles depends on the joint effects of extraction chemistry and amplification strategy and that extraction performance must be judged by fungal enrichment and signal robustness under selective conditions rather than by total DNA concentration alone.

2.2 Introduction

Brown spot needle blight (BSNB), caused by *Lecanosticta acicola*, is an important foliar disease of affecting majority of pine species. Infected needles typically develop small yellow lesions that enlarge into brown or orange-brown spots, often surrounded by a yellow halo, followed by necrosis above the infection point, premature needle cast, loss of photosynthetic area, growth reduction, and, in severe cases, mortality. The pathogen has attracted increasing attention because its geographic range and impact have expanded in recent decades, and climatic suitability models suggest that large pine-growing regions remain vulnerable to further spread and establishment (van der Nest et al., 2019; Tubby et al., 2023; Ogris et al., 2023).

Visual observations of pathogenic symptoms are often insufficient in determining the causal agent of plant pathogens as, especially in the case of BNSB, symptoms of different pathogens can frequently overlap. In terms of molecular diagnostics, nucleic acid testing has revolutionized the efficiency, accuracy, and length of time of properly assessing the presence of a variety of pathogens from viruses to fungi. Nucleic acid testing (NAT) is a highly sensitive detection method that utilizes direct amplification of the nucleic acid or a target signal to verify its presence in small amounts. Due to its ability to perform well with a relatively small limit of detection (LoD), its uses in forest pathology are

easily recognized as plant material is notably resistant to complete lysis due to the presence of cellulose in the cell wall. Consequently, the quality and quantity of extracted nucleic acids directly influence the performance of downstream applications such as PCR and CRISPR-based assays. The amplification of impurities and off-target effects, respectively, are common issues due to the high sensitivity and specificity of these techniques if DNA quality is poor (Lucena-Aguilar et al. 2016; Garrett 2001). For this reason, the method of DNA extraction is crucial and should be evaluated for purity of sample, cost-effectiveness, time involving hands-on manipulation, and scalability (Boesenberg-Smith et al. 2012).

Because BSNB is often diagnosed and studied from infected needles rather than from pure culture, molecular recovery of pathogen DNA directly from plant tissue is highly important. Earlier work on pine needle blight pathogens showed that direct molecular detection from infected needles is feasible and that multiple commercial extraction procedures can yield DNA of sufficient quality for PCR-based diagnosis. More recent work has also shown that pine needle tissues can be processed successfully for direct pathogen detection after lesion-focused subsampling and tissue grinding, confirming that infected needle tissue is a practical source of diagnostic DNA (Ioos et al., 2010; Aglietti et al., 2021).

The presence of secondary metabolites in plant tissue (i.e, polysaccharides, phenolic compounds, alkaloids, saponins, and resin) are released as a result of the plant's defense system when broken down in the process of DNA extraction. Polysaccharides and phenolic compounds are the most difficult to remove in the extraction and purification

process as they often co-precipitate with DNA (Pratyusha 2022). Both of these unique and variable secondary metabolites present a separate issue that lead to contamination of genomic DNA. Polysaccharide contamination inhibits the activity of several PCR polymerases and ligases and falsely inflates the amount of DNA present upon extraction due to co-precipitation. The concentrated presence of cellulose within the cell wall also presents an issue in sample homogenization as the intense procedure of physical lysis in turn also degrades the high molecular weight of DNA. While polyphenol contamination frequently presents struggles in plant DNA isolation as when cell lysis begins, polyphenols are released from vacuoles and quickly oxidize causing irreversible enzymatic oxidization of DNA that leaves it with a brown coloration and unusable for downstream applications (Varma et al. 2007). For this reason, the selection of an efficient method for DNA extraction is crucial and should be evaluated for purity of sample, cost-effectiveness, time involving hands-on manipulation, and scalability (Boesenberg-Smith et al. 2012).

The main challenge, however, is that infected needles are mixed-template material. DNA extracted from diseased pine needles contains host pine DNA together with fungal DNA, and the host fraction may be much more abundant than the pathogen fraction. In addition, conifer tissues are chemically difficult substrates because polyphenols, polysaccharides, resins, and other secondary metabolites can reduce DNA purity and inhibit downstream PCR. For that reason, an extraction method that produces a high total DNA concentration is not automatically the best method for pathogen recovery if much of that DNA is host-derived or co-purified with inhibitors (Kim et al., 1997; Porebski et al., 1997; Sahu et al., 2012; Rezadoost et al., 2016).

DNA isolation from fungal material faces similar issues in extraction of quality gDNA. Fungal cell walls can be difficult to lyse efficiently without shearing or degrading DNA (Langsiri et al. 2025). The composition of fungi also exhibits parallel contamination opportunities. Uniquely, however, due to the vast variation in fungal specimens and minimal fungal pathogen coverage, metagenomic sequencing can often produce misidentifications when short-read sequences are provided due to low quality DNA (Li et al. 2021). Pushing the importance of high quality gDNA extraction to generate longer sequences for more accurate fungal identification.

For fungal community and pathogen-focused studies, the internal transcribed spacer (ITS) region is widely accepted as the principal fungal barcode, and ITS2-targeting primers are commonly favored because shorter amplicons reduce some forms of PCR bias and can perform better when template is degraded, scarce, or inhibitor-rich. Primer choice is nevertheless not neutral: different ITS primer pairs can produce markedly different estimates of fungal abundance, composition, and taxonomic recovery, especially in plant-associated samples in which host co-amplification is a major concern (Schoch et al., 2012; Lindahl et al., 2013; Ihrmark et al., 2012; Li et al., 2020).

A further strategy for reducing plant background is the use of peptide nucleic acid (PNA) clamps. PNA molecules bind target host sequences during PCR and block their efficient amplification, thereby enriching microbial or fungal templates. PNA-based blocking has been effective in several microbiome studies, but the success of a clamp depends strongly on host-sequence compatibility, and even single mismatches can substantially reduce blocking efficiency. Thus, a clamp that works in one plant host cannot

be assumed to work equally well in pine without validation (Lundberg et al., 2013; Fitzpatrick et al., 2018; Viotti et al., 2024).

Considering these factors, BSNB detection requires extraction workflows that cope with inhibitor-rich host tissue and amplification systems must balance total signal against fungal selectivity. This chapter focuses on comparing extraction and amplification strategies for recovering *L. acicola* DNA from infected loblolly pine needles and using those results to propose a simplified, diagnostically useful workflow.

2.2.1 Objective and Hypothesis

The objective of this study was to identify extraction and amplification conditions that recover more *Lecanosticta acicola* DNA from BSNB-infected pine needles while minimizing plant DNA contamination. A second objective was to use the comparative results to propose a simplified workflow for routine fungal DNA extraction from infected needles. Three main hypotheses guided these objectives:

1) The central hypothesis was that the most informative comparison would come from infected pine needles rather than from pure *L. acicola* material. Pure fungal samples should behave largely as fungal-positive controls because they contain mostly fungal DNA and little host material, whereas infected needles directly test the real biological problem of host-pathogen mixtures. On that basis, the fungal-to-plant DNA ratio in infected needles was expected to be the most meaningful performance criterion. 2) Primer choice and PNA clamping would strongly influence host carryover. Based on previous work comparing gITS7/ITS4, fITS7/ITS4, and 5.8S-Fun/ITS4-Fun in plant-associated samples showed that primer selection was the dominant factor affecting plant-

fungal co-amplification. In that study, broad gITS7-based amplification produced more plant-associated carryover, fITS7 generally gave a favorable balance between fungal recovery and selectivity, and 5.8S-Fun/ITS4-Fun, particularly with PNA, gave the strongest host suppression but not always the highest total fungal read number. Informing expectations for this study that the broadest assay would be expected to maximize total signal, whereas the more selective assays are expected to improve the fungal-to-plant balance (Viotti et al., 2024; Taylor et al., 2016). 3) Plant-oriented extractions were expected to recover high amounts of total DNA from infected needles, but not necessarily the highest proportion of fungal DNA. By contrast, fungal-oriented kits or fungal-friendly lysis workflows were expected to perform better if they disrupted fungal cell walls efficiently while limiting the recovery of plant background. This distinction between total yield and selective fungal enrichment is especially important in conifer tissues, where host-derived compounds can dominate the extract and interfere with downstream amplification (Kim et al., 1997; Rezadoost et al., 2016; Folorunso et al., 2025).

2.3 Materials and Methods

2.3.1 Sample Origin and Experimental Design

Pure cultures of *L. acicola* were obtained from Dr. Janna Willoughby's lab at the College of Forestry, Wildlife, and Environment at Auburn University, Auburn, Alabama, USA. The isolates used in this study were donated by collaborators from an origin site in east Alabama. Cultures were maintained on MEA at room temperature or in liquid YEPD

prior to acquisition, and in –20 °C prior to DNA extraction. Any distinctions in mycelium origin are noted.

Mycelium extractions and amplification were used as fungal-positive controls.

Symptomatic loblolly pine needles exhibiting signs of brown spot needle blight were obtained in field collections coordinated by the lab teams of Dr. Janna Willoughby and Dr. Lori Eckhardt (College of Forestry, Wildlife, and Environment, Auburn, Al, USA). In Fall 2025, infected needles were received from both Dr. Willoughby's and Eckhardt's lab for DNA extraction, and in Spring 2026, additional needles were collected and provided by solely Dr. Eckhardt's lab.

Asymptomatic ("healthy") loblolly pine needles were also obtained from Dr. Eckhardt's lab during the same collection periods. Healthy pine needles were used as plant-background controls and non-infected reference material in this study and stored at –80 ° C until DNA extraction.

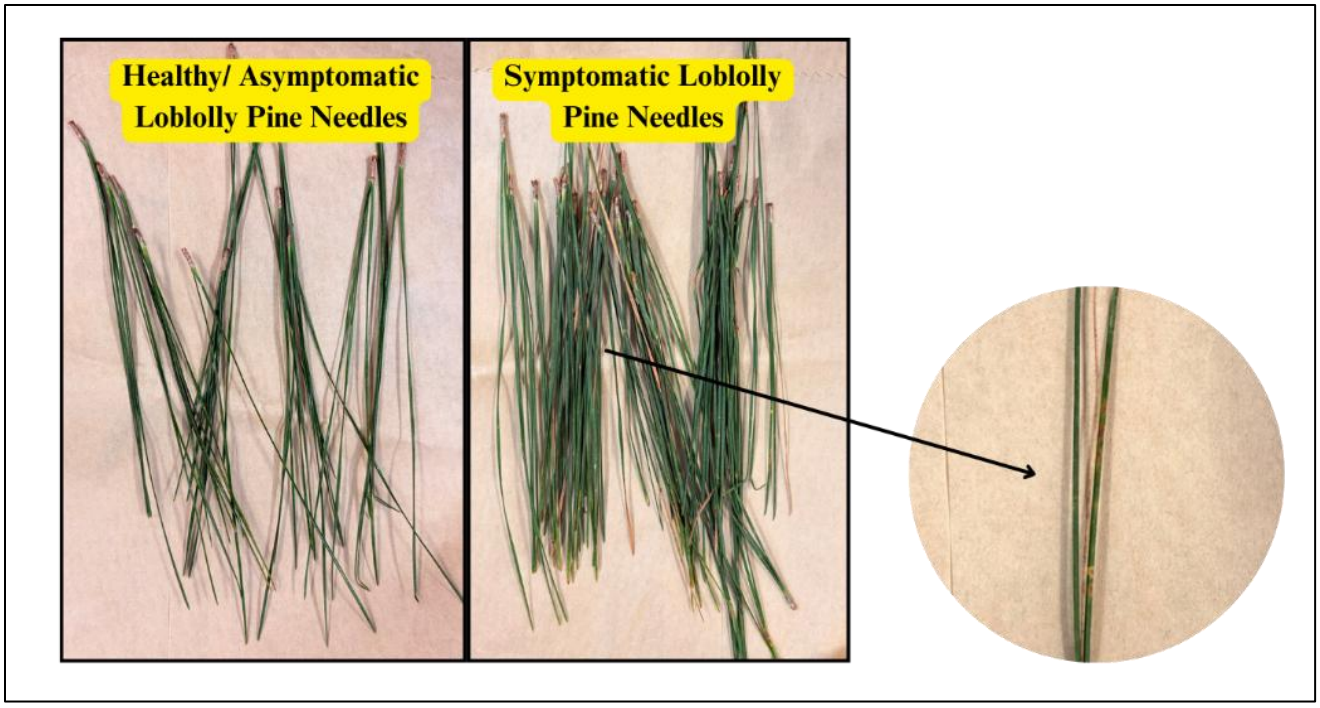

Figure 2.1 Field collected asymptomatic or “Healthy” loblolly pine needles pictured on the right and symptomatic loblolly pine needles showing brown spots and yellow halos. The image to the far right shows these symptoms at a closer view.

DNA extraction methods and performance was compared among four commercial extraction kits (A. Zymo YeaStar Genomic DNA Kit (D2002), B. ZymoBIOMICS DNA Miniprep Kit with Lysis Tubes (D4300), C. Quick-DNA Fungal/Bacterial Miniprep Kit (D6005), and D. Quick-DNA Plant/Seed Miniprep Kit (D6020)) and against a standard, needle-optimized CTAB protocol using both symptomatic and asymptomatic loblolly pine needles as starting material. *L. acicola* cultures provided source material for two extraction kits focused on fungal DNA (A. Zymo YeaStar Genomic DNA Kit and C. Quick-DNA Fungal/Bacterial Miniprep Kit). Fungal culture and infected needle samples each had two biological replicates, where each replicate consisted of tissue from the same independent site and or independently grown culture plate. Each infected needle sample And ran one additional validation batch to verify that the best-performing method is reproducible and robust.

Each extract was assessed under six amplification conditions: gITS7 + ITS4, fITS7 + ITS4, 5.8S-Fun + ITS4-Fun, gITS7 + ITS4 + PNA, fITS7 + ITS4 + PNA, and 5.8S-Fun + ITS4-Fun + PNA. This design allowed independent evaluation of extraction chemistry, primer specificity, and the effect of host-blocking treatment. The order of samples and extraction kits was randomized to minimize systematic bias associated with processing order. All samples received an input 50mg of biomass and an elution volume of 50 µl to ensure uniformity of all yield in fungal DNA copies per mg tissue. Mechanical disruption of starting biomass will be standardized using Precellys Evolution Touch Homogenizer at fixed setting for all methods except Zymo's Yeastar Genomic DNA Kit which does not call for tissue lysis. Lastly, all samples are RNase treated to reduce viscosity and improve

quantification ability. Any protocol modifications were documented, and their effects on performance were assessed.

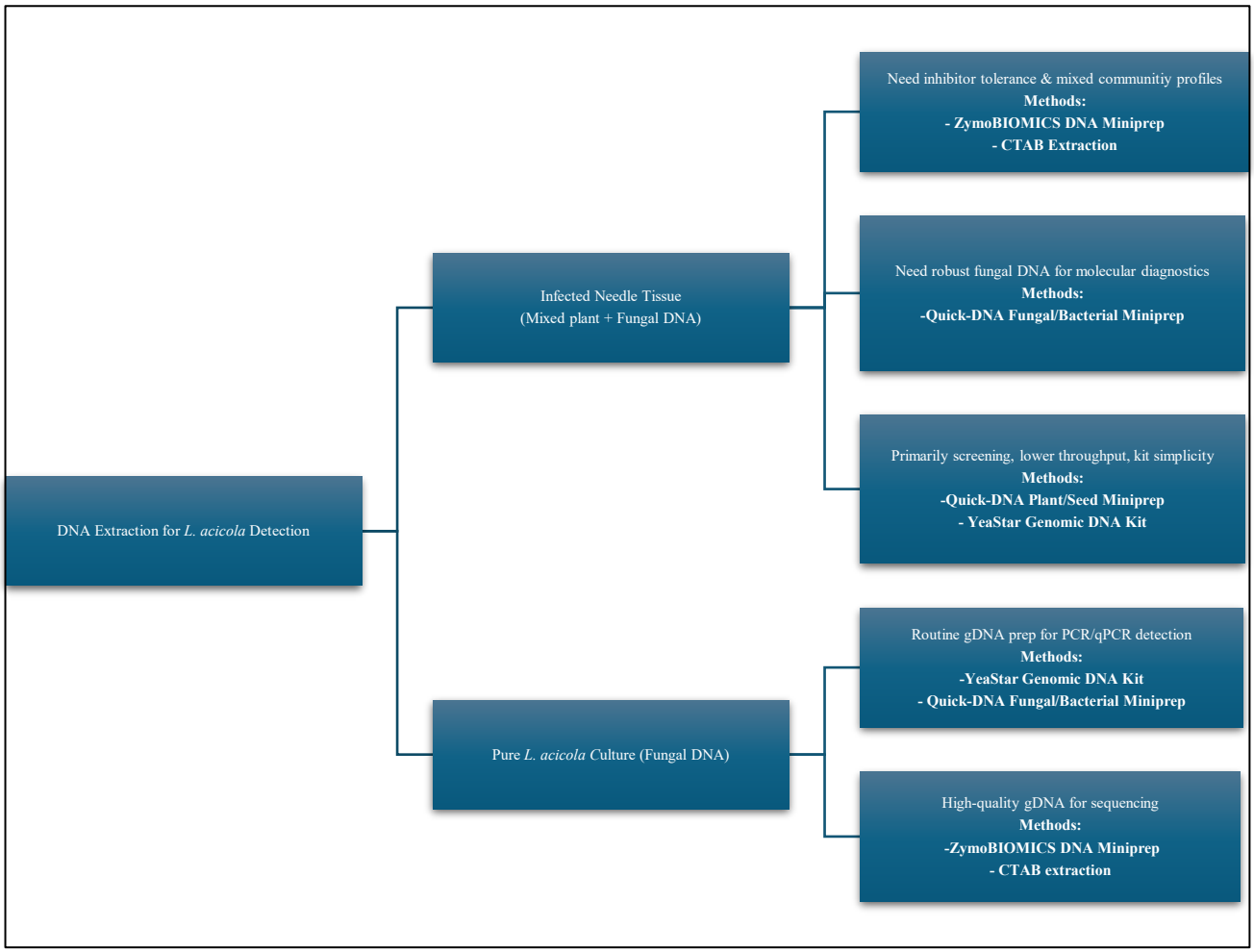

Figure 2.2 Decision tree summarizing conditions under which each DNA extraction method (ZymoBIOMICS, Quick-DNA Fungal/Bacterial, YeaStar, Quick-DNA Plant/Seed, CTAB) is preferred for recovering Lecanosticta acicola DNA from infected needles or pure cultures

2.3.2 DNA Extraction Workflows

Genomic DNA extractions using the Zymo YeaStar Genomic DNA Kit were performed according to the manufacturer's instructions, using 50 mg of loblolly pine needle or *L. acicola* fungal tissue as input with a final elution volume of 50 µl using nuclease-free water. For infected needle tissue, two alternative sample preparation methods were evaluated. In the first method (“wash-shed” treatment), approximately 50

mg of infected needle segments were incubated in 400 µl nuclease-free water for 5 minutes at room temperature and intensely vortexed for 5 minutes with 1-minute rests every minute. This wash was repeated once, and 200 µl of the resulting suspension was used as biological input for each extraction and extraction replicate. In the second method (“bead-bashing treatment), each of the 50 mg of infected needle tissue samples were placed in 2 mL bashing-bead tube containing 0.1 and 0.5 mm beads and 750 µl water to be mechanically disrupted prior to extraction. 200 µl of this suspension from each respective sample was used as input for extraction. For this kit, a total of seven needle samples and three fungal samples were processed. An additional DNA wash step, using the kit’s provided wash buffer, was included before elution to improve removal of residual carryover and salt contaminants.

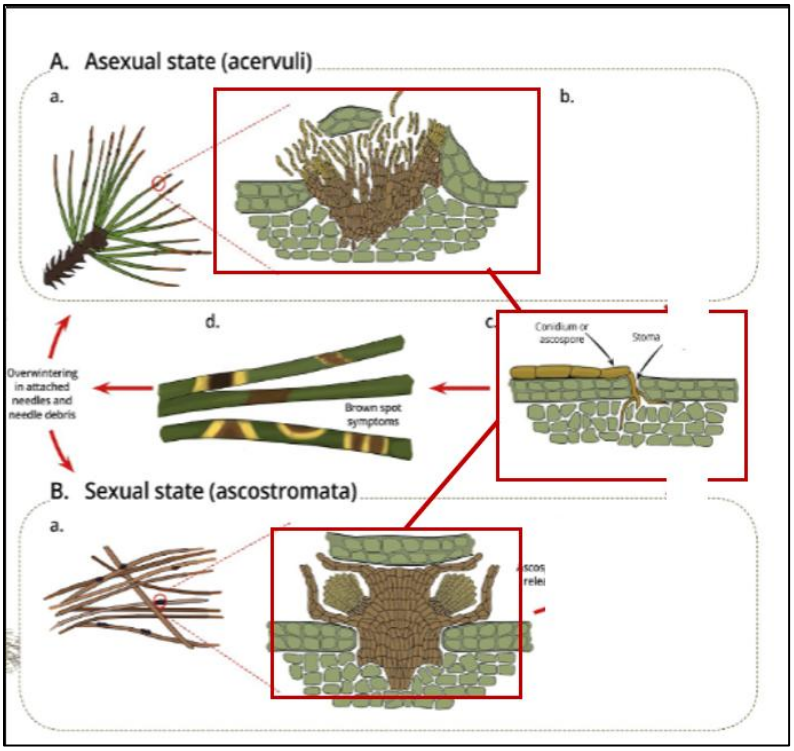

Figure 2.3 . Life cycle of Lecanosticta acicola on pine needles, showing asexual acervuli and sexual ascostromata developing on needle surfaces, spore release through stomata, and overwintering on infected needle debris. Adapted from van der Nest et al. (2019).

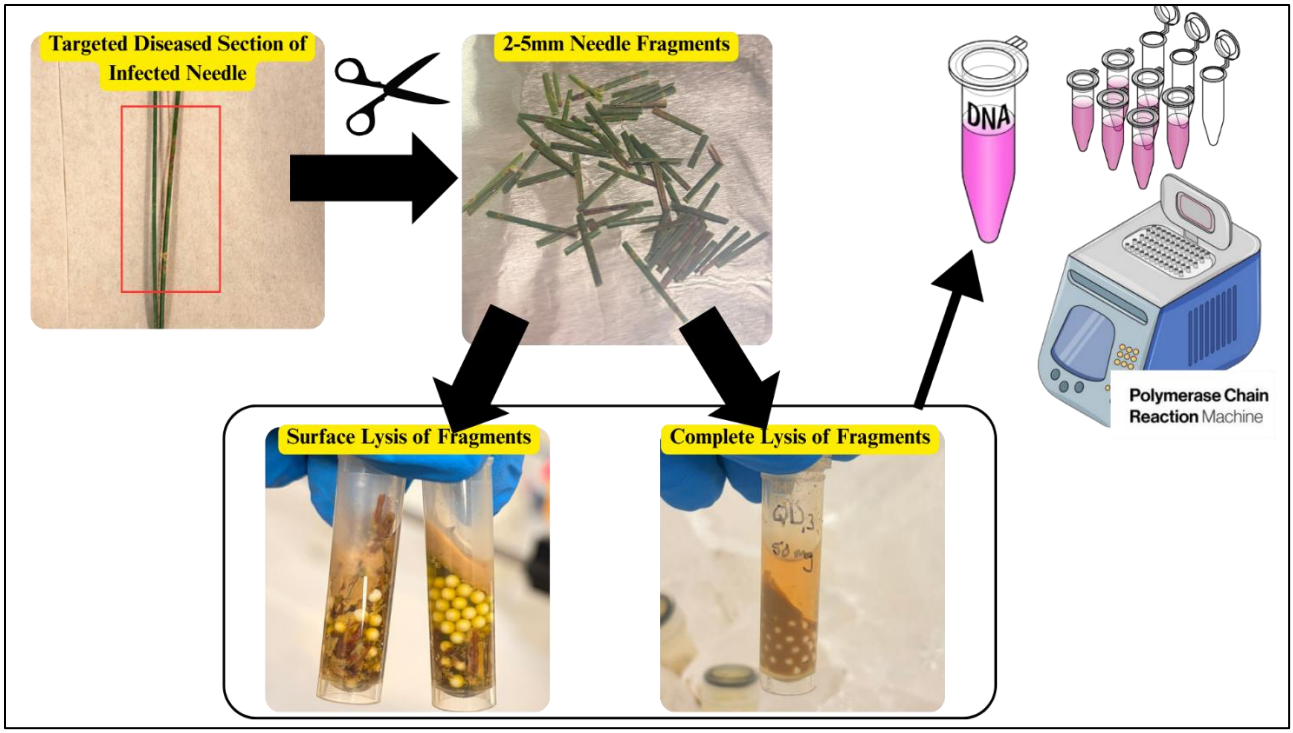

Figure 2.4 Sample preparation workflow for DNA extraction from Lecanosticta acicola-infected loblolly pine (*Pinus taeda*) needles**.** Visually symptomatic needle sections were targeted and excised into 2–5 mm fragments to concentrate diseased tissue prior to lysis. Fragments were then subjected to either surface lysis, in which bead-beating disrupts the outer needle surface while preserving the structural integrity of the tissue, or complete lysis, in which full mechanical homogenization is performed via bead-beating to fully disrupt needle tissue. Both approaches were evaluated to determine the effect of lysis intensity on DNA yield, purity, and the efficiency of downstream PCR amplification

Extractions using the Quick-DNA Fungal/Bacterial Miniprep Kit were executed according to the manufacturer's instructions using the same standardized tissue input and elution volume as described above. Sample preparation of needles followed the same wash-shed and bashing-bead procedure described for Zymo YeaStar Genomic DNA Kit.

A total of seven needle samples and three fungal samples were processed using this kit, and additional DNA wash step was included prior to elution.

Extractions performed using the ZymoBIOMICS DNA Miniprep Kit were completed as per the provided protocol with the standardized tissue input and elution volume described above. A total of four needle samples were processed with this kit. All samples underwent mechanical disruption in supplied bead-beating tubes, with the bashing bead lysis step repeated three times for each sample to maximize tissue disruption, based on preliminary observations that a single cycle did not provide adequate lysis. Lastly, an additional wash step was performed prior to elution.

Genomic DNA extracted with the Quick-DNA Plant/Seed Miniprep Kit was completed using the supplier's protocol using the standardized tissue input and elution volume as described above. A total of four samples were processed using this protocol, with an additional DNA wash step performed prior to elution.

The genomic DNA extracted from infected needle tissue using a fungal CTAB extraction method (Carter-House et al. 2020 Oct 26). Needle tissue was homogenized using liquid nitrogen, and 100 mg of ground tissue was used as input for each extraction. The CTAB lysis buffer formulation differed from the original protocol and was prepared from 2 g CTAB, 1 mL 1 M Tris-HCl (pH 8.0), 0.4 mL 0.5 M EDTA (pH 8.0), 2.8 mL 5 M NaCl, and 20 µL β-mercaptoethanol, brought to 100 mL with nuclease-free water. To each sample, CTAB lysis buffer (1,560 µl), 1% PVP (175 µl), and Proteinase K (10 µl) were added. Samples were treated with Phenol: Chloroform: Isoamyl alcohol (25:24:1, PCI), Chloroform: Isoamyl alcohol (24:1, CI), and washed with 70% ethanol. Precipitated DNA was then eluted in 50 µL of prewarmed nuclease-free water.

2.3.3 DNA Purification, Quantification, and Quality Assessment

To purify genomic DNA for downstream applications, DNA clean-up kits were utilized. Fungal gDNA extracted from infected needle tissue was purified with the OneStep PCR Inhibitor Removal Kit from Zymo Research following the manufacturer's protocol, to remove pine needle derived secondary metabolites that inhibit enzymatic reactions such as PCR. Genomic DNA extracted from *L. acicola* fungal tissue was purified using DNA Clean & Concentrator-5 (Zymo Research) following the protocol as supplied. All samples were eluted to the standardized volume of 50 µL using prewarmed nuclease-free water.

DNA concentration and purity were assessed before and after purification using a NanoDrop Ultra spectrophotometer from Thermo Fisher Scientific. Concentrations were recorded in ng/µL, and purity was evaluated using A260/280 and A260/230 absorbance ratios. Samples with A260/280 ratios between 1.8 and 2.0 and A260/230 ratios between 2.0 and 2.2 were considered to have acceptable purity for downstream applications (Matlock 2015). Samples meeting these criteria after extraction did not undergo additional purification.

All DNA samples were subjected to PCR to evaluate amplification performance regardless of initial purity ratios. However, only gDNA that met the defined purity criteria after extraction and, if needed, purification was used for amplicon sequencing and CRISPR-Cas9 detection assays.

2.3.4 ITS2-Targeted qPCR Primers and PNA Clamp

To further assess the relative amount of fungal versus plant DNA recovered from different extraction methods, ITS-2 targeted qPCR assays were performed with three fungi-specific primer combinations and a peptide nucleic acid (PNA) clamp. Primer sets included the fITS7/ITS4 pair, 5.8S-Fun/ITS4-Fun pair, and the more universal gITS/ITS4 pair that amplifies fungi and plants. Primer selection was based upon the published evaluations of ITS2 primers in Viotti et al. 2024. According to a recent systematic comparison, the approximate amplicon size is about 292 bp for fITS7/ITS4 and gITS7/ITS4 and about 440 bp for 5.8S-Fun/ITS4-Fun (Ihrmark et al., 2012; Taylor et al., 2016; Viotti et al., 2024). A PNA clamp that targets sequences unique to plants was used to enhance detection of fungal ITS2 signal by suppression of plant DNA amplification.

For each sample, qPCR reaction were set up in 20 µL containing 10 µL Luna Universal qPCR Master Mix (New England Biolabs, Ipswich, MA, USA), 0.5 µL of each primer, and a standardized amount of template DNA at 5 ng across samples. Each extract was run with all primer combinations with and without PNA clamp. The PNA sequence targeted conserved plant rDNA and was added at the manufacturer recommended concentration; PNA-assisted reactions included an elevated temperature clamp step prior to primer annealing. These qPCR assays were used to quantify the relative contribution of fungal DNA to plant DNA and evaluate the influence of PNA clamping on community composition.

Table 2.1 ITS2-targeted qPCR primer sets used in Chapter 2.

Target Locus	Primer Pair	Forward Primer	Reverse Primer	Amplicon (bp)	Assay Type	Purpose
ITS2	fITS7 / ITS4	fITS7	ITS4	292	ITS2 qPCR	Fungal-biased ITS2 amplification from mixed needle DNA
ITS2	gITS7 / ITS4	gITS7	ITS4	292	ITS2 qPCR	Broad ITS2 assay (fungi + plant) used as reference signal
ITS2	5.8S-Fun / ITS4-Fun	5.8S-Fun	ITS4-Fun	440	ITS2 qPCR	More selective fungal ITS2 assay; used with or without PNA clamp

2.3.5 Statistical Analysis

All statical analyses were performed in R version 4.3.2 (R Core Team, Vienna, Austria) and Excel and were considered significant at $P < 0.05$. gDNA concentrations (ng/μL) and purity ratios (A260/280 and A260/230) were summarized as mean ± standard deviation for each extraction kit used and tissue type. Kruskal-Wallis tests were used to evaluate the differences in yield and purity across extractions kits and tissue type, with commercial kits and tissue type categorized as fixed effects (Desneux and Pourcher 2014). When global tests were significant, post hoc pairwise comparisons among commercial kits were produced using Dunn's test for post hoc comparisons.

Within each extraction workflow, the broad gITS7 + ITS4 condition was normalized to 1.0 and used as the reference amplification signal. All other primer and primer+PNA conditions were expressed relative to that reference. This made it possible to compare

how strongly each extraction method retained amplifiable signal when the assay shifted from broad amplification to more selective fungal-oriented conditions. Fungal and plant outputs were also summarized as relative proportions in a stacked comparison across extraction methods. This second analysis was critical because the central question of the study was not simply which method produced the strongest signal, but which method yielded the best balance between fungal DNA recovery and plant DNA exclusion.

2.4 Results

2.4.1 Comparison of DNA Yield and Purity

To test the efficiency of DNA extraction method, DNA concentration and spectrophotometric purity were assessed for all kits and tissue types. Fungal gDNA extractions from infected needle tissue generally yielded lower DNA concentrations and poorer A260/230 ratios than fungal extractions, whereas ZymoBIOMICS Plant produced the highest yields from needle tissue and Quick-DNA Fungal generated the highest yields from fungal tissue. Across infected needle samples, ZymoBIOMICS Plant had the highest mean yield (62.9 ng ng/µL ± 36.7 SD), followed by Quick-DNA Fungal (9.8 ng/µL ± 19.7 SD), YeaStar (3.4 ng/µL ± 2.5 SD), CTAB (3.6 ng/µL ± 2.8 SD), and Quick-DNA Plant (2.0 ng/µL ± 0.8 SD). Fungal extractions showed strong kit-dependent differences in yield, with Quick-DNA Fungal having a mean of 120.4 ng/µL ± 14.9 SD compared to 53.0 ng/µL ± 15.5 SD for YeaStar. These patterns are summarized below in Table 2.2.

Spectrophotometric purity ratios also varied by kit and tissue type. For infected needle tissue, mean A260/280 ratios ranged from suboptimal values for YeaStar (0.99 ±

0.15) to near-ideal means for Quick-DNA Plant (1.84 ± 0.29), Quick-DNA Fungal/Bacterial (1.79 ± 0.79), ZymoBIOMICS Plant (1.72 ± 0.21), and intermediate purity for CTAB (1.36 ± 0.16). As anticipated, A260/230 ratios for infected needle tissue were low across all extraction kits (all means ≤ 0.41), except ZymoBIOMICS Plant where it exhibited higher and more variable A260/230 values (mean 1.38 ± 0.82). Healthy needle tissue extractions were used as a comparative baseline for purity ratios. In fungal culture extractions, Quick-DNA Fungal/Bacterial reached substantially higher A260/230 ratios (mean 1.71 ± 0.19) than YeaStar (0.95 ± 0.12).

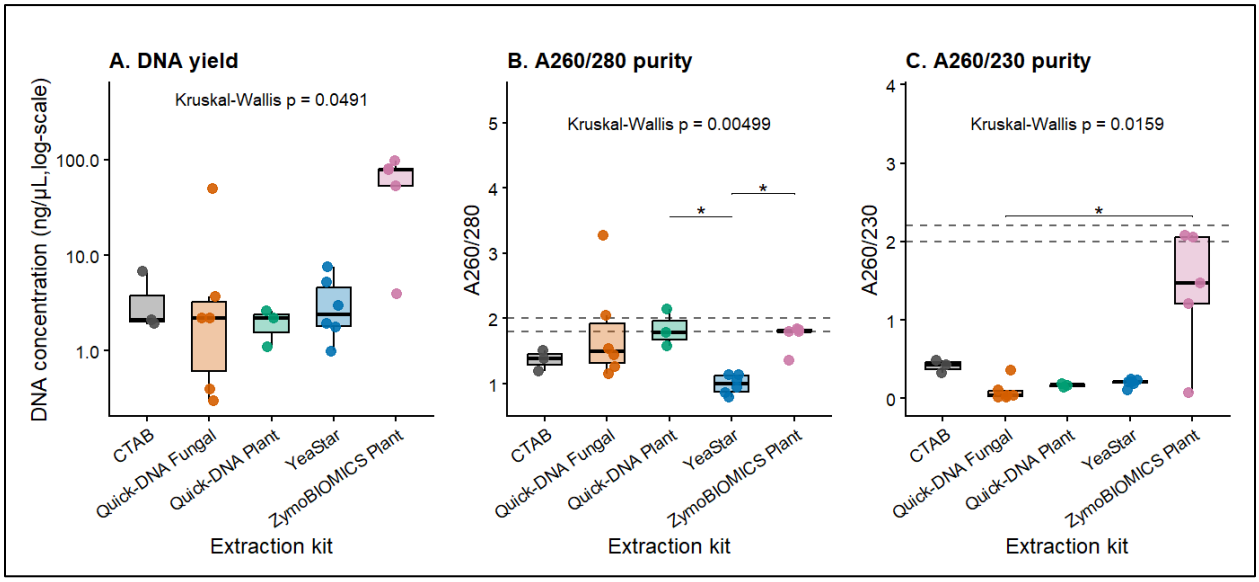

Figure 2.4. Extraction kit performance for infected needle tissue. (A) DNA concentration (ng/µL, log scale), (B) A260/280, and (C) A260/230 for infected needle samples extracted with each kit. Points represent individual biological replicates; boxes show the mean average for each kit; dashed lines indicate acceptable purity ratio ranges.

Fungal DNA recovery differed significantly among kits for infected needle tissue (Kruskal-Wallis H=9.53, df = 4, p = 0.049), leading with ZymoBIOMICS Plant showing the

highest mean concentration (62.9 ± 36.7 ng/μL), followed by Quick-DNA Fungal bead-bashing (2.7 ± 0.9 ng/μL), YeaStar bead-bashing (4.6 ± 3.3 ng/μL), CTAB (3.6 ± 2.8 ng/μL), and Quick-DNA Plant (2.0 ± 0.8 ng/μL; Figure 2.4, Panel A). Additionally, spectrophotometric purity differed significantly across fungal DNA recovery from infected needle extraction procedures, both for A260/280 ($H = 14.86$, $df = 4$, $p = 0.005$) and A260/230 ($H = 12.20$, $df = 4$, $p = 0.016$; Figure 2.4, Panels B–C). Dunn's post hoc tests showed that ZymoBIOMICS Plant had significantly higher A260/230 values than Quick-DNA Fungal on infected needles tissue (Bonferroni-adjusted $p = 0.021$). For yield from infected tissue, the global test was significant but no individual pairwise comparison remained significant after Bonferroni correction. In contrast, healthy needle samples showed no significant differences among kits for yield or purity ratios ($p = 0.302$), indicating that extraction kit effects were most pronounced in infected tissue. Together, these results confirm that kit choice is meaningful for gDNA extraction from infected pine needles and that ZymoBIOMICS Plant stands out in absolute yield and A260/230 purity from this tissue type.

For fungal tissue, Quick-DNA Fungal and YeaStar were compared, and Kruskal-Wallis tests indicated significant differences between the two in yield and both purity metrics ($H = 3.86$, $df = 1$, $p \approx 0.050$). Quick-DNA Fungal provided both higher yields and A260/230 ratios than YeaStar. Together these results show that kit choice is substantially influential on both yield and purity metrics, with ZymoBIOMICS Plant excelling in yield on infected needles and Quick-DNA Fungal performing best overall on fungal cultures.

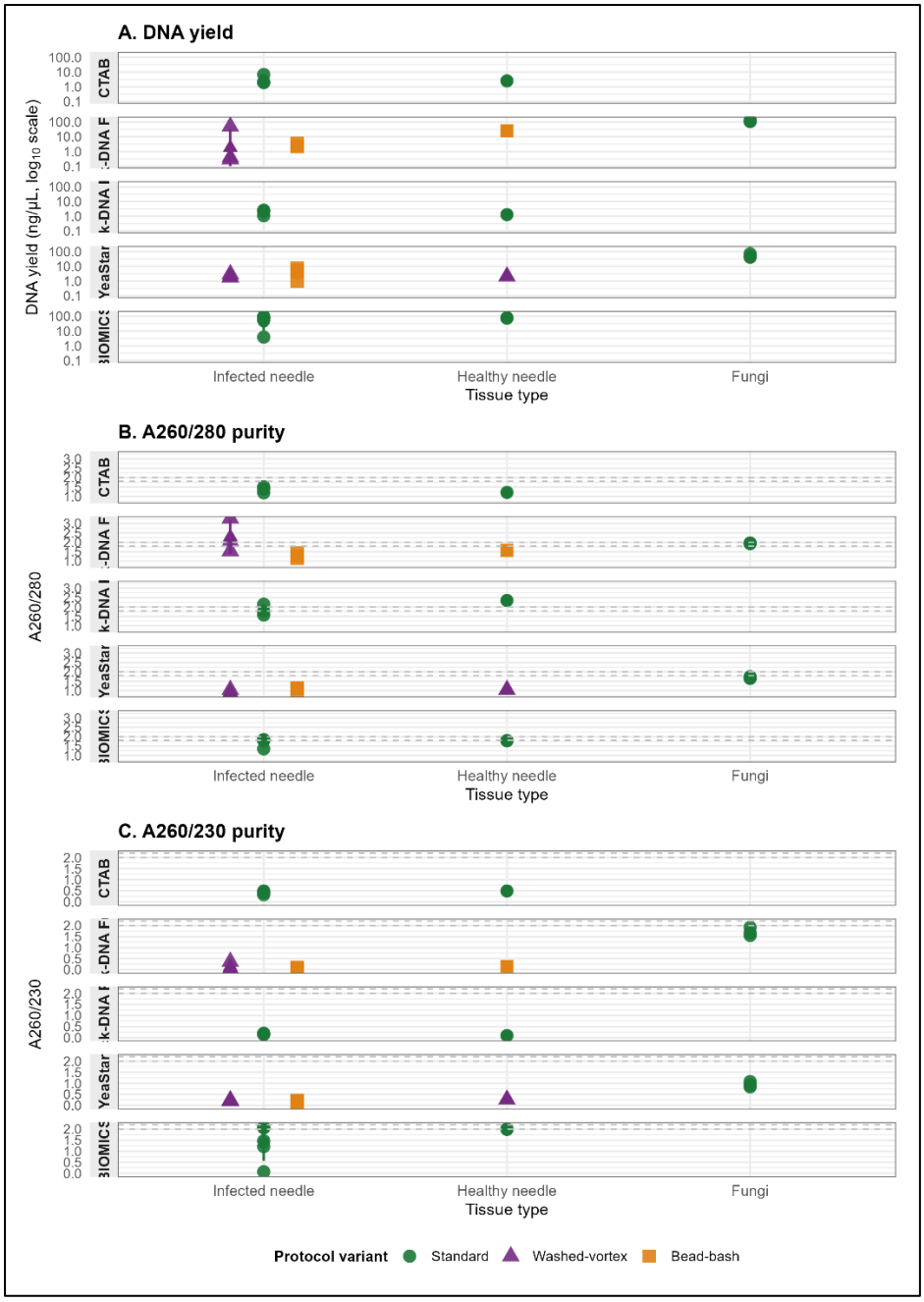

Figure 2.5 Tissue- and protocol-level extraction performance within each DNA extraction kit. For each kit (rows), DNA yield (A; ng/µL on a log1010 scale), A260/280 purity ratio (B), and A260/230 purity ratio (C) are shown for three tissue types: brown spot needle blight–infected needles, healthy needles, and L. acicola fungal cultures. Points represent individual replicates and are colored and shaped by protocol variant (Standard,

Washed-vortex, Bead-bash), with mean ± SD overlaid for each kit × tissue × protocol combination. Dashed lines in panels B and C indicate commonly used purity targets (A260/280 ≈ 1.8–2.0; A260/230 ≈ 2.0–2.2). Because most subgroups have n = 1–3 replicates, these results are descriptive and were not subjected to formal within-panel hypothesis testing.

2.4.2 ITS-2 Primers and PNA Clamp Effects Across Extraction Methods

Across all extraction workflows, the same first-order pattern was observed: the broad primer pair gITS7 + ITS4 consistently produced the highest normalized signal and served as the 1.0 reference condition (Figure 2.5-2.10). Every fungi-focused primer set and every PNA-assisted condition yielded a lower total relative signal than this broad reference. Showing that, regardless of extraction method, the broad assay recovered the largest pool of amplifiable ITS templates.

However, this overall result should not be misread as proof that gITS7 + ITS4 is the best condition for fungal DNA extraction. In the present experiment, total signal and fungal selectivity were clearly not the same thing. The broad primer pair most likely produced the largest signal partly because it tolerated plant co-amplification, whereas the more selective primer systems and PNA-supported reactions deliberately narrowed the target space. Therefore, the key question sought to answer which extraction method preserved the most useful signal after the system became more selective. A second broad result was that extraction workflows differed greatly in how much signal they retained after leaving the broad reference condition. Based on the plotted values, the average retention of the five nonreference conditions was approximately 0.72 for YeaStar, 0.54 for Quick-DNA Plant, 0.35 for Quick-DNA Fungal, 0.18 for ZymoBIOMICS, and only

0.10 for CTAB. In other words, YeaStar was the most stable method across changing primer strategies, whereas CTAB was by far the least stable (Figure 1-6).

A) Quick-DNA Fungal

Under the Quick-DNA Plant workflow, the broad gITS7 + ITS4 condition was again the strongest, but the decline in signal under alternative primer conditions was moderate rather than catastrophic. The fITS7 + ITS4 and gITS7 + ITS4 + PNA conditions retained approximately 0.39 and 0.42 of the reference signals, making them the best-performing nonreference options in this workflow. The 5.8S-Fun + ITS4-Fun condition fell to roughly 0.33, while the two more selective PNA-assisted fungal-oriented conditions were lower still, around 0.29 to 0.30.

This pattern suggests three things (Figure 2). First, the Quick-DNA Fungal extraction was compatible with selective amplification, because alternative primer conditions still yielded measurable signal rather than collapsing completely. Second, the method appeared especially tolerant of fITS7 + ITS4 and gITS7 + ITS4 + PNA, indicating that the extract remained amplifiable even when conditions became more restrictive. Third, the drop seen with 5.8S-Fun-based conditions shows that the fungal-focused assays exacted a clear signal cost, which is important if pathogen biomass in the infected tissue was already low.

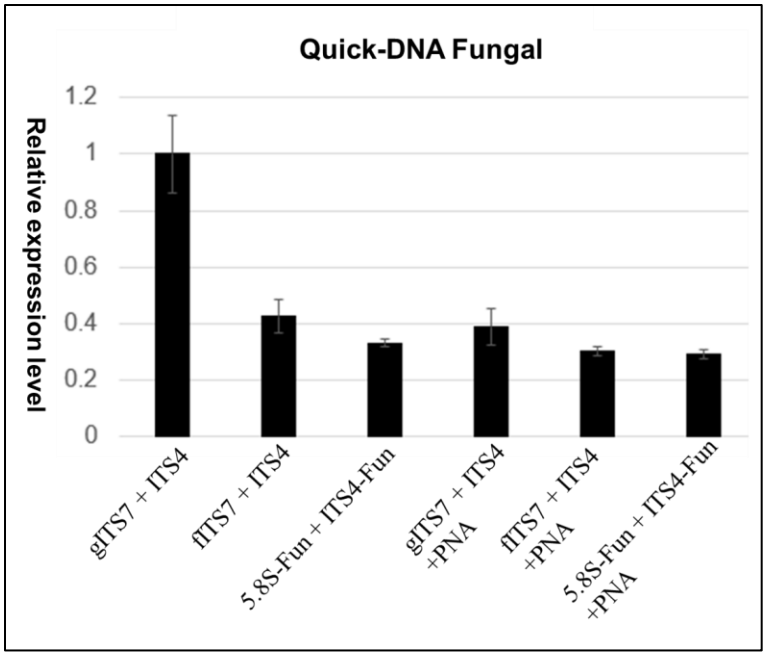

Figure 2.5 Relative total amplified DNA yield across primer combinations using the Quick-DNA Fungal extraction kit. The combined plant and fungal DNA signal amplified with gITS7 + ITS4 was set to 1 and used as the normalization reference. Bars represent the relative total amplified DNA levels obtained with the other primer combinations compared with this reference, and error bars indicate variability among replicates.

The stacked fungal-versus-plant comparison adds a second layer of interpretation. Quick-DNA Fungal produced a fungal fraction of about 0.46 and a plant fraction of about 0.54. This was not the best fungal enrichment overall, but it was clearly one of the stronger methods. When interpreted together with the moderate retention of nonreference signal, this indicates that Quick-DNA Fungal offered a good compromise between maintaining amplifiable DNA and preferentially recovering fungal representation. In practical terms, it behaved like a credible fungal-enrichment method for mixed infected needles, even though it did not reach the fungal dominance observed with YeaStar (Figure 4).

B) Quick-DNA Plant

Quick-DNA Plant gave a noticeably different response profile (Figure 3). Although the broad gITS7 + ITS4 condition still ranked first, the alternative primer sets retained relatively strong signal compared with most other methods. The fITS7 + ITS4 condition remained high at about 0.66, and gITS7 + ITS4 + PNA was also relatively robust at about 0.60. Even the more restrictive 5.8S-Fun-based conditions remained around 0.45 to 0.51. In simple amplification terms, this method was considerably more stable than Quick-DNA Fungal, ZymoBIOMICS, or CTAB. At first glance, those values might seem to identify Quick-DNA Plant as a top-performing extraction. However, the fungal-versus-plant summary revealed the weakness of this interpretation. Only about 0.29 of the recovered signals was fungal, whereas 0.71 remained plant- derived. Thus, Quick-DNA Plant preserved signal well, but much of that preserved signal appears to have been host-associated rather than pathogen-enriched.

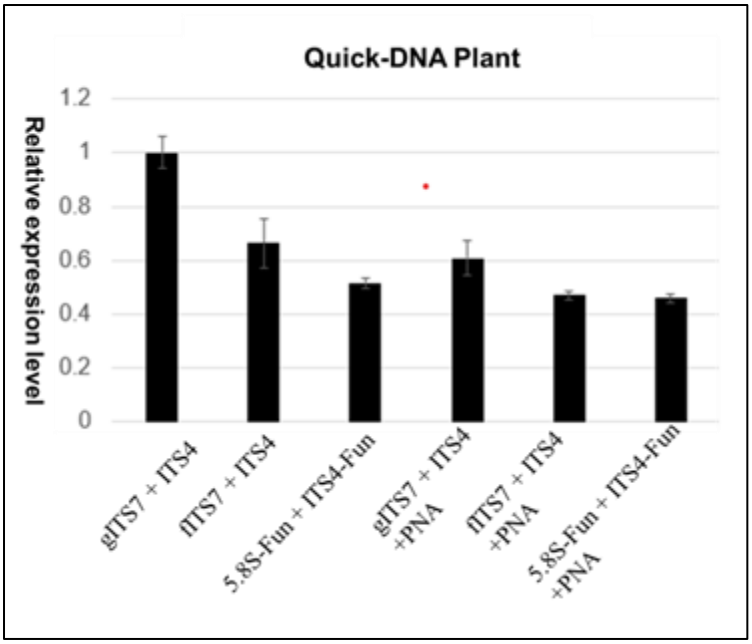

Figure 2.6 Relative total amplified DNA yield across primer combinations using the Quick-DNA Plant extraction kit. The combined plant and fungal DNA signal amplified with gITS7 + ITS4 was set to 1 and used as the normalization reference. Bars represent the relative total amplified DNA levels obtained with the other primer combinations compared with this reference, and error bars indicate variability among replicates

This distinction is one of the most important outcomes of the experiment. Quick-DNA Plant performed relatively well if judged only by how much amplification remained under alternative primer systems. But when the biological goal shifted from “strong PCR” to “high fungal selectivity,” its ranking dropped substantially. In other words, this workflow was good at extracting DNA from infected needles, but less good at shifting the mixture toward *L. acicola*. For the purpose of fungal enrichment, that makes it clearly inferior to YeaStar and weaker than Quick-DNA Fungal.

C) ZymoBIOMICS

The ZymoBIOMICS workflow showed one of the strongest penalties when the assay moved away from the broad reference condition (Figure 3). After normalization to gITS7 + ITS4 = 1.0, the other five bars clustered at low values. The fITS7 + ITS4 and gITS7 + ITS4 + PNA conditions were both around 0.23, while 5.8S-Fun + ITS4-Fun, fITS7 + ITS4 + PNA, and 5.8S-Fun + ITS4-Fun + PNA fell further to approximately 0.14 to 0.16.

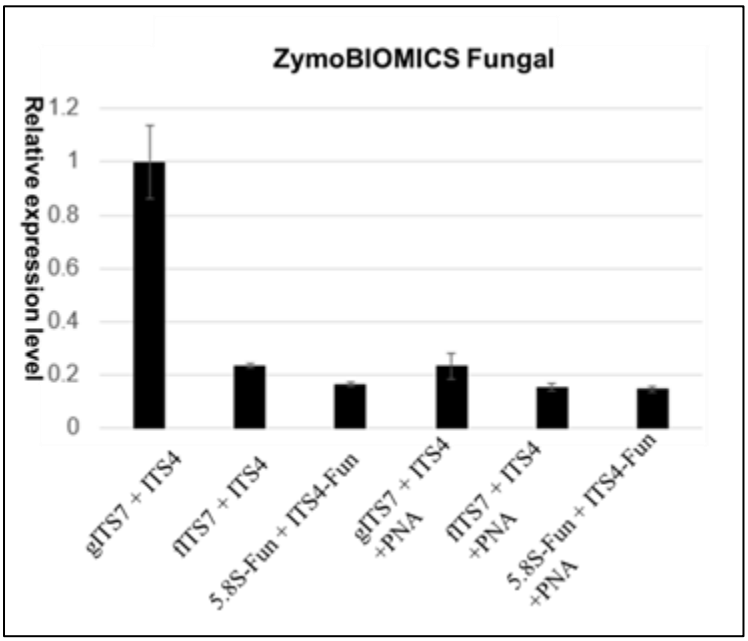

Figure 2.7 Relative total amplified DNA yield across primer combinations using the ZymoBIOMICS kit. The combined plant and fungal DNA signal amplified with gITS7 + ITS4 was set to 1 and used as the normalization reference. Bars represent the relative total amplified DNA levels obtained with the other primer combinations compared with this reference, and error bars indicate variability among replicates

This profile indicates that ZymoBIOMICS was highly dependent on the broadest primer condition and lost much of its usable signal under more selective assays. That is an important result because the earlier extraction-yield summary suggested that high-

yield workflows could appear attractive in infected-needle tissue. The present amplification results show that whatever advantage the workflow may have had in total DNA recovery did not translate into strong selective fungal detection. The stacked comparison confirms this interpretation. ZymoBIOMICS contained only about 0.15 fungal DNA and about 0.85 plant DNA. That is a strongly plant-dominated output, and it places this workflow among the weaker options for the central goal of fungal enrichment. The result therefore argues against using total DNA yield as the sole criterion for method selection in infected pine needles. A method can recover plenty of amplifiable DNA and still perform poorly for pathogen-focused molecular work if that DNA is dominated by host background.

D) YeaStar

YeaStar showed the most even and most favorable amplification profile of all tested methods (Figure 4). Although gITS7 + ITS4, again, remained the strongest condition, the nonreference bars stayed much closer to the reference than in any other workflow. The values were approximately 0.83 (fITS7 + ITS4), 0.77 (5.8S-Fun + ITS4-Fun), 0.75 (gITS7 + ITS4 + PNA), 0.64 (fITS7 + ITS4 + PNA), and 0.60 (5.8S-Fun + ITS4-Fun + PNA).

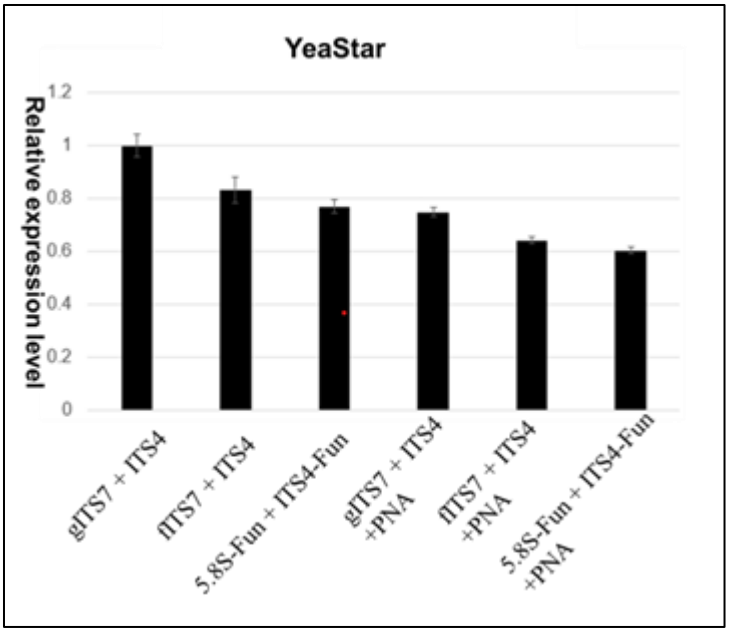

Figure 2.8 Relative total amplified DNA yield across primer combinations using the YeaStar kit. The combined plant and fungal DNA signal amplified with gITS7 + ITS4 was set to 1 and used as the normalization reference. Bars represent the relative total amplified DNA levels obtained with the other primer combinations compared with this reference, and error bars indicate variability among replicates

YeaStar retained amplification power even when the assay became more selective, which means the extraction produced DNA that was amplifiable and remained useful under more stringent fungal-oriented conditions. Second, the lowest YeaStar value was still about 0.60, which exceeded nearly all nonreference values observed for the other extraction methods. Third, the method appears to have buffered the trade-off between selectivity and total signal better than any other workflow in the dataset.

This strong performance was reinforced by the fungal-versus-plant summary, where YeaStar showed the highest fungal fraction overall, approximately 0.60 fungal and 0.40 plant. This means that YeaStar was the only tested workflow in which fungal DNA

clearly exceeded plant DNA in the final stacked comparison. Expressed as a fungal: plant DNA ratio, this corresponds to roughly 1.5, far above Quick-DNA Fungal (~0.85), Quick-DNA Plant (~0.41), ZymoBIOMICS (~0.18), and CTAB (~0.11). Thus, YeaStar did not merely maintain amplification across primer systems; it also produced the strongest net fungal enrichment. This result shows that the best-performing method for fungal enrichment was not the method expected to dominate based solely on raw plant-tissue DNA yield. Instead, YeaStar seems to have shifted the extract composition in a way that favored fungal recovery relative to the host. For the present experiment, that makes YeaStar the strongest extraction workflow overall.

E) CTAB

CTAB showed the weakest performance in the dataset. As with the other methods (Figure 5), gITS7 + ITS4 was normalized to about 1.0. But all five alternative conditions collapsed to extremely low values, approximately 0.09 to 0.11. Unlike the other extraction methods, CTAB did not show a meaningful separation among fungi-focused primers or PNA-assisted conditions; once the system left the broad mixed-template assay, the signal remained uniformly poor.

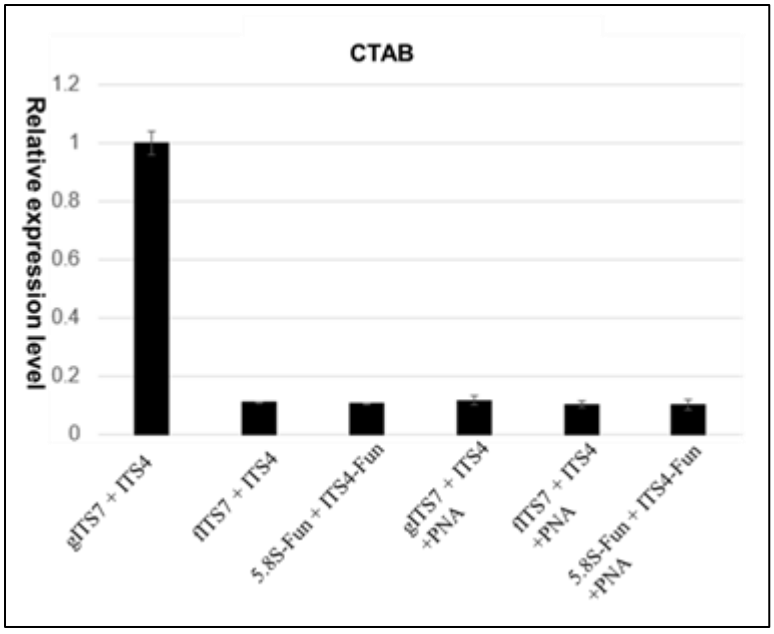

Figure 2.9 Relative total amplified DNA yield across primer combinations using the CTAB extraction method. The combined plant and fungal DNA signal amplified with gITS7 + ITS4 was set to 1 and used as the normalization reference. Bars represent the relative total amplified DNA levels obtained with the other primer combinations compared with this reference, and error bars indicate variability among replicates

The stacked proportion plot agreed completely with this conclusion. CTAB yielded only about 0.10 fungal DNA and about 0.90 plant DNA, making it the most plant-dominated and least favorable workflow for fungal enrichment. Therefore, while CTAB remains an important historical benchmark for difficult plant tissues, it was not competitive here as a practical default method for BSNB-infected needles.

The stacked comparison in Figure 6 provided the clearest answer to the biological question of the study. Ranked from best to worst by fungal proportion, the methods were YeaStar (~0.60 fungal), Quick-DNA Fungal (~0.46), Quick-DNA Plant (~0.29),

ZymoBIOMICS (~0.15), and CTAB (~0.10). This ranking differed from what might have been concluded from total amplification alone.

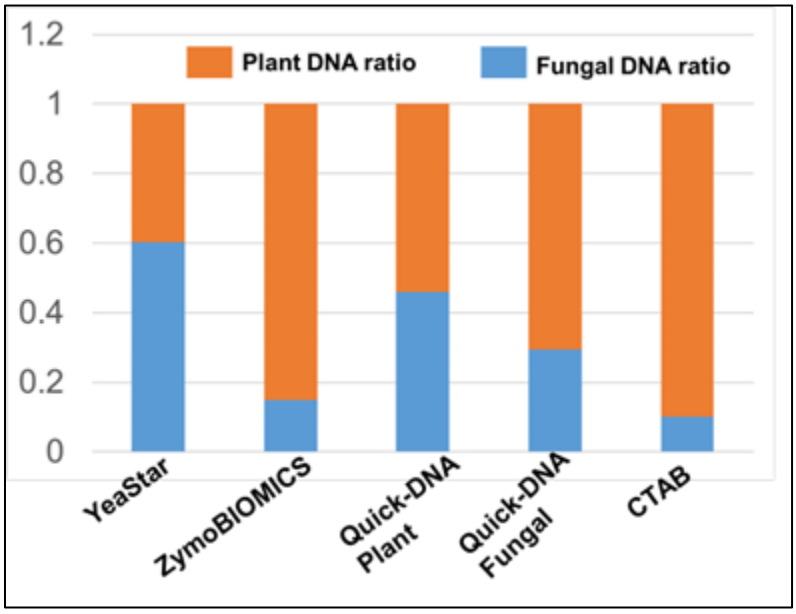

Figure 2.10 Comparison of plant and fungal DNA composition among DNA extraction methods. The stacked bar chart presents the relative fractions of plant DNA and fungal DNA recovered under each extraction condition. Within each treatment, plant and fungal DNA ratios sum to 1, allowing direct comparison of host-versus-fungal DNA balance across methods.

The contrast between YeaStar and Quick-DNA Plant is especially revealing. Quick-DNA Plant retained more signal than Quick-DNA Fungal across the alternative primer conditions, but its fungal fraction was much lower. YeaStar, by contrast, paired the best fungal proportions with the most stable nonreference amplification profile. This shows that the crucial factor of a successful extraction method in mixed infected needles is high DNA recovery, along with high recovery of the correct fraction of the mixture. The comparison also showed that the experiment separated two related but distinct properties

of performance: signal robustness and fungal selectivity. YeaStar was strong in both. Quick-DNA Plant was strong mainly in signal robustness. Quick-DNA Fungal was intermediate but clearly favorable for selectivity. ZymoBIOMICS and CTAB were weak for both outcomes. This separation is crucial to the interpretation of the dataset and strongly supports the original rationale for evaluating fungal-to-plant balance rather than total DNA concentration alone.

2.5 Discussion

“Because *L. acicola* produces acervuli and ascostromata on needle surfaces **(Figure 2.X)**, the wash-shed pre-treatment is expected to enrich surface propagules without full needle lysis…”

The concentration of secondary metabolites in host plant tissue can muddy DNA metrics and directly inhibit DNA polymerases during amplification, making otherwise high-yield extracts unsuitable for conventional PCR detection and downstream molecular assays (Porebski et al., 1997; Boesenberg-Smith et al., 2012; Matlock, 2015). This is especially true for conifers, where needles and woody tissues are rich in polyphenols, polysaccharides, and resins that co-precipitate with DNA and either reduce amplification efficiency or produce spurious melt curves and off-target products if they are not adequately removed (Kim et al., 1997; Sahu et al., 2012; Lucena-Aguilar et al., 2016). In the infected-needle yield and purity plots, these matrix effects are evident in the consistently depressed A260/230 values across most kits despite high DNA concentrations, underscoring that apparent high yield does not automatically translate

into diagnostically useful template (Figures 2.X–2.Y). The fact that even aggressive bead-beating and inhibitor-removal columns did not fully normalize A260/230 in infected needles highlights how chemically demanding BSNB lesions are as substrates compared with healthy needles and pure fungal cultures. For pathogens embedded within needle tissue, these matrix effects can be as limiting as assay sensitivity itself, so extraction choice becomes a central part of the diagnostic design rather than an interchangeable pre-analytical step (Boesenberg-Smith et al., 2012; Langsiri et al., 2025).

In addition to the inhibitory effects of secondary metabolites, fungal DNA recovery can be depressed simply because abundant host DNA overwhelms the pathogen template, rendering the pathogen undetectable or detectable only at exceedingly small apparent yields even when infection is present (Ioos et al., 2010; Desneux and Pourcher, 2014). This template masking is a realistic risk in BSNB because loblolly needles contain far more host biomass than fungal biomass, especially early in the disease when lesions are small. In this context, having an enriched fungal DNA yield from infected needle tissue is more valuable than a baseline fungal DNA yield. Extracts dominated by host DNA tend to raise the effective limit of detection and generate unreliable DNA metrics and distinction for assays designed for *L. acicola*. The results of this chapter support the central hypothesis that extraction performance should be assessed by fungal enrichment in mixed host–pathogen tissues particularly in loblolly pine needles where host DNA and inhibitors can easily dominate the extract. This distinction is visible when comparing the infected-needle yield figure with the stacked fungal to plant proportion figure: workflows that appear favorable based on concentration alone, such as ZymoBIOMICS, rank poorly

once fungal representation is taken into account, whereas YeaStar and Quick-DNA Fungal move to the top of the ranking despite only moderate yields (Figures 2.X and 2.Z).

Across all extraction workflows and amplification conditions, the most informative metric for BSNB in this study was the ratio of fungal to plant DNA recovered from infected loblolly needles. When methods were ranked by fungal proportion, YeaStar produced the highest fungal fraction (~0.60), followed by Quick-DNA Fungal (~0.46), whereas Quick-DNA Plant (~0.29), ZymoBIOMICS (~0.15), and CTAB (~0.10) remained strongly plant-dominated. This ranking differed from what would have been concluded from total amplification or spectrophotometric yield alone, which initially favored ZymoBIOMICS because of its high concentration and relatively strong A260/230 purity. The stacked comparison of fungal versus plant signal (Figure 2.Z) provides a compact visual summary of this ranking and makes clear that workflows differed more in selectivity than in gross amplification capacity. Importantly, the same figure also shows that even the best-performing methods did not completely eradicate host DNA, which is realistic for BSNB and supports the idea that the goal is not a pure fungal extract but a reproducible and favorable fungal: plant balance.

Kit-by-kit performance is also dependent on the kit chemistry and targeted DNA. Assessing the most successful assay in this study, YeaStar relies on yeast lytic enzymes optimized for fungal cell walls and includes gentle column cleanup, a combination that has been effective for fungal DNA recovery in other systems (Carter-House et al., 2020; Langsiri et al., 2025). In infected needles, this chemistry appears to lyse *L. acicola* effectively while leaving many pine cells under-lysed, particularly when the wash-shed

pre-treatment is used to enrich surface acervuli and ascostromata. The washed-needle workflow effectively skims pathogen structures from lesion surfaces before full mechanical homogenization, which reduces the amount of deep host tissue carried into the final extract while still capturing lesion-associated fungal biomass (Figure 2.2). As a result, even when bead-bashing introduces more host tissue into the extract, fungal DNA remains a large fraction of the total, and amplification remains robust across more selective ITS2 primer and PNA combinations. These trends are consistent with the infected-needle extraction figure, where YeaStar's DNA concentrations are moderate but its non-reference ITS2 response bars remain closer to the gITS7+ITS4 reference than any other kit, and with the fungal: plant stacked bars where YeaStar occupies the top position (Figures 2.X–2.Z). Comparatively, regarding extraction chemistry, Quick-DNA Fungal uses aggressive bead beating, a chaotropic lysis buffer, and β-mercaptoethanol to target tough microbial cell walls, similar to other workflows developed for metagenomic fungal DNA extraction (Desneux and Pourcher, 2014; Langsiri et al., 2025). This chemistry efficiently disrupts *L. acicola* tissue and spores but also brings substantial pine DNA into solution, especially when whole needle segments are homogenized. Subsequently, it showed an intermediate fungal fraction (~0.46) and moderate retention of non-reference signal. In practice, Quick-DNA Fungal behaves as a useful compromise because its more fungal-enriching chemistry but lesser selectivity than YeaStar. A difference that is especially visible under the most selective 5.8S-Fun + ITS4-Fun + PNA conditions where YeaStar retains slightly stronger normalized signal. In the ITS2 response plots, Quick-DNA Fungal's non-reference bars sit below those of YeaStar yet remain clearly higher than the corresponding bars for Quick-DNA Plant and

ZymoBIOMICS, reinforcing this intermediate position and suggesting that it is a credible runner up option when YeaStar is unavailable (Figure 2.Y).

Quick-DNA Plant is explicitly designed for plant tissues, combining large 2.0 mm beads, plant-tuned lysis buffer, and a PCR-inhibitor removal column to recover clean host DNA (Karakousis and Langridge, 2003). That design choice is reflected in the results: the workflow preserved signal well across alternative primer systems and produced some of the highest normalized amplification values under non-selective assays, but it yielded a strongly plant-dominated extract. This is apparent in the side-by-side comparison of extraction profiles, where Quick-DNA Plant shows high normalized signals across primer conditions but a low fungal fraction in the stacked bar figure (Figures 2.X and 2.Z). ZymoBIOMICS, a microbiome-oriented kit, produced high total yields and generally good purity from infected needles, yet performed poorly once assays became more selective. With repeated bead beating, this workflow appears to lyse substantial amounts of pine tissue alongside fungal structures, and the inhibitor-removal chemistry does little to preferentially favor fungal templates over plant templates (Desneux and Pourcher, 2014; Lucena-Aguilar et al., 2016). As a result, the apparent advantage of ZymoBIOMICS in the yield and A260/230 figures disappears when ITS2 signal is normalized and partitioned into fungal and plant fractions, where the method clusters near the lower end of the fungal-enrichment spectrum (Figures 2.X and 2.Z). CTAB, finally, provided broad plant lysis but poor selective recovery that despite acceptable yields, CTAB extracts supported only weak amplification under selective ITS2/PNA conditions and mainly plant-dominated in the stacked comparison (Carter-House et al., 2020). The amplification decline for these two workflows is captured in the non-reference bar plots, where normalized signals drop

sharply once the system moves away from gITS7+ITS4 toward more fungal-focused assays (Figure 2.Y). Together, these patterns reinforce that common extraction chemistries and microbiome-oriented kits are not automatically appropriate for conifer lesion diagnostics without explicit evaluation of fungal selectivity. For diagnostics, this informs that these kits are better suited to host genotyping or reference pine DNA work than to BSNB detection from lesion tissue, unless paired with strong downstream host-blocking strategies.

Fungal recovery in this system is not determined by extraction chemistry alone; suppression of plant DNA carryover during amplification is equally important for making fungal signal visible against a pine background (Ioos et al., 2010; Li et al., 2021). Work in plant microbiome and root–fungus systems has shown that ITS2 marker choice, lineage-specific primers, and PCR conditions can strongly influence apparent fungal abundance and diversity in mixed plant tissues, independent of extraction method (Schoch et al., 2012; Lindahl et al., 2013; Ihrmark et al., 2012; Li et al., 2020). PNA clamps targeting chloroplast and mitochondrial or ribosomal sequences were used to suppress host plant co-amplification so that fungal ITS reads are not drowned out by host amplicons (Lundberg et al., 2013; Fitzpatrick et al., 2018; Viotti et al., 2024). However, these studies also emphasize that PNA clamping is rarely perfect: PNA clamps usually suppress host amplification only partially and cannot fully rescue datasets that begin from host-dominated templates (Lundberg et al., 2013; Viotti et al., 2024). The partial reduction of plant signal observed in this study, especially in healthy-needle controls and in Quick-DNA Plant and ZymoBIOMICS extracts, fits that broader pattern and shows that PNA is best as a fine-tuning tool for favorable extraction workflows rather than a universal

fix for host-heavy DNA. The present results fit this pattern across the three ITS2 primer systems. The broad gITS7 + ITS4 primer set consistently produced the strongest total signal across extraction workflows but also tolerated the most host co-amplification. The fITS7 + ITS4 combination provided a useful compromise between total amplification and fungal orientation, particularly for YeaStar and Quick-DNA Fungal extracts, and is a practical default choice for routine ITS2-based detection from BSNB-infected needles (Ioos et al., 2010). The more selective 5.8S-Fun + ITS4-Fun assays, especially with PNA, improved fungal-to-plant balance but at a noticeable cost in total signal making them better suited for high-specificity confirmation over screening assays. These trade-offs are clearly illustrated in the primer-response figures, where non-reference bars shrink progressively as assays become more selective, even under the best extraction workflows, and where the combination of fITS7 + ITS4 with PNA on YeaStar or Quick-DNA Fungal extracts emerges as a reasonable compromise for field-facing diagnostics (Figure 2.Y).

Healthy pine needle controls play a key role in this interpretation. Under PNA-assisted conditions, strong reduction of plant-derived amplification in healthy controls would indicate that the clamp is well matched to pine rDNA, whereas weak reduction would suggest poor sequence compatibility and raise questions about whether the PNA treatment is worth the additional cost and complexity (Lundberg et al., 2013; Viotti et al., 2024). Even when PNA is partially effective, it functions best as a refinement for a fungal-enriching extraction workflow rather than as a work-around for plant-heavy extracts, a conclusion that is reinforced by the poor performance of CTAB and ZymoBIOMICS under PNA-assisted 5.8S-Fun assays.

From a forest diagnostic perspective, BSNB-infected loblolly needles treated wtih YeaStar and Quick-DNA Fungal produced the most diagnostically useful extracts because they enriched *L. acicola* DNA relative to host DNA and maintained usable amplification under increasingly selective ITS2/PNA conditions. This study's results support adopting fungal-oriented workflows as the default for *L. acicola* detection and using plant-optimized protocols primarily when host genotyping or reference plant DNA is the main goal (Ioos et al., 2010; Datta, 2021). Conceptually, these choices are summarized in the Chapter 2 decision-tree figure, which routes samples toward YeaStar or Quick-DNA Fungal for pathogen-focused diagnostics and toward plant-oriented kits when host targets are of primary interest (Figure 2.1). Cost, equipment, and time, however, are also to be considered. The kit-based workflows use standard microcentrifuge equipment, modest hands-on time, and avoid hazardous organic solvents, making them realistic options for small diagnostic labs and cooperatives (Desneux and Pourcher, 2014; Carter-House et al., 2020). CTAB remains valuable when high-molecular-weight plant DNA is the target and organic solvents are acceptable, but its labor-intensive handling, safety considerations, and poor fungal enrichment make it a weaker default choice for BSNB diagnostics (Carter-House et al., 2020). In forestry and nursery fields, the additional training, fume-hood access, and waste-disposal requirements associated with CTAB are unlikely to be justified when kit-based workflows can deliver equal or better fungal selectivity with simpler steps.

Conifers are notoriously difficult matrices for pathogen DNA recovery, a challenge that has been documented for other tree–fungus systems such as *Heterobasidion annosum* infections of Norway spruce (*Picea abies*), where secondary metabolites and

high phenolic content interfere with both extraction and amplification (Baldi and La Porta, 2020; Langsiri et al., 2025). Only five extraction workflows and a limited number of disruption treatments were evaluated in this study, so additional protocols, including simpler phenol-free or dipstick-style extractions, could potentially provide equal or better fungal enrichment (Boesenberg-Smith et al., 2012; Baldi and La Porta, 2020). Infected loblolly pine needle collection and sampling was limited to East Alabama, meaning that performance rankings might differ in other pine species, climates, or needle blight complexes with multiple co-occurring pathogens (Mullett et al., 2018; Ogris et al., 2023). Lastly, fungal and plant proportions were inferred from ITS2 qPCR and primer/PNA response rather than from metagenomic sequencing, so the fungal: plant ratios reported here represent amplifiable ITS templates rather than absolute genome copy numbers (Li et al., 2021). These limitations mean that the rankings proposed here should be treated as an evidence-based starting point rather than a universal prescription but still provide guidance for BSNB-focused extraction choices.

Despite these limitations, this study demonstrates that fungal-enriching workflows such as YeaStar and Quick-DNA Fungal materially improve the sensitivity and reliability of molecular assays for *L. acicola*. The optimized workflows identified here provide the pre-analytical backbone for Chapter 3, where they are coupled with CRISPR-based detection of *L. acicola* and used to test how improved extraction and amplification translate into faster, field-aligned diagnostics for brown spot needle blight.

2.6 Conclusions

The present work provides a clear, empirically grounded ranking of extraction options for BSNB-infected needles and demonstrates that fungal-enriching workflows such as YeaStar and Quick-DNA Fungal materially improve the sensitivity and reliability of molecular assays for L. acicola. For on site or near site diagnostics in forestry settings, where time and equipment are constrained, these results suggest that fungi targeted extraction chemistries combined with ITS2 primer/PNA systems that limit plant co amplification are a more promising foundation than generic plant or microbiome kits (Baldi and La Porta, 2020; Ioos et al., 2010). In the broader context of woody plant pathology, they also reinforce the idea that building robust diagnostic pipelines for emerging threats like BSNB requires attention not only to the detection technology (qPCR, LAMP, CRISPR-Cas) but also to the pre-analytical steps that determine how much pathogen DNA is actually present and visible in the first place.

3 Chapter 3. CRISPR-Cas9 Target Validation of *Lecanosticta acicola* in Loblolly Pine Trees

3.1 Abstract

Lecanosticta acicola, the fungal causal agent of brown spot needle blight (BSNB), is difficult to confirm visually due to similar infectious mechanisms shared with Dothistroma needle blight (DNB) that cause tree mortality. Accurate species-level identification requires molecular confirmation, and CRISPR-based diagnostics offer a promising framework because of their ability to utilize guide-directed target recognition

for rapid, programmable readouts adaptable to field deployment. However, before further implementation of additional CRISPR-Cas systems, the target locus and guide RNA must perform direct efficient cleavage of the target sequence in vitro. This chapter describes the design and in vitro evaluation of sgRNAs targeting the translation elongation factor 1-alpha (TEF1) and the internal transcribed spacer (ITS) loci of *L. acicola*. Three TEF-targeting guides (TEF-50rev, TEF-76rev, TEF-177rev) and three ITS-targeting guides (100rev) were designed for Streptococcus pyogenes Cas9 using the NEB EnGen sgRNA synthesis workflow. After confirming sgRNA synthesis and RNP assembly using a PvuII-linearized pBR322 positive control, each TEF-specific guide was tested in in vitro ribonucleoprotein (RNP) cleavage assays against amplified *L. acicola* TEF template. Cleavage was not clearly resolved on agarose gel but was confirmed by polyacrylamide gel electrophoresis, demonstrating that the TEF locus is a viable CRISPR target in *L. acicola*. A qPCR comparison using ITS-targeted assays provided a quantitative reference and showed strong amplification efficiency. These results establish the biochemical proof-of-principle for CRISPR-mediated detection assays of L. acicola DNA and lay the foundation for future development of a deployable CRISPR diagnostic for BSNB.

3.2 Introduction

Loblolly pines (*P. taeda)* are one of the most harvested and widely planted conifer species of the Southeastern United States (Pokhrel et al. 2026), subsequently making them a major timber crop in the southern United States (U.S.). As of 2010, loblolly pines make up over 45% of commercial forest land and produces around $30 billion in revenue for the south U.S. (Zhang et al. 2010). First noted in 2013, loblolly pine defoliation due to

fungal phytopathogens has expanded in its geographical range and intensity. Leading to concerns about environmental perseveration of the crop and subsequent economic losses (Datta 2021).

Lecanosticta acicola is the causal agent of Brown Spot Needle Blight and notably the most prolific fungal pathogen among pine species in the southeast (van der Nest et al. 2019; Datta 2021). *L. acicola* (formerly known as *Mycosphaerella dearnessii*) was first discovered in Central America but is most recognized for its presence in the southeastern U.S. for its pathological effects and spread among longleaf pines (van der Nest et al. 2019). The humid climate of the southeast creates optimal conditions for *L. acicola's* reproductive and overwintering states which rely on warm and wet weather. Areas where the pathogen has been recorded are often naturally humid, close to the sea, or urban areas. Even in exceptionally favorable conditions, the pathogen has the potential to infect pine species less susceptible to infection (van der Nest et al. 2019). The pathogen's geographic range and apparent impact have expanded in recent decades, and climatic suitability models suggest that large pine-growing regions remain vulnerable to further establishment and spread (Ogris et al. 2023; Matallana-Ramirez et al. 2021).

The symptoms of infection begin with a small, yellow spot at the point of infection on the needle which develops into a narrow brown band, with definite yellow margins as the infection progresses. Fatal symptoms of the infection present points of infection along the shaft just above the dead tip of the needle from which the needle begins to die back from (Siggers 1932). The oldest aged, infected needles are the most damaged and are subsequently shed in early fall, and when infection is aggressive, premature defoliation occurs resulting in reduced photosynthetic ability of the tree. Infected needles and needle

debris that accumulate beneath trees acts as reservoirs of inoculum, allowing the pathogen to jump to new growth needles and nearby trees, carrying on the disease cycle (Siggers 1932; Skilling and Nicholls 1975). Once infection takes root, the pathogen can be present in its asymptomatic form from a few weeks to three months (Skilling and Nicholls 1975), making early observation-based detection a challenge.

A central diagnostic problem is that BSNB symptoms are not unique. Needles with brown bands, yellow halos, and dead tips can closely resemble damage caused by *Dothistroma* needle blight (DNB) and other stressors, including abiotic injury and insect feeding. *Dothistroma septosporum* (Dorog.) M. Morelet and *Dothistroma pini* Hulbary are the fungal causal agents of DNB affecting over sixty pine species (Barnes et al.). The blight results in characteristic red, conversely to brown, bands at the spot of the infection, and parallelly, causes tree mortality and stunted growth consequence of needle defoliation (Gibson et al. 1967). The pathogen conjointly thrives in warm, humid climates leading to common misidentification of the two diseases. Historical accounts even indicate the confusion on symptomatology; in 1944, Siggers identified previous distinctions of *L. acicola* exhibited symptoms more attributable to *Dothistroma pini* (Siggers 1944).

Management of BSNB in the United States has relied on a combination of controlled burning, seasonal thinning, and, less commonly, fungicide applications (Tainter and Baker 1996; Skilling and Nicholls 1975). The effectiveness of these practices relies on the ability to detect the presence of BSNB in forest stands early enough to justify, application of interventions, and the saplings ability to withstand treatment. In crowns, BSNB can present as diffuse thinning and discolored foliage that is difficult to distinguish

from other needle diseases by eye alone, especially early in the epidemic or when multiple agents are present. Because visual detection can be hard to confirm, other approaches (e.g. spore traps, microscopy, molecular diagnostics, and remote sensing) have been deployed for accurate and reliable detection to support timely management decisions (Singh et al. 2025; EPPO 2015).

Polymerase chain reaction (PCR) -based detection is commonly used for identification due to its high specificity, sensitivity, and analytical efficiency. Species-specific PCR and qPCR assays allow for the distinction of *L. acicola* from *D. septosporum* and *D. pini* by targeting and amplifying the Translation Elongation Factor 1-α (*TEF1-α*) gene and Internal Transcribed Spacer (ITS) region in combination (Huang 1995; van der Nest et al. 2019). However, these approaches require specialized equipment, controlled laboratory conditions, and trained personnel to perform assays and interpret data, and they rely on careful primer design and optimization. These constraints limit their use as true point-of-care (POC) tools in nurseries, inspection stations, and remote forest sites (Huang et al. 2023). Consequently, there is a clear need for additional detection methods that maintain the sequence-level specificity of PCR while being more portable, operationally simple, and better suited to field deployment for BSNB diagnostics.

3.2.1 CRIPSR-Based Detection of Plant Pathogens and POC Applicability

The CRISPR-Cas systems (Clustered Regularly Interspaced Short Palindromic Repeats and associate nucleases) first recognized as adaptive immune mechanisms in bacteria and archaea but have since been developed into powerful tools for genome editing, functional genomics, and nucleic-acid detection (Rocafort et al. 2022). The

CRIPSR-Cas9 complex can target and cleave specific DNA signatures within the pathogen's genome with two key components, a single-guide RNA (sgRNA) directs the Cas9 endonuclease to a specific DNA sequence via a 20-nucleotide protospacer region complementary to the target and recognition of a short protospacer adjacent motif (PAM) in the DNA. The RNA-guided Cas9 introduces a double-strand break at a defined position upstream of the PAM. The guide RNA consists of the variable protospacer fused to a conserved scaffold that folds into a structure recognized by Cas9, ensuring that different guides can all dock into the same protein framework. These components of the sgRNA are bound to Cas9 via a non-variable 80-nucleotide scaffold structure unique to the Cas9 protein (Krappmann 2017; Pozharskiy et al. 2025; Rocafort et al. 2022). The CRISPR-Cas9 system has received most recognition for its exploitation of DNA repair pathways after cleavage to knock out, rewire, or replace genes resulting in altered function of genes (Krappmann 2017). However, the same sequence-specific cutting activity can be repurposed for analytical applications as when Cas9 cleaves a defined amplicon only when a target is present, that cut serves as a yes/no biochemical readout of target recognition.

For diagnostics, however, a different family of CRISPR nucleases has become even more prominent. Cas12a (formerly Cpf1) and Cas13 retain the guide-directed recognition of a specific DNA or RNA target, but once activated, exhibit collateral nuclease activity against reporter molecules such as short-labeled single-stranded DNA or RNA, respectively (Lei et al. 2022). This collateral cleavage activity enables the nuclease to cleave fluorescent sensors, in addition to the target DNA, that produces a visual confirmation of the systems activity once cut. These properties underpin platforms

such as DETECTR (DNA Endonuclease Targeted CRISPR Trans Reporter), where isothermal amplification (e.g., RPA or LAMP) increases target copy number and Cas12a then converts target recognition into a strong fluorescent or lateral flow readout (Chen et al. 2018; Lei et al. 2022). Recent RPA–Cas12a and LAMP–Cas12a assays for woody and perennial pathosystems including oak wilt (*Bretziella fagacearum*), *Fusarium circinatum* on pines, citrus Huanglongbing, grapevine trunk pathogens, pine wood nematode, and multiple *Phytophthora* species affecting forest and orchard hosts. *(*Bourgault et al. 2022; Chen et al. 2023; Wang et al. 2025; Dai et al. 2023; Guo et al. 2023).

In forestry, these features map directly onto operational constraints. Foresters and land managers rarely have access to thermocyclers, real-time qPCR instruments, or molecular-diagnostic expertise, but are responsible for decisions about thinning, sanitation harvests, and movement of planting stock. Conventional PCR and qPCR remain the laboratory gold standard for *L. acicola* detection, especially when TEF1-α and ITS are targeted in combination to separate BSNB from *Dothistroma* needle blight. At the same time, these assays require controlled laboratory settings, careful primer optimization, and trained personnel to interpret results. CRISPR-based diagnostics offer a way to compress this complex workflow into simpler, more portable formats that are easier to interpret at or near the sampling site. Considering climatic shifts towards warmer climates, difficulty in precise visual detection, and the potential for long, cryptic infection periods to erode pine productivity, rapid and reliable detection of *L. acicola* is particularly important.

At the same time, CRISPR diagnostics are dependent on the underlying guide–target interaction as sgRNAs that may look acceptable in silico do not always perform well in practice. Guide efficiency can vary with sequence composition, local chromatin or amplicon context, PAM accessibility, RNA stability, and guide–target thermodynamics (Jinek et al. 2012; Hsu et al. 2013). For this reason, in vitro screening of candidate sgRNAs is as an essential empirical step before guides move forward into diagnostic or gene-editing workflows (Grainger et al. 2017; Kellner et al. 2019). In the context of BSNB, the TEF1 locus is an attractive CRISPR target because it is a well-supported marker for fungal species discrimination and has already underpinned species-specific PCR and LAMP assays for *L. acicola* directly from infected needles. Demonstrating that TEF-targeting guides can form active CRISPR–Cas9 ribonucleoprotein (RNP) complexes and cleave amplified *L. acicola* TEF sequences in vitro provides the biochemical proof-of-principle required before investing in a full Cas12a-based point-of-care assay (Jinek et al. 2012; Kellner et al. 2019).

Building on the extraction findings in Chapter 2, this chapter evaluates whether *L. acicola* DNA targets can be effectively amplified, sequence-confirmed, and recognized by CRISPR-Cas reagents in vitro. In this framework, CRISPR–Cas9 RNP assay serve as the staple biochemical validation step on which any future Cas12a-based BSNB test may rest. The objective of this study was to: 1) Confirm amplification and sequence identity of diagnostic *L. acicola* diagnostic loci, 2) Design and evaluate sgRNAs that target selected loci using in vitro by assessing Cas9-mediated cleavage assays, and 3) Use the resulting proof-of-principle to inform future development of a POC CRISPR diagnostic mechanism for BSNB.

3.3 Materials and Methods

3.3.1 Biological Samples and Experimental Design

Lecanosticta acicola isolates used in this study for target confirmation originated from Dr. Willoughby's lab as tissue culture biomaterial. Cultures were maintained on malt extract sugar MEA medium at room temperature and stored at -20℃ prior to DNA extraction. Genomic DNA was extracted using the Quick-DNA Fungal/Bacterial Miniprep Kit (Zymo Research, Irvine, CA, USA), following the optimized fungal workflow described in Chapter 2, and purified with the DNA Clean & Concentrator-5 kit (Zymo Research, Irvine, CA, USA). To compensate for low biomass and ensure sufficient template for downstream PCR and CRISPR assays, approximately 300 mg wet weight of fungal tissue was processed per extraction. These culture-derived extracts served as positive controls and as source material for amplifying TEF and ITS targets used in in vitro CRISPR–Cas9 cleavage assays.

Loblolly pine needles were sampled from forest stands in east Alabama forests to collect both symptomatic and asymptomatic needles. Dr. Willoughby's and Dr. Eckhardt's lab team facilitated field sampling. Symptomatic needle selection was based on the presence of brown bands, yellow halos, and dead needle tips characteristic of brown spot needle blight. While visually healthy needles from the same sites served as noninfected reference material. All needle samples were transported on ice and stored at -80 ℃ until DNA extraction. For laboratory processing, needles cut into 6–12 mm (~¼–½ inch) fragments targeting visible lesions to were used concentrate diseased tissue. Healthy fragments were cut to the same length from mid-needle sections without specific targeting.

To extract needle DNA, two workflows were used, the E-Z Plant DNA DS Kit (Omega Bio-tek, Norcross, GA, USA) was applied to both symptomatic and asymptomatic needles with approximately 10 mg input biomass per extraction. Then, second, selected samples used the optimized plant-oriented workflow from Chapter 2 based on the Quick-DNA Plant Kit (Zymo Research, Irvine, CA, USA), providing a comparative plant-extraction reference for downstream assay performance. Extracted DNA concentrations and spectrophotometric purity(A260/A230) ratios from all sample types were measured and recorded on a NanoDrop spectrophotometer. Extract quality and fragment size were visualized on 1.5% agarose gels by gel electrophoresis run at 100 V for 30 minutes. Sample IDs, wet weights (mg), extraction conditions, and DNA yields (ng/μL), logged systematically, connected field collections with subsequent PCR, qPCR, and CRISPR assays. An overview of sample origin, extraction workflows, and downstream PCR and CRISPR assays is summarized in Figure 3.1.

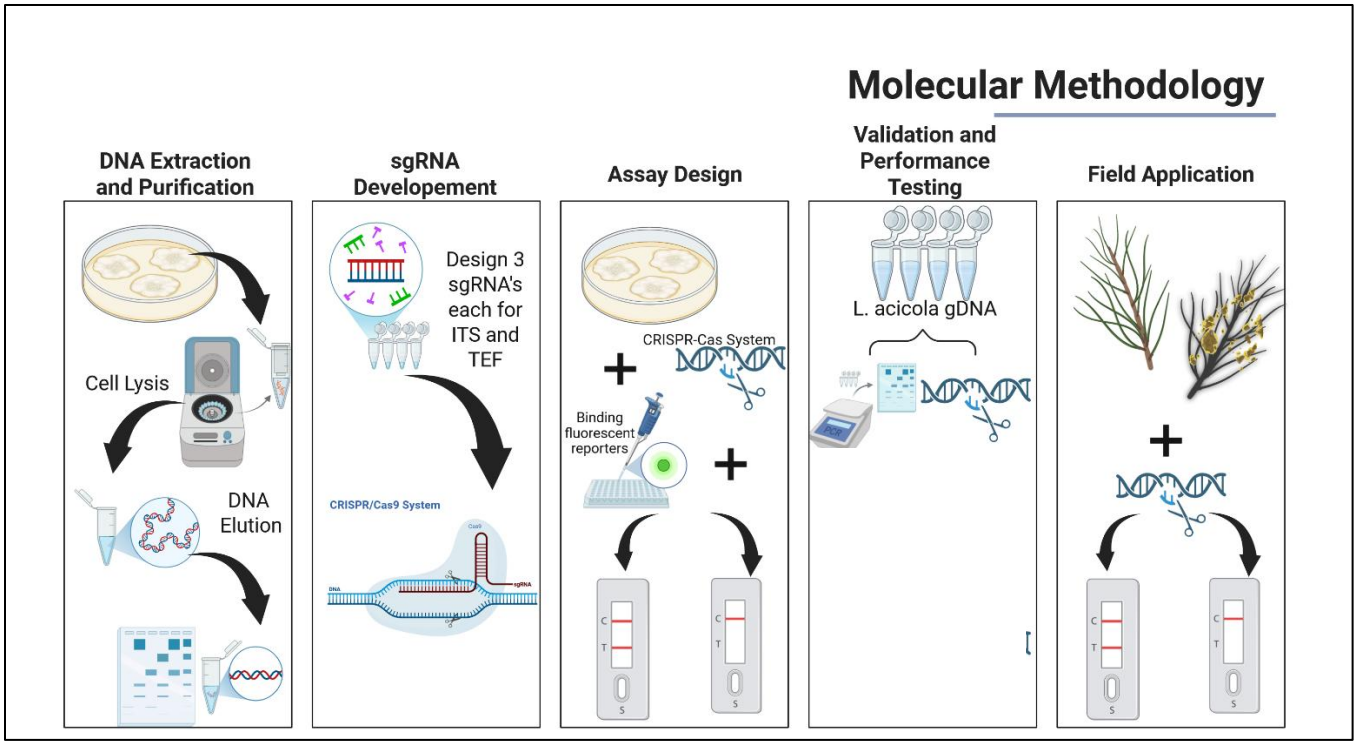

Figure 3.1 Biological samples and experimental workflow for CRISPR–Cas9 target validation of *Lecanosticta acicola***.** Symptomatic and asymptomatic loblolly pine (*Pinus taeda)* needles collected from east Alabama stands and *L. acicola* cultures from laboratory isolates served to generate mixed host-pathogen and culture-derived DNA templates. Treated with optimized extraction workflows from Chapter 2 TEF and ITS targets amplified, these extracts provided substrates for PCR/qPCR confirmation and in vitro CRISPR–Cas9 (RNP) cleavage assays used to validate TEF as a CRISPR-compatible diagnostic tool. Generated by BioRender.com.

3.3.2 Target Selection and Guide RNA Design

Primary targets for *L. acicola* detection focused on two primary loci, the ITS region and TEF1-a gene. These selections were based upon their use in previous use in forestry diagnostics to discriminate *L. acicola* from closely related *Dothistroma* species (loos et al.

2010). ITS amplicons of ~500 bp and TEF1-a fragments of ~450-500 bp were confirmed within template DNA samples by sequencing facilitated by Plasmidsaurus Selected sequences for further use showed high percent similarity to reference *L. acicola* ITS and TEF1-α sequences in NCBI to confirm locus identity. Primer mapping of the TEF1-A region using the EF1-728F/EF-2 primer sets confirmed expected amplicon size and showed multiple candidate Cas9 target sites with appropriate PAM motifs.

Primer mapping of the TEF1-α region with EF1-728F/EF-2 confirmed the expected amplicon size and revealed multiple candidate Cas9 sites with (NGG) PAMs. TEF-targeting sgRNAs designed for *Streptococcus pyogenes* Cas9 were selected based on compatible PAM sequences within the TEF amplicon. For the ITS-targeting, primers and restriction-site mapping guided placement of candidate protospacers away from primer binding regions. Benchling was used to evaluate both loci to verify PAM presence, GC content, and avoid primer-dimer effects.

Three oligonucleotides targeting TEF1-α (TEF-50rev, TEF-76rev, TEF-177rev) and three ITS-targeting oligos (ITS-100rev, ITS-103rev, ITS-300rev) served as the main sgRNA panel. Using the NEB EnGen sgRNA Synthesis Kit (S. pyogenes), each user-designed oligo required the T7 promoter, a 20-nt protospacer, and the overlap needed for scaffold completion. sgRNA templates were transcribed in vitro using the EnGen kit (New England Biolabs, Ipswich, MA, USA), purified with RNA Clean & Concentrator (Zymo Research, Irvine, CA, USA), quantified by NanoDrop, and quality-checked by PAGE or 1% bleach–agarose gels prior to RNP assembly.

3.3.3 CRISPR-Cas Assay Configuration

In vitro CRISPR-Cas9 reactions were assembled as ribonucleoprotein (RNP) complexes using recombinant *S. pyogenes* Cas9 and custom synthesized sgRNAs targeting the ITS or TEF1-a amplicons of *L. acicola*. Cas9 nucleases used in this study included Cas9 Nuclease, S. pyogenes (Intact Genomics) in initial reactions and EnGen Seq1 Cas9 in later runs. RNP assembly reactions ran in 30 µL mixes containing 10x reaction buffer, Cas9 nuclease, sgRNA, and substrate DNA in nuclease-free water. To allow for RNP complex formation, reactions were pre-incubated at 25 ℃ for 10 minutes. After RNP–DNA incubation at 37 °C for 15 minutes to 1 hour depending on Cas9 preparation, Proteinase K was added to terminate reactions and dissociate Cas9 from the cleaved DNA. Crucial for removing residual Cas9 bound to DNA which interferes with gel resolution of digestion products (New England Biolabs, 2025c). Products were resolved on 1-1.5% agarose gels by gel electrophoresis ran at 100 V for 30 minutes.

Each run included a negative control lacking one critical component: 1) without sgRNA, 2) without Cas9, or 3) without DNA, as well as DNA-only controls to monitor nonspecific cleavage or contamination. Before testing target-specific guides against fungal DNA PvuII-linearized pBR322 served as the control substrate to validate the overall workflow using EnGen sgRNA Control Oligo directed cleavage. Reaction conditions were optimized iteratively by varying total reaction volume, sgRNA and substrate DNA concentrations (30-300 nM), and Cas9 volume while preserving the target 10:10:1 molar ratio. Optimization experiments compared the three different sgRNAs designed to target the TEF1 region against the same amplicon to assess efficiency.

Another comparison evaluated alternative Cas9 preparations between Cas9 Nuclease and EnGen Seq1 Cas9 under identical buffer and DNA conditions as well.

3.3.4 PCR Amplification

Primer selection was based off the amplification and target efficiency of a set of seven primer sets. Initial screening evaluated commonly targeted loci used in multilocus barcoding and phylogenetic analysis of *Lecanosticta* spp., including ITS, TEF-1, TEF1-a, β-tubulin, MS204, RPB2, and fungal universal 18s rRNA for qPCR normalization. Primary focus was the PCR amplification of the ITS and TEF1-a sequences from *L. acicola* genomic DNA were amplified with ITS primer pair ITS1-F/ITS4-R, TEF-1 and TEF1-a primer sets LATEF-F/LATEF-R and EF1-728F/EF-2R. Primer sets were obtained from Dr. Willoughby's lab, originally designed and compiled using Siddique et al. (2022) and additional primers were ordered based on prior use in van der Nest et al. (2019). The summarized and complete primer panel is in Table 3.1.

Within this panel, the primary focus for CRISPR target development was robust PCR amplification of ITS and TEF1-α from *L. acicola* genomic DNA. Amplified ITS primers consisted of ITS1F/ITS4 and ITS3/ITS4 combinations, while TEF-1/TEF1-α were targeted used the LAtef-F/LAtef-R and EF1-728F/EF-2 primer sets. TEF1-α was prioritized because it is an informative fungal marker for species-level discrimination and has already lead species-specific PCR and LAMP assays for *L. acicola*. Amplicon sizes were ~ 500 bp for ITS and ~450–500 bp for TEF1-α, consistent with expectations from the literature and primer-mapping analyses.

Conventional PCR reactions assembly was in 25 µL volumes containing 2× Taq DNA polymerase master mix, forward and reverse primers, nuclease-free water, and 10–

100 ng standardized genomic DNA inputs. Selected reactions substituted with Q5 High-Fidelity Master Mix to generate higher-fidelity PCR products for sequencing and for potential use as CRISPR substrates, reducing polymerase-induced errors in the target region. Thermocycling followed the general PCR program described in Chapter 2, with annealing temperatures adjusted by gradient PCR (55–68 °C) to identify optimal conditions for each primer set. Each run included a no-template control (NTC) to monitor contamination and a positive control consisting of *L. acicola* culture DNA known to amplify at the target locus. Amplification success was visualized on 1–1.5% agarose gels run at 100 V for approximately 30 minutes, and products with bands at the expected size were submitted to Plasmidsaurus for sequencing to confirm locus identity. Confirmed ITS and TEF1-α amplicons then served directly as substrate DNA for subsequent CRISPR–Cas9 experiments.

Table 3.1 Primer sets targeting ITS and TEF1-α loci of Lecanosticta acicola used for conventional PCR, qPCR, and amplicon generation for CRISPR–Cas9 substrates.

Target / locus	Primer name	Sequence (5'–3')	Direction	Application	Reference / source
TEF region	LAtef-F	GCAAATTTTCGCCGTTTATC	Forward	Conventional PCR	Ioos et al. 2010
TEF region	LAtef-R	TGTGTTCCAAGAGTGCTTGC	Reverse	Conventional PCR	Ioos et al. 2010
TEF region	LAtef-F1	CCTCCTTCACTTTCCCTTC	Forward	qPCR	Ioos et al. 2010
TEF region	LAtef-R1	TGTGGGAGATAGGCTTGTCA	Reverse	qPCR	Ioos et al. 2010
18S rRNA	18S uni-F	GCAAGGCTGAAACTTAAAGGAA	Forward	qPCR reference	Siddique et al. 2022
18S rRNA	18S uni-R	CCACCACCCATAGAATCAAGA	Reverse	qPCR reference	Siddique et al. 2022
Fungal ITS	ITS1F-F	CTTGGTCATTTAGAGGAAGTAA	Forward	PCR / amplicon	Gardes & Bruns 1993
Fungal ITS	ITS3-F	GCATCGATGAAGAACGCAGC	Forward	PCR / amplicon	White et al. 1990
Fungal ITS	ITS4-R	TCCTCCGCTTATTGATATGC	Reverse	PCR / amplicon	van der Nest et al. 2019
TEF1 locus	EF1-728F	CAT CGA GAA GTT CGA GAA GG	Forward	PCR / sequencing	Carbone & Kohn 1999
TEF1 locus	EF-2	GGA RGT ACC AGT SAT CAT GTT	Reverse	PCR / sequencing	O'Donnell et al. 1998

Table 3.2 Additional primer sets targeting β-tubulin, MS204, RPB2, and universal 18S rRNA used for multilocus screening and qPCR normalization

Target / locus	Primer name	Sequence (5'–3')	Direction	Application	Reference / source
β-tubulin 1	B11a	TTC CCC GCT CTC CAC CTC TTC ATG	Forward	PCR	van der Nest et al. 2019
β-tubulin 1	B11b	GAC GAG AGT CAT GTT GAT GTC	Reverse	PCR	van der Nest et al. 2019
β-tubulin (β-SandyR)	B12a	GGR CGA GGV ACT TAC TTG GAC	Forward	PCR	van der Nest et al. 2019
β-tubulin (β-SandyR)	B12b	GGT ACA ACA CTG AAG AAG CCT TTC	Reverse	PCR	van der Nest et al. 2019
MS204 locus (Cerato-specific)	MS204F cerato	AAC CAC CTC TAC TAC CTA CAC C	Forward	PCR	Burgess et al. 2018
MS204 (Cerato-specific)	MS204R Cerato	GAT GAG GCC GAG GTG AAA CTC	Reverse	PCR	Burgess et al. 2018
RPB2	RPB2-5F2	GAY GAR TGY CCD GGR ATG TC	Forward	PCR	Liu et al. 1999
RPB2	RPB2-7cR	CCC ATR GCT TGY TTR CCC AT	Reverse	PCR	Liu et al. 1999

3.3.5 Analytical Sensitivity, Limit of Detection, and Assay Specificity

Serial dilutions of purified *L. acicola* ITS and TEF gene amplicons and extracted gDNA determined analytical sensitivity for PCR, qPCR, and CRIPSR-Cas9- based readouts. Ten-fold and two-fold dilution series were prepared to span template DNA inputs from high copy number down to near-single copy equivalents. NanoDrop concentrations and amplicon length provided the basis for template mass estimates. Each dilution level included three replicate reactions. The LOD refers to the lowest concentration at which a clear band of the expected size was consistently visible and distinguishable from no-template controls and background smearing in at least two independent runs For qPCR assays targeting ITS and TEF, Cq values across the dilution series generated standard curves, and the Azure Cielo real-time PCR system automatically determined thresholds and baselines.

Assay specificity examination at both template and matrix levels evaluated detection ability between the levels. At the template level, host-only DNA, no-template controls, and confirmed *L. acicola* DNA established the baseline for non-target amplification and detection. At the matrix level, infected and healthy needle extracts determined whether the complex plant–fungal DNA background produced nonspecific products or altered the LOD relative to culture-derived DNA.

3.3.6 Comparison to qPCR Reference Assays

qPCR quantification cycle values and amplification curves served as the quantitative reference method for comparison to CRISPR-Cas9 outcomes. Standard curves generated from serial dilutions of gDNA spanning 20 ng to1.25 ng per reaction estimated amplification efficiency, dynamic range, and quantification limits for ITS and

TEF region targeted assays. qPCR reactions followed he Luna Universal qPCR Master Mix protocol (New England Biolabs) with primer annealing temperatures adjusted based on gradient optimization, and each run included no-template controls to monitor contamination. For each sample-locus combination, qPCR quantification cycle (Cq) values and amplification curves were recorded, while CRISPR-Cas 9 assays provided qualitative data in the form of presence or absence of expected bands and cleavage patterns on agarose gels.

3.3.7 Data Analysis

Diagnostic performance and comparative analyses for qPCR and CRISPR assays used R (R Foundation for Statistical Computing). For qPCR, the study estimated sensitivity, dynamic range, and amplification efficiency from standard curves generated with serial dilutions of *L. acicola* DNA. Statistical approaches followed frameworks commonly used in recent CRISPR-based diagnostic validation studies. The study calculated diagnostic metrics such as sensitivity, specificity, positive predictive value (PPV), and negative predictive value (NPV). Using 2×2 confusion matrices, CRISPR assay signals served as the index test and qPCR results as the reference standard. When Cas9-based assays did not produce robust signals, the study described performance qualitatively in the Results section rather than reporting unstable numerical estimates.

3.4 Results

3.4.1 Amplification and Sequence Confirmation of ITS and TEF targets

In this study, genomic DNA extractions from loblolly pine needles fell into three groups: older infected needles, freshly collected infected needles, and healthy needles that served as plant-background controls. Fresh infected needles consistently yielded the strongest combination of DNA concentration and purity, with genomic DNA in the range of ~ 167–176 ng/μL and A260/280 ratios near 1.8, while older infected tissue and healthy needles produced lower yields and more pronounced evidence of secondary-metabolite carryover typical of conifer material. These extraction results identified fresh infected needles as the primary template source for locus-specific PCR in Chapter 3.

PCR screening focused on the internal transcribed spacer (ITS) region and the translation elongation factor 1-alpha (TEF-1a) locus. On 1.5% agarose gels, amplification of the ITS region from fresh infected needle DNA with the ITS1-F/ITS4-R primer pair produced a single discrete band at the expected size, whereas the ITS negative control lane remained blank. This outcome confirmed that the extraction and PCR conditions could recover a clean ITS product from diseased needles and that visible amplification did not simply reflect contamination or non-specific primer binding. In the same run, a TEF-related primer pair (LATEF-F/LATEF-R) produced a band from an infected needle sample (Figure 3.2). A broader primer comparison then evaluated several loci (18S rDNA, BT-1, β-tubulin, TEF-1 locus, RPB2, ITS, and LATEF) across DNA templates from infected needles, healthy needles, and *L. acicola* cultures. This screen established a pattern that only the TEF-1 locus primers and the ITS primer pair generated amplicons that both produced strong, locus-appropriate bands on gel and matched the reference

sequences for *L. acicola* upon sequencing. Whereas 18S, BT-1, β-tubulin, RPB2, and LATEF either failed to amplify consistently or did not yield clear sequence matches. On that basis, ITS and TEF-1a were prioritized as the most reliable loci for subsequent target confirmation and CRISPR assay development within this chapter. In the TEF-1a sequencing panel, selected amplicons from extracted infected needle DNA produced over 90% alignment with reference sequences from NCBI Database for the *L. acicola* TEF1a gene (MW660834.1, isolate UASc and KJ938449.1, isolate Mx1). While the ITS amplicon played a complementary role by demonstrating that a standard fungal barcode can be amplified directly from infected needles with clean negative controls.

Table 3.3 Sequencing and alignment summary for TEF-1a amplicons used in CRISPR target validation.

Sample ID	Primer Set	Template Type	Amplicon Length (bp)	BLAST accession	Locus	Alignment Range
C2	EF1-a	*L. acicola* culture	~542	MW660834.1	TEF1-a	11–542
C4	EF1-a	Infected Needle	~400	KJ938449.1	TEF1-a	191–329

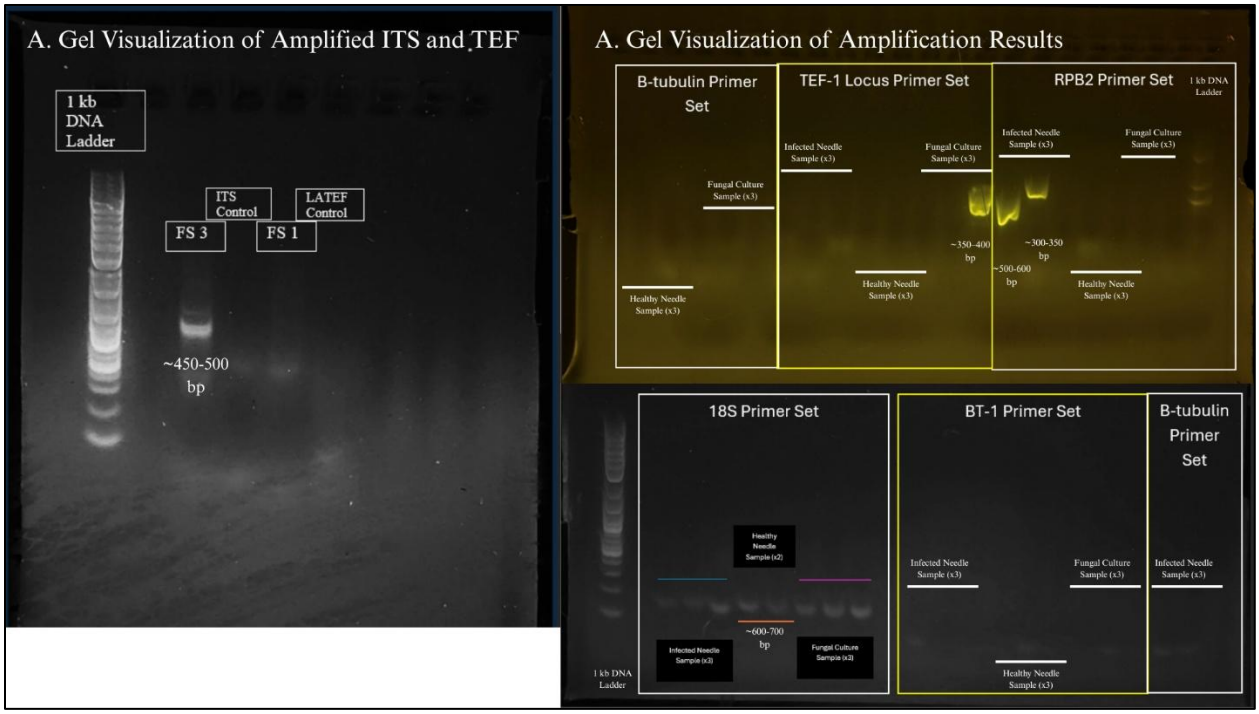

Figure 3.2 PCR amplification of ITS and TEF-related loci from loblolly pine needle DNA and Lecanosticta acicola cultures. (A) 1.5% agarose gel showing successful amplification of the ITS region from fresh infected loblolly pine needles using the ITS1-F/ITS4-R primer pair, with no band in the ITS negative control lane, and a TEF-related amplicon produced by the LATEF primer set along with its negative control. (B) Representative gel from a multi-locus primer screen (18S rDNA, BT-1, β-tubulin, TEF-1 locus, RPB2, ITS, and LATEF) across templates from infected needles, healthy needles, and L. acicola cultures.

3.4.2 sgRNA Screening and Cas9 RNP Cleavage of the TEF Locus

Three sgRNAs (TEF-50rev, TEF-76rev, TEF-177rev) targeted the confirmed TEF1-α amplicon. In vitro transcription with the EnGen sgRNA Synthesis Kit, followed by

RNA Clean & Concentrator purification and PAGE or bleach–agarose checks, produced guides of the expected size and integrity for all three TEF protospacers.

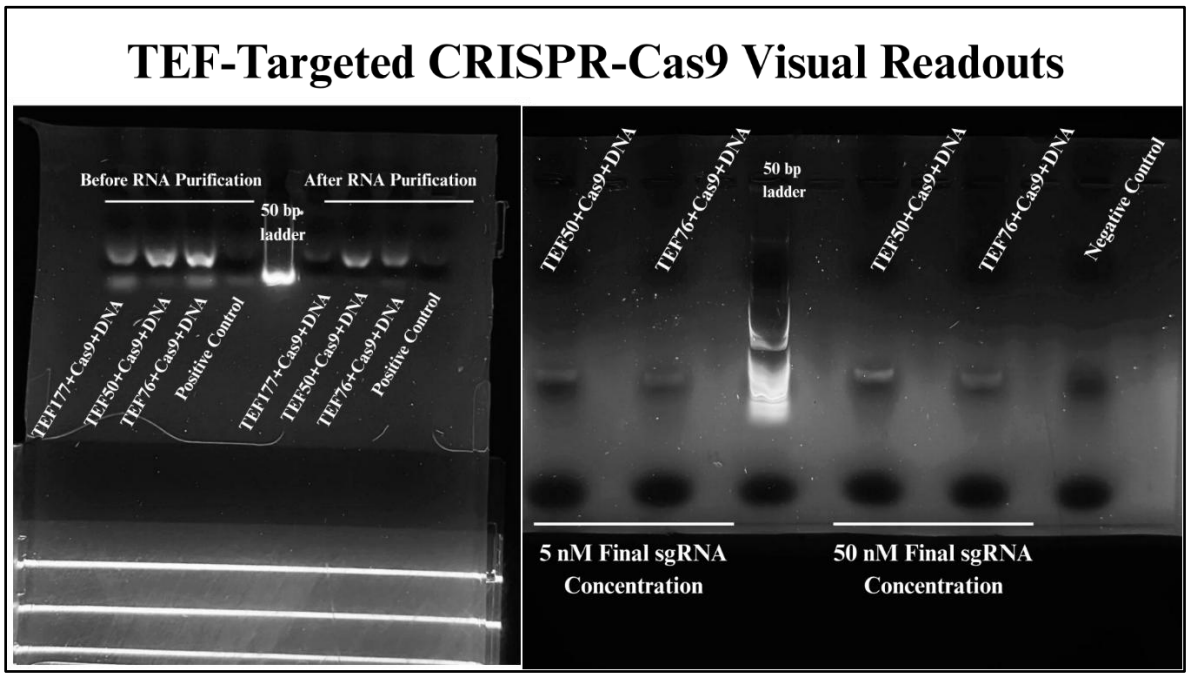

Figure 3.3 TEF-targeted CRISPR-Cas9 visual readouts on agarose gels. 1.5% agarose gels show TEF-specific sgRNAs (TEF177, TEF50, TEF76) before and after RNA purification (left panel) and TEF RNP reactions at 5 nM and 50 n final sgRNA concentrations (right panel).

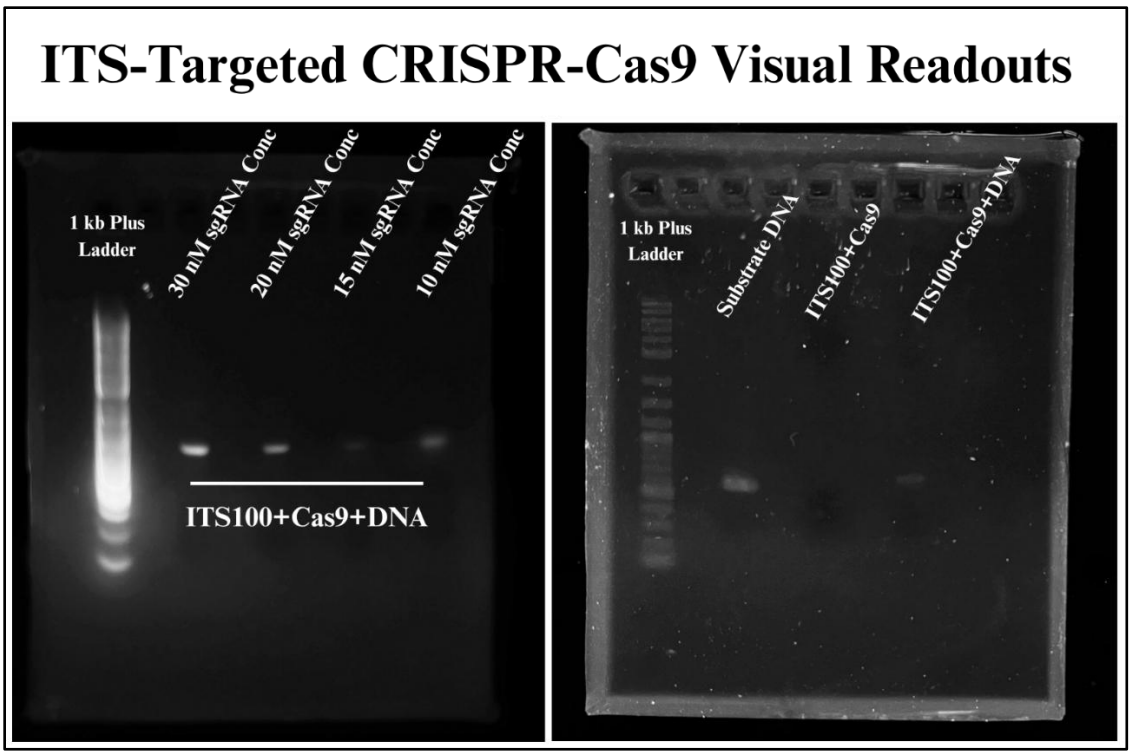

Figure 3.4 ITS-targeted CRISPR-Cas9 visual readouts. Agarose gels show ITS-directed Cas9 reactions across an sgRNA concentration series (10–30 nM; left panel) and a substrate-plus-Cas9 control comparison (right panel). ITS100-based RNP reactions produced weak or indistinct band shifts relative to substrate-only and Cas9-only lanes, indicating limited or inconsistent cleavage activity under the conditions tested.

Before testing fungal targets, the Cas9 workflow was validated using PvuII-linearized pBR322 and the EnGen sgRNA Control Oligo. Complete reactions containing template DNA, Cas9, sgRNA, and Mg^{2+} produced the expected digestion pattern on 1% agarose, whereas lanes lacking Cas9, sgRNA, or Mg^{2+} retained intact substrate, confirming that sgRNA synthesis, RNP assembly, and reaction conditions were functional (Figure 3.5).

After the control workflow was validated, sequence-confirmed TEF amplicons were advanced into target-specific Cas9 ribonucleoprotein assays. Purified TEF substrates derived from confirmed sequencing samples were combined with Cas9 and TEF-targeting sgRNAs under standard preincubation and cleavage conditions. Initial agarose-based visualization of these reactions produced only faint or subtle changes relative to intact controls, and several runs showed little to no clearly resolved fragment separation on 1–1.5% agarose gels. However, the small size and close spacing of expected fragments limited agarose resolution (Figure 3.5). Higher-resolution PAGE revealed clearer digestion patterns where complete reactions containing TEF DNA, Cas9, and the most effective TEF guide produced additional lower-migrating fragments that were absent from Cas9-only, sgRNA-only, and DNA-only controls (Figure 3.6). These PAGE results confirm that at least one TEF-targeting sgRNA formed an active Cas9 RNP that recognized and cleaved the amplified TEF locus from *L. acicola* in vitro.

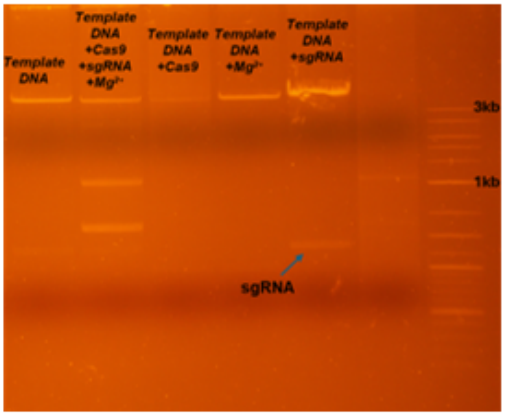

Figure 3.3. Cas9/sgRNA-mediated in vitro digestion of PvuII-linearized pBR322.In vitro cleavage reactions were performed using PvuII-linearized pBR322 as the DNA substrate and an sgRNA synthesized from the EnGen sgRNA Control Oligo, S. pyogenes. Reactions were assembled according to NEB® protocols at a 20:20:1 molar ratio of Cas9:sgRNA:target site in 30 µl total volume. Reaction products were mixed with Gel Loading Dye, Purple (6X) (NEB #B7024), separated on a 1% TBE agarose gel, and visualized by ethidium bromide staining. The 1 kb Plus DNA Ladder (NEB #N3200) was used as the molecular size marker. Lane 1, template DNA only; Lane 2, template DNA + Cas9 + sgRNA + Mg^{2+}; Lane 3, template DNA + Cas9; Lane 4, template DNA + Mg^{2+}; Lane 5, template DNA + sgRNA; Lane M, DNA ladder. Cleavage products were detected only in the complete reaction containing Cas9, sgRNA, and Mg^{2+}, whereas the control lanes lacking one or more required components retained the intact linear DNA substrate. The fast-migrating band in Lane 5 corresponds to free sgRNA.

Figure 3.5 Cas9/sgRNA digestion of PvuII-linearized pBR322 positive-control substrate, showing cleavage only in the complete reaction containing template DNA, Cas9, sgRNA, and Mg^{2+}.

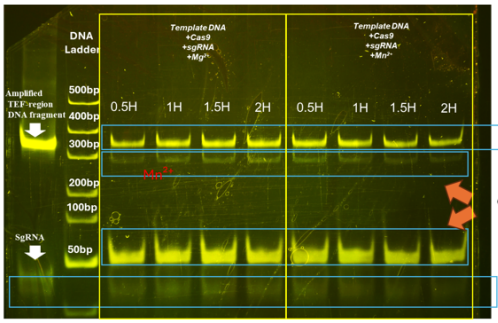

Figure 3.4. In vitro CRISPR-Cas9 ribonucleoprotein digestion of the amplified TEF locus from *Lecanosticta acicola. The* translation elongation factor 1-alpha (TEF; EF-1α) locus amplified from Lecanosticta acicola was used as the substrate for an in vitro CRISPR-Cas9 cleavage assay to validate TEF as a target for CRISPR-based diagnostic protocol 1. TEF was selected because it is a robust fungal marker for species-level discrimination and has previously been used successfully for L. acicola detection. TEF-targeting sgRNAs were designed for Streptococcus pyogenes Cas9 according to the NEB EnGen sgRNA synthesis workflow, following initial validation of sgRNA synthesis using the kit-provided positive control. The amplified TEF fragment was incubated with Cas9 and TEF-specific sgRNA to form an active ribonucleoprotein (RNP) cleavage system. Control reactions lacking individual components of the cleavage system were included to confirm that digestion depended on the complete RNP complex. The intact TEF amplicon is visible in the control lane, whereas cleavage-dependent changes were expected only in the complete reaction containing template DNA, Cas9, sgRNA, and Mg^{2+}. Although cleavage products were not clearly resolved on agarose, the corresponding acrylamide gel assay confirmed successful digestion of the TEF target, indicating that the selected TEF sequence is compatible with CRISPR-mediated recognition and cleavage. The weak agarose resolution most likely reflects the limited ability of agarose to separate small or closely sized digestion fragments from a short PCR amplicon. This experiment provides the key biochemical proof-of-principle that the TEF locus of L. acicola is a valid CRISPR target and establishes the molecular foundation for subsequent development of a TEF-based CRISPR diagnostic assay.

Figure 3.6 In vitro Cas9 digestion of the TEF amplicon from Lecanosticta acicola, showing intact substrate in control lanes and additional lower-migrating fragments in complete reactions containing Cas9, TEF-specific sgRNA, and Mg^{2+}.

The averaged gel metrics showed that ITS and TEF contributed vastly different amounts of usable substrate across the experiment. ITS runs yielded a mean relative substrate of ~ 1.31 (n = 13), with lower signal in ratio tests (0.79, n = 4) and modest enrichment in ITS-oriented sgRNA-screening gels (1.55, n = 9), indicating reliable but relatively limited template for intensive follow-up work. In contrast, TEF runs averaged roughly 3.03 relative substrate overall (n = 37), with especially strong contributions from purity-test gels (5.43, n = 16) and solid performance in fungal-versus-needle comparisons (1.56, n = 7), even though TEF-linked sgRNA-screening gels themselves showed more moderate values (0.93, n = 9). Taken together, these trends (Figure 3.7) show that ITS supported early screening and reference assays, whereas TEF consistently supplied more abundant, cleaner DNA across the roles most critical for CRISPR optimization.

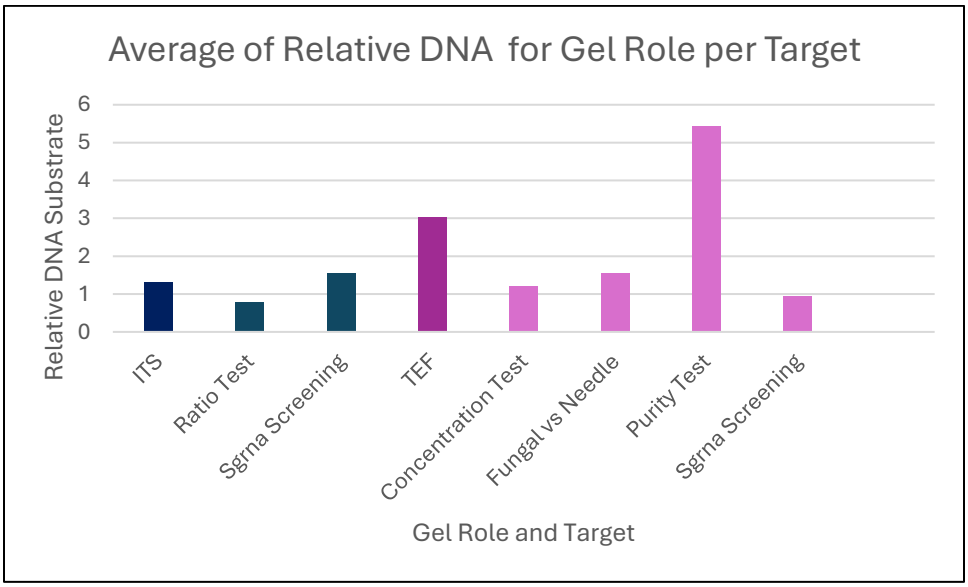

Figure 3.7 Average relative DNA substrate across gel roles for ITS and TEF targets. Bar heights show the mean relative substrate values for ITS (overall 1.31; ratio tests 0.79, n = 4; ITS-focused sgRNA-screening gels 1.55, n = 9) and TEF (overall 3.03; concentration tests 1.20, n = 5; fungal-versus-needle gels 1.56, n = 7; purity-test gels 5.43, n = 16;

TEF-focused sgRNA-screening gels 0.93, n = 9). TEF consistently contributed more abundant and cleaner DNA in the gel roles most relevant to CRISPR optimization.

3.4.3 Comparison of ITS-targeted qPCR Reference Assays

Quantitative PCR (qPCR) assays provided a conventional molecular reference for evaluating how the TEF-targeted Cas9 cleavage assay compared with an established detection method. The ITS-targeted qPCR assay produced a highly linear standard curve across the 1.25–20 ng DNA input range, with Cq values decreasing as $\log_{10}$ DNA input increased, a slope of approximately –3.70, and an R^2 of 0.997, corresponding to an efficiency of about 86.3%. Within this range, the ITS assay reliably detected *L. acicola* genomic DNA down to 1.25 ng per reaction, with Cq values rising from ~8 cycles at 20 ng to ~13 cycles at 1.25 ng, indicating robust performance defining a limit of detection.

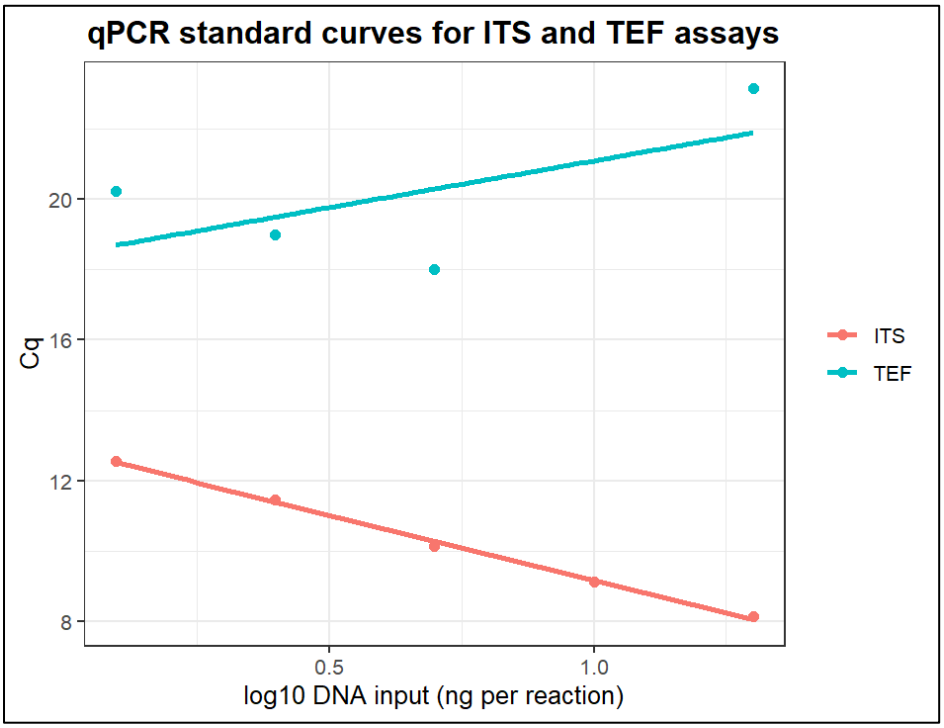

Figure 3.8 Standard curves for ITS and TEF qPCR assays generated from five-point dilution series (20–1.25 ng per reaction), showing linear Cq responses to DNA input for ITS (R^2 = 0.997, efficiency ≈ 86.3%) and a weaker, more variable relationship for TEF (R^2 = 0.373, efficiency ≈ −58.0%).

In contrast, the TEF-targeted qPCR assay displayed weak, inconsistent quantitative behavior. Its standard curve showed a slope of 2.65, an R^2 of 0.373, and an apparent efficiency around 58.0%, with Cq values that did not follow a consistent trend with DNA input, making this assay unsuitable for quantitative interpretation in its current configuration. For that reason, subsequent comparisons in this chapter treat ITS qPCR as the primary quantitative benchmark and interpret TEF-associated CRISPR cleavage qualitatively, focusing on presence/absence and fragment patterns rather than precise quantification.

3.5 Discussion

This study evaluated whether *Lecanosticta acicola* DNA targets from loblolly pine can be amplified, sequence-confirmed, and recognized by CRISPR–Cas9 nuclease in vitro, with the ultimate goal of informing a future Cas12a-based point-of-care (POC) diagnostic for brown spot needle blight. Overall, the results support the central hypothesis that the TEF1-α locus functions as a CRISPR-compatible target for *L. acicola*, whereas the initial ITS-directed guide assessed here showed weaker and less consistent activity. This work builds upon the upstream sample selection and extraction choices from Chapter 2 to directly influence CRISPR assay feasibility, because those determine whether fungal DNA targets are present at sufficient quality and abundance for both PCR/qPCR and downstream RNP cleavage. (Baldi and La Porta 2020).

The first objective was to confirm that diagnostically relevant loci from L. acicola can be amplified from realistic forestry samples, not just pure cultures. The multi-locus primer screens and gel visualizations demonstrate that the ITS region and TEF1-related amplicons can be recovered from infected loblolly pine needles, while healthy needle controls and no-template controls remained free of bands at the expected sizes (Figure 3.2). These outcomes align with previous work that uses ITS and TEF1-α to distinguish L. acicola from Dothistroma spp. and confirm that the optimized workflows from Chapter 2 generate DNA suitable for locus-specific amplification in host–pathogen mixtures. (Ioos et al. 2010; van der Nest et al. 2019; Janoušek et al. 2016). Sequencing selected ITS and TEF1 amplicons provided high similarity to reference *L. acicola* sequences in NCBI, reinforcing locus identity and confirming that the amplified products correspond to diagnostically meaningful regions. (Janoušek et al. 2016; Seo et al. 2012). These findings parallel TEF-based PCR and LAMP assays that successfully detect *L. acicola* directly from pine needles and highlight TEF1 as a robust fungal marker for species-level discrimination in this pathosystem. (Janoušek et al. 2016; Bakhsha et al. 2021; van der Nest et al. 2019). By establishing that infected needles yield clean, sequence-confirmed targets, this chapter moves the system from theoretical target selection into a verified molecular context that can support CRISPR assay development.

The core hypothesis for the CRISPR component of this chapter was that at least one TEF1-α-targeting sgRNA could form an active Cas9 ribonucleoprotein (RNP) that cleaves amplified *L. acicola* TEF DNA in vitro, thereby validating TEF as a CRISPR-compatible diagnostic target. (Jinek et al. 2012; Kellner et al. 2019). TEF1-α already carries strong support as a diagnostic marker in fungal systematics and

BSNB-specific assays, and previous studies show that TEF has high amplification success and species-level resolving power within *Lecanosticta* and related taxa. (van der Nest et al. 2019; Janoušek et al. 2016; Bakhsha et al. 2021). The present work extends that evidence by demonstrating that TEF not only amplifies and discriminates *L. acicola* in PCR-based assays but also supports sequence-specific CRISPR recognition and cleavage when targeted by a properly configured guide and nuclease. The sgRNA panel (TEF-50rev, TEF-76rev, TEF-177rev) followed the NEB EnGen design framework, using NGG-adjacent protospacers within the confirmed TEF amplicon and incorporating the T7 promoter and scaffold-overlap sequence in each user-designed oligo. (New England Biolabs 2025a, 2025b). This approach reflects current best practice, where multiple candidate guides are tested per locus because in silico scores do not always predict in vitro performance. (Hsu et al. 2013; Grainger et al. 2017). In this study, all three TEF guides produced sgRNA of the expected length and integrity on PAGE or bleach–agarose gels (Figure 3.3, left panel), indicating that the synthesis pipeline and RNA handling were adequate for RNP assembly.

The decisive evidence for TEF compatibility comes from the in vitro RNP cleavage assays. (Jinek et al. 2012; Grainger et al. 2017). After validating the overall NEB workflow with PvuII-linearized pBR322 and the EnGen control sgRNA (Figure 3.5), sequence-confirmed TEF amplicons were incubated with Cas9 and TEF-specific sgRNAs under recommended pre-incubation and cleavage conditions. (New England Biolabs 2025c). Agarose gels showed only subtle band shifts and faint additional bands relative to undigested controls, likely due to the small fragment sizes and close spacing of expected products, but acrylamide gels resolved distinct lower-migrating bands that

appeared only in complete Cas9+sgRNA+Mg^{2+} reactions (Figure 3.6). (Bio-Rad 2014; Thermo Fisher Scientific 2025). These PAGE results confirm that at least one TEF-targeting guide generated an active Cas9 RNP that recognized and cleaved the amplified TEF locus from *L. acicola* in vitro, satisfying the central biochemical requirement for a CRISPR-based diagnostic target. (Jinek et al. 2012; Kellner et al. 2019). By coupling TEF's prior success in PCR and LAMP diagnostics with direct CRISPR-mediated cleavage, this work transforms TEF from a candidate marker into a validated CRISPR target for *L. acicola*. (Janoušek et al. 2016; Bakhsha et al. 2021). This validation is especially important because TEF exhibits intraspecific diversity, and guide design must consider conservation across lineages to avoid false negatives in diverse field populations. (Ogris et al. 2023; Matallana-Ramirez et al. 2021; van der Nest et al. 2019). Future work should therefore survey TEF sequence variation at the sgRNA-binding and PAM-adjacent sites across multiple *L. acicola* isolates, but the current results show that at least one TEF region can support reliable CRISPR recognition under laboratory conditions. (Janoušek et al. 2016; Bakhsha et al. 2021).

One of the most conspicuous technical outcomes in this chapter is the contrast between weak or ambiguous TEF cleavage patterns on agarose and clearer digestion products on acrylamide. (Figure 3.5; Figure 3.6). This pattern agrees with broader electrophoresis literature, which emphasizes that agarose gels are well suited for larger fragments and gross size differences, whereas PAGE provides superior resolution for short PCR fragments and digestion products that differ by tens of base pairs or less. (Bio-Rad 2011; Bio-Rad 2014). In this study, the PvuII-linearized pBR322 control produced a clear multi-band pattern on agarose because the substrate is large and

digestion generates fragments with large size differences, whereas the TEF amplicon is short and Cas9 cleavage likely yields products that are close in size to each other and to the uncleaved amplicon. (New England Biolabs 2021). This illustrates that faint or unresolved TEF digestion on agarose does not contradict successful cleavage, but that visualization sensitivity depends on gel matrix and fragment size. (Bio-Rad 2011; Thermo Fisher Scientific 2025). Acrylamide's smaller pore size and sharper banding pattern detect partial cleavage and minority fragments more effectively, which explains why TEF digestion products appear clearly in Figure 3.6 despite equivocal agarose results in Figure 3.5. (Bio-Rad 2014; Thermo Fisher Scientific 2025). This interpretation aligns with manufacturer guidance and CRISPR methods papers that recommend PAGE when users need to verify digestion of short amplicons or distinguish subtle size shifts. (Grainger et al. 2017; New England Biolabs 2025c).

This observation carries practical implications for CRISPR assay development beyond this thesis. (Kellner et al. 2019; Rocafort et al. 2022). When early optimization runs rely only on agarose gels, researchers may underestimate guide performance or misclassify weakly positive guides as inactive, particularly for short diagnostic amplicons. (Bio-Rad 2011; Thermo Fisher Scientific 2025). Incorporating at least one PAGE-based validation step into guide screening workflows can prevent premature rejection of viable targets and guides, especially in plant pathology systems where amplicon sizes often fall in the few-hundred-base-pair range. (Grainger et al. 2017; New England Biolabs 2025c).

A secondary question in this chapter was whether the ITS-targeting sgRNA would perform comparably to TEF-specific guides in Cas9 RNP assays. The sgRNA targeting ITS (100rev) based RNP reactions produced only weak, indistinct band shifts across the

tested sgRNA concentration series, and digestion patterns remained difficult to interpret when compared with substrate-only and Cas9-only controls (Figure 3.4). These results suggest that, under the conditions used here, the ITS-directed guide displayed limited or inconsistent cleavage activity, even though ITS amplification and qPCR performed well in conventional assays. (Ioos et al. 2010). Several factors may explain the difference between TEF and ITS performance like how guide efficiency depends on more qualities than target identity. Protospacer GC content, secondary structure, and local sequence context can influence RNP binding and cleavage kinetics (Hsu et al. 2013). Additionally, ITS amplicon design prioritized primer placement and restriction-site mapping for PCR and qPCR workflows, and guide placement had to avoid primer binding regions, which may have constrained access to optimal Cas9 sites (Ioos et al. 2010). Along with, sgRNA stability being a known bottleneck in RNA-based systems as any degradation during synthesis, cleanup, or storage would reduce effective guide concentration and exaggerate differences among guides. (New England Biolabs 2025b; New England Biolabs 2025c).

From a diagnostic perspective, these findings do not diminish ITS as a valuable qPCR locus, but it does highlight that locus performance in amplification assays does not guarantee equal performance in CRISPR cleavage assays (Wu et al. 2025; Cao et al. 2024). In the context of BSNB diagnostics, the present results support a strategy where TEF serves as the primary CRISPR-targeted locus, while ITS remains central for qPCR benchmarking and for confirmatory testing when needed (Janoušek et al. 2016; Bakhsha et al. 2021). Future work can revisit ITS targeting using alternative guide sites, nucleases

with different PAM requirements, or Cas12a-based systems where guide architecture and DNA recognition differ from Cas9. (Chen et al. 2018; Lei et al. 2022)

In Chapter 2, it was established that fungal-enriching extraction workflows, particularly kits optimized for fungal cells or mixed fungal–plant tissues, substantially improve the sensitivity and reliability of molecular assays for *L. acicola* in needles (Baldi and La Porta 2020). Our CRISPR-Cas9 assays build directly on that foundation by showing that TEF and ITS targets amplified from those optimized extracts can serve not only in qPCR readouts but also as substrates for CRISPR-Cas recognition and cleavage. In practical terms, this means that any future Cas12a-based POC assay for BSNB will depend heavily on upstream choices that maximize fungal DNA content and minimize inhibitors, just as much as it will depend on downstream guide and nuclease design (Luchi et al. 2020; Wu et al. 2025).

Altogether, this study outlines a diagnostic pipeline for *L. acicola.* Infected needles collected from operational forestry settings can be processed with fungal-focused extraction chemistries that enrich target pathogen DNA, and TEF-targeted primers are able to amplify a short diagnostic fragment that both confirms locus identity and feeds a CRISPR-based detection module (Janoušek et al. 2016; Bakhsha et al. 2021). In a laboratory context, Cas9-based cleavage and PAGE confirmation provide a robust quality-control step that validates guide function and target compatibility before those components are translated into Cas12a-driven collateral-cleavage readouts suitable for lateral-flow or fluorescence-based field devices. (Kellner et al. 2019; Chen et al. 2018; Lei et al. 2022).

Limitations of this study can also guide the next steps toward a field-deployable CRISPR diagnostic. The TEF-targeted RNP assays relied on a limited number of isolates and guides so, broader inclusivity testing across diverse *L. acicola* lineages will be necessary to ensure that TEF guide sites remain conserved and that polymorphisms do not compromise sensitivity (Janoušek et al. 2016; van der Nest et al. 2019; Ogris et al. 2023). Another limitation is present considered all CRISPR evaluations occurred under controlled laboratory conditions with purified amplicons, which simplifies matrix effects compared with crude or minimally processed needle extracts that a POC assay would encounter (Baldi and La Porta 2020; Wu et al. 2025). Lastly, the work used Cas9 as a proof- of-principle nuclease because its cleavage products are straightforward to interpret by gel electrophoresis, but the envisioned diagnostic ultimately depends on Cas12a or related nucleases that couple target recognition to collateral reporter cleavage (Kellner et al. 2019; Chen et al. 2018; Lei et al. 2022). Translating a TEF-validated Cas9 target into a Cas12a mechanism will require careful PAM and guide redesign, empirical tuning of isothermal amplification conditions, and validation of readouts in formats such as lateral-flow (Gootenberg et al. 2017; Bourgault et al. 2022; Wang et al. 2025).

Despite these limitations, this chapter provides the essential biochemical validation that the TEF locus supports CRISPR-Cas9 mediated recognition of *L. acicola* DNA and guide-directed nucleases can distinguish fungal targets in mixed host–pathogen samples. (Jinek et al. 2012; Kellner et al. 2019; Janoušek et al. 2016). By anchoring future Cas12a assay development in a TEF region that already supports both PCR-based diagnostics and Cas9-mediated cleavage, the work reduces downstream risk and focuses

optimization on readout and field-adaptation challenges rather than on fundamental target compatibility. (Bakhsha et al. 2021; Wu et al. 2025; Cao et al. 2024).

3.6 Conclusions

Overall, chapter 3 demonstrates that diagnostically relevant loci from *Lecanosticta acicola*, specifically the translation elongation factor 1-alpha (TEF-1a) locus, can be reliably amplified from realistic forestry samples rather than only from pure cultures. Building on the fungally enriching extraction workflows developed in Chapter 2, locus-specific PCR from fresh infected loblolly pine needles produced clean ITS and TEF amplicons that matched reference *L. acicola* sequences and remained free of bands in healthy-needle and no-template controls, confirming that these targets are both accessible and specific in host–pathogen mixtures. Within this framework, TEF1 emerged as a particularly strong candidate for CRISPR-based diagnostics. TEF-targeted primers generated robust, sequence-confirmed amplicons, and multiple Streptococcus pyogenes Cas9 guide RNAs designed against this locus supported detectable in vitro cleavage when assembled into RNP complexes and evaluated on polyacrylamide gels. Although cleavage patterns on agarose gels were ambiguous, PAGE gel analysis resolved clear digestion of the TEF substrate, underscoring that guide performance can be underestimated when only low-resolution gels are used to screen CRISPR reactions on short diagnostic amplicons.

These findings provide biochemical proof-of-principle that guided CRISPR–Cas9 nucleases can recognize and cleave L. acicola TEF targets in mixed host–pathogen DNA, bridging the gap between sequence-level assay design and functional validation. At the

same time, the work highlights several limitations such as having only a small panel of sgRNAs and loci were tested, guide performance was evaluated under laboratory conditions rather than in fully integrated point-of-care formats, and assay readouts relied on gel-based visualization rather than portable fluorescence or lateral-flow devices. Despite these constraints, the TEF-based CRISPR validation completed here establishes a low-risk, well-characterized target region that can be ported into Cas12a-driven collateral-cleavage platforms and other CRISPR diagnostic architectures. Combined with the optimized extraction and amplification pipeline from Chapter 2, this chapter therefore lays the molecular foundation for future development of field-aligned BSNB diagnostics that couple fungally enriched needle extracts, TEF-targeted amplification, and CRISPR-mediated detection into a cohesive workflow for *L. acicola* surveillance in operational forestry settings.

3.7 References

A phenol/chloroform-free method to extract nucleic acids from recalcitrant, woody tropical species for gene expression and sequencing - PubMed. [accessed 2026 Apr 5]. https://pubmed.ncbi.nlm.nih.gov/31171930/.

Aglietti C, Meinecke CD, Ghelardini L, Barnes I, van der Nest A, Villari C. 2021. Rapid Detection of Pine Pathogens Lecanosticta acicola, Dothistroma pini and D. septosporum on Needles by Probe-Based LAMP Assays. Forests. 12(4):479. doi:10.3390/f12040479.

Bakhsha M, Barnes I, van der Nest MA, Wingfield MJ, Mesanza N. 2021. A rapid and highly specific molecular assay for the detection of Lecanosticta acicola, the causal agent of brown spot needle blight of pines. Forests. 12:479.

Barbier FF, Chabikwa TG, Ahsan MU, Cook SE, Powell R, Tanurdzic M, Beveridge CA. 2019. A phenol/chloroform-free method to extract nucleic acids from recalcitrant, woody tropical species for gene expression and sequencing. Plant Methods. 15:62. doi:10.1186/s13007-019-0447-3.

Barnes I, Crous PW, Wingfield BD, Wingfield MJ. Multigene phylogenies reveal that red band needle blight of Pinus is caused by two distinct species of Dothistroma, D. septosporum and D. pini.

Barnes I, Van der Nest A, Mullett MS, Crous PW, Drenkhan R, Musolin DL, Wingfield MJ. 2016. Neotypification of Dothistroma septosporum and epitypification of D. pini, causal agents of Dothistroma needle blight of pine. Forest Pathology. 46(5):388–407.

Bio-Rad. 2025. Gel electrophoresis guide and overview of agarose versus polyacrylamide applications. Bio-Rad Laboratories.

Boesenberg-Smith KA, Pessarakli MM, Wolk DM. 2012. Assessment of DNA Yield and Purity: an Overlooked Detail of PCR Troubleshooting. Clinical Microbiology Newsletter. 34(1):1–6. doi:10.1016/j.clinmicnews.2011.12.002.

Borodušķe A, Ķibilds J, Fridmanis D, Gudrā D, Ustinova M, Seņkovs M, Nikolajeva V. 2023. Does peptide-nucleic acid (PNA) clamping of host plant DNA benefit ITS1 amplicon-based characterization of the fungal endophyte community? Fungal Ecology. 61:101181. doi:10.1016/j.funeco.2022.101181.

Bourgault É., Gauthier M, Potvin A, Stewart D, Chahal K, Sakalidis ML, Tanguay P. 2022. Benchmarking a fast and simple on-site detection assay for the oak wilt pathogen Bretziella fagacearum. Frontiers in Forests and Global Change. 5:1068135. doi:10.3389/ffgc.2022.1068135.

Bourgault Émilie, Gauthier M-K, Potvin A, Stewart D, Chahal K, Sakalidis ML, Tanguay P. 2022. Benchmarking a fast and simple on-site detection assay for the oak wilt pathogen Bretziella fagacearum. Front For Glob Change. 5. doi:10.3389/ffgc.2022.1068135. [accessed 2026 Apr 4]. https://www.frontiersin.org/journals/forests-and-global-change/articles/10.3389/ffgc.2022.1068135/full.

Broders K, Munck I, Wyka S, Iriarte G, Beaudoin E. 2015. Characterization of Fungal Pathogens Associated with White Pine Needle Damage (WPND) in Northeastern North America. Forests. 6(11):4088–4104. doi:10.3390/f6114088.

Broughton JP, Deng X, Yu G, Fasching CL, Servellita V, Singh J, Chiu CY. 2020. CRISPR–Cas12-based detection of SARS-CoV-2. Nature Biotechnology. 38(7):870–874. doi:10.1038/s41587-020-0513-4.

Carter-House D, Stajich J, Unruh S, Kurbessoian T. 2020 Oct 26. Fungal CTAB DNA Extraction protocol materials. [accessed 2026 Mar 22]. https://www.protocols.io/view/fungal-ctab-dna-extraction-bp2l6n64dgqe/v1.

Chen JS, Ma E, Harrington LB, Da Costa M, Tian X, Palefsky JM, Doudna JA. 2018. CRISPR-Cas12a target binding unleashes indiscriminate single-stranded DNase activity. Science. 360(6387):436–439. doi:10.1126/science.aar6245.

Chen Q, Wu J, Tang C, Wang Y. 2024. CRISPR-based platforms for the specific and dual detection of defoliating/nondefoliating strains of Verticillium dahliae. Pest Management Science. 80(4):2042–2052. doi:10.1002/ps.7940.

Chen Z, Yang X, Xia H, Wu C, Yang J, Dai T. 2023. A Frontline, Rapid, Nucleic Acid-Based Fusarium circinatum Detection System Using CRISPR/Cas12a Combined

with Recombinase Polymerase Amplification. Plant Disease. 107(6):1902–1910. doi:10.1094/PDIS-05-22-1234-RE.

Climate at a Glance | National Centers for Environmental Information (NCEI). [accessed 2026 Mar 26]. https://www.ncei.noaa.gov/access/monitoring/climate-at-a-glance/statewide/mapping.

Curti LA, Primost I, Valla S, Alegre DI, Perglione CO, Repizo GD, Lara J, Parcerisa I, Palacios A, Llases ME, et al. 2021. Evaluation of a Lyophilized CRISPR-Cas12 Assay for a Sensitive, Specific, and Rapid Detection of SARS-CoV-2. Viruses. 13(3):420. doi:10.3390/v13030420.

Dai T, Chen Z, Guo Y, Ye J. 2023. Rapid detection of the pine wood nematode *Bursaphelenchus xylophilus* using recombinase polymerase amplification combined with CRISPR/Cas12a. Crop Protection. 170:106259. doi:10.1016/j.cropro.2023.106259.

Datta D. 2021. Identification and Distribution of Fungal Pathogens Associated with Loblolly Pine Defoliation and Tree Mortality in the Southeastern United States [Master of Science thesis]. [Auburn, Alabama]: Auburn University.

Desneux J, Pourcher A-M. 2014. Comparison of DNA extraction kits and modification of DNA elution procedure for the quantitation of subdominant bacteria from piggery effluents with real-time PCR. MicrobiologyOpen. 3(4):437. doi:10.1002/mbo3.178.

EPPO. 2015. PM 7/46 (3) Lecanosticta acicola (formerly Mycosphaerella dearnessii), Dothistroma septosporum (formerly Mycosphaerella pini) and Dothistroma pini. doi:10.1111/epp.12217. [accessed 2026 Mar 27]. https://onlinelibrary.wiley.com/doi/epdf/10.1111/epp.12217.

Farrall T, Abeynayake SW, Webster W, Fiorito S, Dinsdale A, Whattam M, Campbell PR, Gambley C. 2024. Development of a rapid, accurate, and field-deployable LAMP-CRISPR-Cas12a integrated assay for Xylella fastidiosa detection and surveillance. Australasian Plant Pathology. 53(1):115–120. doi:10.1007/s13313-023-00954-4.

Fitzpatrick CR, et al. 2018. Chloroplast sequence variation and the efficacy of peptide nucleic acids for blocking host amplification in plant microbiome studies. Microbiome. 6:144.

Folorunso TR, et al. 2025. Optimized protocol for culturing and extracting DNA from fungal isolates associated with brown spot needle blight in pine trees. PLoS ONE. 20:e0337218.

Garrett PE. 2001. Quality control for nucleic acid tests: common ground and special issues. Journal of Clinical Virology. 20(1):15–21. doi:10.1016/S1386-6532(00)00150-5.

Gibson IAS, Christensen PS, Dedan JK. 1967. Further Observations in Kenya on a Foliage Disease of Pines Caused by Dothistroma Pini Hulbary: Iii. the Effect of Shade on the Incidence of Disease in Pinus Radiata. The Commonwealth Forestry Review. 46(3 (129)):239–247.

Grainger R, Brown CM, Hartley JL. 2017. Guide RNA validation for in vitro CRISPR/Cas9 applications. Methods.

Guo Y, Xia H, Dai T, Liu T, Shamoun SF, CuiPing W. 2023. CRISPR/Cas12a-based approaches for efficient and accurate detection of Phytophthora ramorum. Front Cell Infect Microbiol. 13. doi:10.3389/fcimb.2023.1218105. [accessed 2026 Apr 4]. https://www.frontiersin.org/journals/cellular-and-infection-microbiology/articles/10.3389/fcimb.2023.1218105/full.

Hsu PD, Scott DA, Weinstein JA, Ran FA, Konermann S, Agarwala V, Li Y, Fine EJ, Wu X, Shalem O, et al. 2013. DNA targeting specificity of RNA-guided Cas9 nucleases. Nature Biotechnology. 31:827–832.

Hu J-J, Li X-X, Zhao Y-M, Chen W. 2023. One-pot assay for rapid detection of benzimidazole resistance in Venturia carpophila by combining RPA and CRISPR/Cas12a. Journal of Agricultural and Food Chemistry. 71(3):1381–1390. doi:10.1021/acs.jafc.2c07345.

Huang T, Zhang R, Li J. 2023. CRISPR-Cas-based techniques for pathogen detection: Retrospect, recent advances, and future perspectives. Journal of Advanced Research. 50:69–82. doi:10.1016/j.jare.2022.10.011.

Huang Z-Y. 1995. Differentiation of *Mycosphaerella dearnessii* by Cultural Characters and RAPD Analysis. Phytopathology. 85(5):522. doi:10.1094/Phyto-85-522.

Hussain R, Kumar P, Perri E. 2024. A Single Tube RPA/Cas12a Based Diagnostic Assay for Early, Rapid and Efficient Detection of Botrytis cinerea in Sweet Cherry. Plant Disease. doi:10.1094/PDIS-XX-XX-XXXX-XX.

Ihrmark K, et al. 2012. New primers to amplify the fungal ITS2 region—evaluation by 454-sequencing of artificial and natural communities. FEMS Microbiology Ecology. 82:666–677.

Ioos R, Fabre B, Saurat C, Fourrier C, Frey P, Marçais B. 2010. Development, Comparison, and Validation of Real-Time and Conventional PCR Tools for the Detection of the Fungal Pathogens Causing Brown Spot and Red Band Needle Blights of Pine. Phytopathology®. 100(1):105–114. doi:10.1094/PHYTO-100-1-0105.

Islam T, Kasfy SH. 2023. CRISPR-based point-of-care plant disease diagnostics. Trends in Biotechnology. doi:10.1016/j.tibtech.2023.01.003.

Janoušek J, Jankovský L, Konečný A, Wingfield MJ, Barnes I. 2016. Characterization and development of microsatellite markers for Dothistroma pini and Lecanosticta acicola including diagnostic markers for both species. Forest Pathology. 46:125–133.

Jinek M, Chylinski K, Fonfara I, Hauer M, Doudna JA, Charpentier E. 2012. A programmable dual-RNA-guided DNA endonuclease in adaptive bacterial immunity. Science. 337:816–821.

Kais AG. 1975. Environmental factors affecting brown spot infection on longleaf pine. Phytopathology. 65(12):1389–1392.

Karakousis A, Langridge P. 2003. A high-throughput plant DNA extraction method for marker analysis. Plant Mol Biol Rep. 21(1):95–95. doi:10.1007/BF02773402.

Kellner MJ, Koob JG, Gootenberg JS, Abudayyeh OO, Zhang F. 2019. SHERLOCK: nucleic acid detection with CRISPR nucleases. Nature Protocols. 14:2986–3012.

Keriö S, Terhonen E, LeBoldus JM. 2020. Safe DNA-extraction Protocol Suitable for Studying Tree-fungus Interactions. Bio-protocol. 10(11):e3634. doi:10.21769/BioProtoc.3634.

Kim CS, et al. 1997. A simple and rapid method for isolation of high quality genomic DNA from fruit trees and conifers using PVP. Nucleic Acids Research. 25:1085–1086.

Krappmann S. 2017. CRISPR-Cas9, the new kid on the block of fungal molecular biology. Med Mycol. 55(1):16–23. doi:10.1093/mmy/myw097.

Lagner JR, Newberry EA, Rivera Y, Zhang L, Vakulskas CA, Qi Y. 2025. Amplification-free detection of plant pathogens by improved CRISPR-Cas12a systems: a case study on phytoplasma. Frontiers in Plant Science. 16:1544513. doi:10.3389/fpls.2025.1544513.

Langsiri N, Meyer W, Irinyi L, Worasilchai N, Pombubpa N, Wongsurawat T, Jenjaroenpun P, Luangsa-ard JJ, Chindamporn A. 2025. Optimizing fungal DNA extraction and purification for Oxford Nanopore untargeted shotgun metagenomic sequencing from simulated hemoculture specimens. mSystems. 10(6):e01166-24. doi:10.1128/msystems.01166-24.

Lei R, Li Y, Li L, Wang J, Cui Z, Ju R, Jiang L, Liao X, Wu P, Wang X. 2022. A CRISPR/Cas12a-based portable platform for rapid detection of Leptosphaeria maculans in Brassica crops. Front Plant Sci. 13. doi:10.3389/fpls.2022.976510. [accessed 2026 Mar 27]. https://www.frontiersin.org/journals/plant-science/articles/10.3389/fpls.2022.976510/full.

Li N, Cai Q, Miao Q, Song Z, Fang Y, Hu B. 2021. High-Throughput Metagenomics for Identification of Pathogens in the Clinical Settings. Small Methods. 5(1):2000792. doi:10.1002/smtd.202000792.

Li S, et al. 2020. Exploring the accuracy of amplicon-based internal transcribed spacer markers for a fungal community. Molecular Ecology Resources. 20:170–184.

Li ZT, Feng WZ, Zhu ZB, Lu SD, Lin MZ, Dong JL, Wang ZX, Liu FX, Chen QH. 2024. Cas-OPRAD: a one-pot RPA/PCR CRISPR/Cas12a assay for on-site Phytophthora root-rot detection. Frontiers in Microbiology. 15:1390422. doi:10.3389/fmicb.2024.1390422.

Lindahl BD, et al. 2013. Fungal community analysis by high-throughput sequencing of amplified markers—a user's guide. New Phytologist. 199:288–299.

Lucena-Aguilar G, Sánchez-López AM, Barberán-Aceituno C, Carrillo-Ávila JA, López-Guerrero JA, Aguilar-Quesada R. 2016. DNA Source Selection for Downstream

Applications Based on DNA Quality Indicators Analysis. Biopreservation and Biobanking. 14(4):264–270. doi:10.1089/bio.2015.0064.

Luchi N, Ioos R, Santini A. 2020. Fast and reliable molecular methods to detect fungal pathogens in woody plants. Appl Microbiol Biotechnol. 104(6):2453–2468. doi:10.1007/s00253-020-10395-4.

Lundberg DS, et al. 2013. Practical innovations for high-throughput amplicon sequencing. Nature Methods. 10:999–1002.

Luo M, Meng F-Z, Tan Q, Yin W-X, Luo C-X. 2021. Recombinase polymerase amplification/Cas12a–based identification of Xanthomonas arboricola pv. pruni on peach. Frontiers in Plant Science. 12:740177. doi:10.3389/fpls.2021.740177.

Mandal A, Panda S, Rath S, Laha B, Nayak S, Goswami UR. 2022. Field-deployable detection of Candidatus Liberibacter asiaticus using recombinase polymerase amplification combined with CRISPR-Cas12a. Journal of Visualized Experiments. 190:e64070. doi:10.3791/64070.

Matallana-Ramirez LP, Whetten RW, Sanchez GM, Payn KG. 2021. Breeding for Climate Change Resilience: A Case Study of Loblolly Pine (Pinus taeda L.) in North America. Frontiers in Plant Science. 12:606908. doi:10.3389/fpls.2021.606908.

Matlock B. 2015. Assessment of Nucleic Acid Purity. 52646.

Menéndez-Gutiérrez M, Villar L, Díaz R. 2024. Effectiveness of a commercial LAMP-technology kit for rapid detection of Bursaphelenchus xylophilus in Pinus pinaster. Forest Systems. 33(3):20917. doi:10.5424/fs/2024333-20917.

Mu K, Ren X, Yang H, Zhang T, Yan W, Yuan F, Zeng Q. 2022. CRISPR-Cas12a-Based Diagnostics of Wheat Fungal Diseases. Journal of Agricultural and Food Chemistry. 70(23):7240–7247. doi:10.1021/acs.jafc.1c08391.

Mullett MS, Adamson K, Bragança H, Bulgakov TS, Georgieva M, Henriques J, Jürisoo L, Laas M, Drenkhan R. 2018. New country and regional records of the pine needle blight pathogens Lecanosticta acicola, Dothistroma septosporum and Dothistroma pini. Forest Pathology. 48(5):e12440. doi:10.1111/efp.12440.

(NOAA National Centers for Environmental information, Climate at a Glance: Statewide Mapping, published February 2026, retrieved on March 4, 2026 from https://www.ncei.noaa.gov/access/monitoring/climate-at-a-glance/statewide/mapping).

van der Nest A, Wingfield MJ, Janoušek J, Barnes I. 2019. Lecanosticta acicola: A growing threat to expanding global pine forests and plantations. Molecular Plant Pathology. 20(10):1327–1364. doi:10.1111/mpp.12853.

van der Nest A, Wingfield MJ, Ortiz PC, Barnes I. 2019. Biodiversity of Lecanosticta pine-needle blight pathogens suggests a Mesoamerican Centre of origin. IMA Fungus. 10(1):2. doi:10.1186/s43008-019-0004-8.

van der Nest MA, Wingfield MJ, Janoušek J, Barnes I. 2019. Molecular markers and diagnostics for fungal plant pathogens. Molecular Plant Pathology. 20:1039–1055.

New England Biolabs. 2025. EnGen sgRNA synthesis kit, S. pyogenes protocol (E3322). New England Biolabs.

Ogris N, Drenkhan R, Vahalík P, Cech T, Mullett M, Tubby K. 2023. The potential global distribution of an emerging forest pathogen, Lecanosticta acicola, under a changing climate. Front For Glob Change. 6. doi:10.3389/ffgc.2023.1221339. [accessed 2026 Mar 26]. https://www.frontiersin.org/journals/forests-and-global-change/articles/10.3389/ffgc.2023.1221339/full.

Pena JM, Manning BJ, Li X, Fiore ES, Carlson L, Shytle K, Nguyen PP, Azmi I, Larsen A, Wilson MK, et al. 2023. Real-Time, Multiplexed SHERLOCK for in Vitro Diagnostics. The Journal of Molecular Diagnostics : JMD. 25(7):428. doi:10.1016/j.jmoldx.2023.03.009.

PM 7/46 (3) Lecanosticta acicola (formerly Mycosphaerella dearnessii), Dothistroma septosporum (formerly Mycosphaerella pini) and Dothistroma pini. 2015. EPPO Bulletin. 45(2):163–182. doi:10.1111/epp.12217.

Pokhrel NR, Dahlen J, Eberhardt TL, Gandhi KJK, Barnes BF. 2026. Loblolly pine (*Pinus taeda*) trees experiencing dieback have altered resin canals, earlywood, and latewood relative to asymptomatic trees. Forest Ecology and Management. 607:123595. doi:10.1016/j.foreco.2026.123595.

Porebski S, Bailey LG, Baum BR. 1997. Modification of a CTAB DNA extraction protocol for plants containing high polysaccharide and polyphenol components. Plant Mol Biol Rep. 15(1):8–15. doi:10.1007/BF02772108.

Pozharskiy A, Kostyukova V, Adilbayeva K, Taskuzhina A, Gritsenko D. 2025. CRISPR/Cas-based detection systems – emerging tools for plant pathology. Open Agriculture. 10(1). doi:10.1515/opag-2025-0458. [accessed 2026 Mar 27]. https://www.degruyterbrill.com/document/doi/10.1515/opag-2025-0458/html.

Pratyusha S. 2022. Phenolic Compounds in the Plant Development and Defense: An Overview. In: Plant Stress Physiology - Perspectives in Agriculture. IntechOpen. [accessed 2026 Mar 26]. https://www.intechopen.com/chapters/80846.

Rezadoost MH, et al. 2016. An efficient protocol for isolation of inhibitor-free nucleic acids even from recalcitrant plants. 3 Biotech. 6:61.

Rocafort M, Arshed S, Hudson D, Sidhu JS, Bowen JK, Plummer KM, Bradshaw RE, Johnson RD, Johnson LJ, Mesarich CH. 2022. CRISPR-Cas9 gene editing and rapid detection of gene-edited mutants using high-resolution melting in the apple scab fungus, *Venturia inaequalis*. Fungal Biology. 126(1):35–46. doi:10.1016/j.funbio.2021.10.001.

Sahu SK, et al. 2012. DNA extraction protocol for plants with high levels of secondary metabolites and polysaccharides without using liquid nitrogen and phenol. ISRN Molecular Biology. 2012:205049.

Schoch CL, et al. 2012. Nuclear ribosomal internal transcribed spacer (ITS) region as a universal DNA barcode marker for Fungi. Proceedings of the National Academy of Sciences USA. 109:6241–6246.

Shin K, Kwon S-H, Lee S-C, Moon YE. 2021. Sensitive and rapid detection of citrus scab using an RPA-CRISPR/Cas12a system combined with a lateral flow assay. Plants. 10(10):2132. doi:10.3390/plants10102132.

Siddique AB, Albrectsen BR, Ilbi H, Siddique AB. 2022. Optimization of Protocol for Construction of Fungal ITS Amplicon Library for High-Throughput Illumina Sequencing to Study the Mycobiome of Aspen Leaves. Applied Sciences. 12(3):1136. doi:10.3390/app12031136.

Siggers PV. 1932. The Brown-Spot Needle Blight of Longleaf Pine Seedlings. j for. 30(5):579–593. doi:10.1093/jof/30.5.579.

Singh S, Narine LL, Willoughby JR, Eckhardt LG. 2025. Remote sensing-based detection of brown spot needle blight: a comprehensive review, and future directions. PeerJ. 13:e19407. doi:10.7717/peerj.19407.

Skilling DD, Nicholls TH. 1975. Brown spot needle disease--biology and control in Scotch pine plantations. Research Paper NC-109 St Paul, MN: US Dept of Agriculture, Forest Service, North Central Forest Experiment Station. 109. [accessed 2026 Mar 26]. https://research.fs.usda.gov/treesearch/10630.

Sutipatanasomboon A, Wongsantichon J, Sakdee S, Naksith P, Watthanadirek A, Anuracpreeda P, Blacksell SD, Saisawang C. 2024. RPA-CRISPR/Cas12a assay for the diagnosis of bovine Anaplasma marginale infection. Sci Rep. 14(1):7820. doi:10.1038/s41598-024-58169-6.

Tainter FH, Baker FA. 1996. Principles of Forest Pathology. John Wiley & Sons.

Tang C, Wu J, Chen Q, Wang Y. 2023. CRISPR-Cas detection coupled with isothermal amplification of Bursaphelenchus xylophilus. Plant Disease. 107(6):1703–1713. doi:10.1094/PDIS-07-22-1648-SR.

Tarrall T, Abeynayake SW, Webster W, et al. 2024. Development of a rapid, accurate, and field deployable LAMP-CRISPR-Cas12a integrated assay for Xylella fastidiosa detection and surveillance. Australasian Plant Pathology. 53:115–120. doi:10.1007/s13313-023-00954-4.

Taylor DL, et al. 2016. Accurate estimation of fungal diversity and abundance through improved lineage-specific primers optimized for Illumina amplicon sequencing. Applied and Environmental Microbiology. 82:7217–7226.

Thermo Fisher Scientific. 2025. Nucleic acid electrophoresis workflow and comparison of agarose and polyacrylamide gel systems. Thermo Fisher Scientific.

Tripathi L, Ntui VO, Tripathi JN, Kumar PL. 2021. Application of CRISPR/Cas for Diagnosis and Management of Viral Diseases of Banana. Front Microbiol. 11. doi:10.3389/fmicb.2020.609784. [accessed 2026 Mar 27]. https://www.frontiersin.org/journals/microbiology/articles/10.3389/fmicb.2020.609784/full.

Tubby K, et al. 2023. The increasing threat to European forests from the invasive foliar pine pathogen, Lecanosticta acicola. Forest Ecology and Management. 536:120847.

Varma A, Padh H, Shrivastava N. 2007. Plant genomic DNA isolation: An art or a science. Biotechnology Journal. 2(3):386–392. doi:10.1002/biot.200600195.

Viotti C, Chalot M, Kennedy PG, Maillard F, Santoni S, Blaudez D, Bertheau C. 2024. Primer pairs, PCR conditions, and peptide nucleic acid clamps affect fungal diversity assessment from plant root tissues. Mycology. 15(2):255. doi:10.1080/21501203.2023.2301003.

Wang B, Fan A, Liu M, Zhou Y, Zhang W, Yan J. 2025. An Integrated Rapid Detection of Botryosphaeriaceae Species in Grapevine Based on Recombinase Polymerase Amplification, CRISPR/Cas12a, and Lateral Flow Dipstick. Plant Disease. 109(5):1102–1110. doi:10.1094/PDIS-08-24-1615-RE.

Wang Q, Qin M, Coleman JJ, Shang W, Hu X. 2023. Rapid and sensitive detection of Verticillium dahliae from complex samples using CRISPR/Cas12a technology combined with RPA. Plant Disease. 107(8):1664–1669. doi:10.1094/PDIS-08-22-1790-SC.

Wang X, Wang LF, Cao YF, Yuan YZ, Hu J, Chen ZH, Zhu F, Wang XZ. 2022. Bursaphelenchus xylophilus detection and analysis system based on CRISPR–Cas12. Frontiers in Plant Science. 13:1075838. doi:10.3389/fpls.2022.1075838.

Wheatley MS, Duan YP, Yang Y. 2021. Highly sensitive and rapid detection of citrus Huanglongbing pathogen (Candidatus Liberibacter asiaticus) using Cas12a-based methods. Phytopathology. 111(12):2375–2382. doi:10.1094/PHYTO-09-20-0443-R.

White, Bruns T, Lee S, Taylor J. 1990. White, T. J., T. D. Bruns, S. B. Lee, and J. W. Taylor. Amplification and direct sequencing of fungal ribosomal RNA Genes for phylogenetics. p. 315–322.

White TJ, Bruns T, Lee S, Taylor J. 1989. Amplification and Direct Sequencing of Fungal Ribosomal Rna Genes for Phylogenetics. In: Sninsky J and White T. San Diego: CA Academic Press. Vol. 38. p. 315–322.

Xiao J, Li Z, Zhang X. 2025. Improved pine wood nematode disease diagnosis system based on deep learning. Plant Disease. doi:10.1094/PDIS-06-25-XXXX-XX.

Xu T, Cao F, Dai T, Liu T. 2024. RPA-CRISPR/Cas12a-mediated isothermal amplification for rapid detection of Phytopythium helicoides. Plant Disease. 108(12):3463–3472. doi:10.1094/PDIS-06-24-1300-SR.

Xu XQ, Dai TT, Xiong Q, Yang J, Zang JH, Liu TL. 2024. Molecular detection of Phytophthora cinnamomi by RPA-CRISPR/Cas12a–mediated isothermal amplification. Forests. 15(5):772. doi:10.3390/f15050772.

Zang J, Shi L, Liu TL. 2024. Rapid and efficient molecular detection of Phytophthora nicotianae based on RPA-CRISPR/Cas12a. Forests. 15(6):952. doi:10.3390/f15060952.

Zhang Y, Majumdar I, Schelhas J. 2010. Changes in Woodland Use from Longleaf Pine to Loblolly Pine. Sustainability. 2(9):2734–2745. doi:10.3390/su2092734.

Zhou J, Li X, Liu TL. 2023. Rapid detection of Phytophthora cambivora using recombinase polymerase amplification combined with CRISPR/Cas12a. Forests. 14(11):2141. doi:10.3390/f14112141.